m

SECULAR MOTION OF RESONANT ASTEROIDS

G. E. O. GIACAGLIA

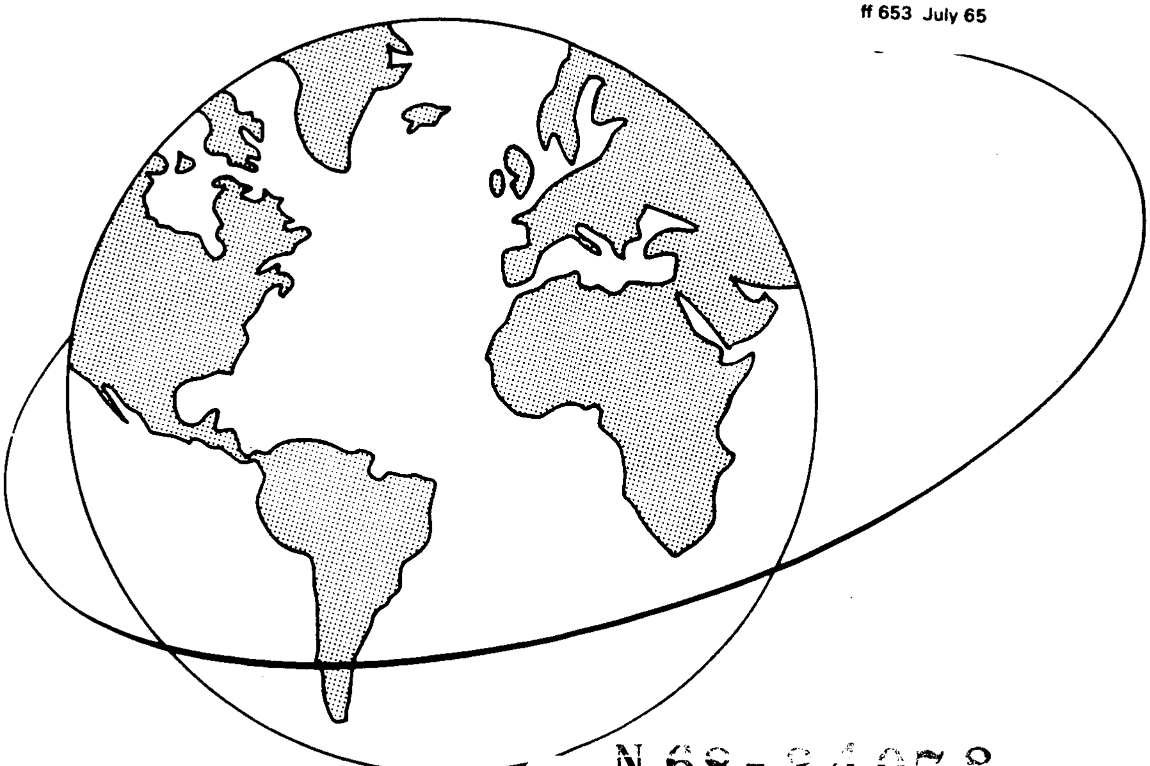

Smithsonian Astrophysical Observatory

SPECIAL REPORT 278

Research in Space Science
SAO Special Report No. 278

SECULAR MOTION OF RESONANT ASTEROIDS

G. E. O. Giacaglia

May 24, 1968

Smithsonian Institution
Astrophysical Observatory
Cambridge, Massachusetts 02138

802-91

PRECEDING PAGE BLANK NOT FILMED.

TABLE OF CONTENTS

LIST OF ILLUSTRATIONS

LIST OF TABLES

ABSTRACT

The secular characteristics of the motion of asteroids in resonance with Jupiter are analyzed. The Trojan group is given special attention by a description of these characteristics in a complete qualitative and quantitative manner. Except for collision orbits, the eccentricity and inclination of the asteroid can take any value. The short-period perturbations caused by Jupiter are averaged by a nonlinear numerical application of von Zeipel's method. Elimination of the resonant argument is carried, in a semianalytical way, to an approximation of the order of the mass of Jupiter. The final system, with one degree of freedom, is represented by isoenergetic curves in the phase plane (ω, e). The various steps of solution allow a description of the general features of motion for a very long time.

RÉSUMÉ

Les caractéristiques séculaires du mouvement des astéroïdes en résonance avec Jupiter sont analysées. Une attention particulière a été portée au groupe Troyen pour lequel la description complète qualitative et quantitative, de ces caractéristiques est présentée. Si l'on excepte le cas des orbites de collision, l'excentricité et l'inclinaison des astéroïdes peuvent prendre n'importe quelles valeurs. La moyenne des pertubbations de courte durée causées par Jupiter est obtenue par une application numérique non-linéaire de la méthode de von Zeipel. L'élimination de l'argument de résonance est poursuivie de manière semi-analytique, jusqu'à un degré d'approximation de l'ordre de la masse de Jupiter. Le système final, à un degré de liberté, est représenté par des courbes d'égale énergie dans le plan des phases (ω, e). Les différentes étapes de solution permettent une description des propriétés générales du mouvement pour une période de temps très étendue.

КОНСПЕКТ

Анализируются вековые характеристики движения астероидов в резонансе с Юпитером. Особое внимание уделяется троянской группе путем описания этих характеристик в полной качественной и количественной форме. За исключением орбит столкновений, экцентриситет и наклон астероида могут принять любую величину. Возмущения короткого периода вызываемые Юпитером, усередняются посредством нелинейного численного применения метода фон Зейпеля. Исключение резонансного аргумента производится полуаналитическим путем,к приближению порядка массы Юпитера. Конечная система с одной степенью свободы изображена изоэнергетическими кривыми в фазовой плоскости (ω,e). Различные шаги решения позволяют описать главные характеристики движения для очень долгого времени.

SECULAR MOTION OF RESONANT ASTEROIDS

G. E. O. Giacaglia

1. INTRODUCTION

Many efforts have been made to describe the properties of two-dimensional orbits, near the 1 / 1 resonance case, in the restricted three-body problem. Most of them make use of a linear analysis; that is, they deal with libration orbits in the vicinity of the triangular equilibrium points. This work tries to eliminate every restriction, with the exception of collision orbits.

The numerical application of von Zeipel's method avoids all questions concerning the convergence of the series for the elimination of short-period terms in the Hamiltonian function. Its validity extends to any value of the osculating eccentricity (less than unity) and of the inclination. Since the departure from the equilibrium Lagrangian points is arbitrary (always assuming that the mean motion is close to that of Jupiter), special cases of interest may be included, such as, for instance, the outer satellites of Jupiter. It is well known that there are satellite problems in which the perturbations from the sun are so severe that both satellite and planetary theories fail to give results valid for longer than a few hundred revolutions. Since secular features may have periods up to several million revolutions, such results are absolutely useless when those features are to be determined. To the present, the best method of analysis of very unusual satellite orbits still remains Kovalevsky's method of computing numerical coefficients for the representative Fourier series.

This work was supported in part by Grant NsG 87-60 from the National Aeronautics and Space Administration.

Pure numerical integration not only gives very restrictive results with little chance of extrapolation but also becomes completely meaningless after a sufficiently long time, owing to round-off and truncation errors. Even if these errors could be efficiently controlled, no available computer is able to perform, in a reasonably short time, an integration for periods of the order of millions of years.

It is hoped that the present research may furnish a way of handling the problem of exceptional planetary and satellite orbits in a more systematic and uniform way. A theory analogous to the one presented here was developed by G. Hori with the collaboration of the author of these notes (Hori and Giacaglia, 1965); it produced highly satisfactory results when applied to the problem of the secular motion of Pluto in resonance with Neptune. In fact, by this method it has been possible to predict all qualitative and approximate quantitative features of that motion; these results agree with the numerical integration performed by Cohen (Cohen and Hubbard, 1965; Cohen, Hubbard, and Oesterwinter, 1967).

It should be remarked that one of the main difficulties found in the development of a general perturbation theory for resonant asteroids with nonzero inclination to the orbital plane of Jupiter is the presence of two slowly varying angular variables: the argument of perihelion and the resonance argument (a linear integral combination of the mean longitudes of the asteroids and Jupiter). With the choice of appropriate variables and a careful application of von Zeipel's method, that doubly degenerate phenomenon can be brought into a form that can be treated mathematically. Moreover, in view of recent results by Arnold (1963), Moser (1967), and Giacaglia (1967) concerning von Zeipel's method, there seems to be some hope that the process will converge. Further, the numerical process allows any values to be used for eccentricity and inclination; this fact overcomes the great obstacle of an analytic development of the disturbing function.

2. GENERAL THEORY

In this section, we consider the motion of an infinitesimal mass point (asteroid) in the gravitational field of two particles (the sun and Jupiter) revolving in circular orbits around their common center of mass. The model and units used throughout are those of the three-dimensional restricted problem of three bodies (Szebehely, 1967). We will assume that the mean motion of the asteroid and that of Jupiter are in a close, low-order, rational relation.

The equations of motion of the asteroid can be written

$$\dot{\ell}_j = -\frac{\partial f^*}{\partial L_j} \ , \ \dot{L}_j = +\frac{\partial f^*}{\partial \ell_j} \ , \ j = 1, 2, 3 \quad , \tag{1}$$

where $\ell_1 = \ell$, $\ell_2 = g$, $\ell_3 = h = \Omega - \lambda_1$, $L_1 = L$, $L_2 = G$, and $L_3 = H$ are the usual Delaunay variables, with the exception of h, the longitude of the ascending node reckoned from the instantaneous position of Jupiter, which is defined by its mean longitude λ_1. The origin is taken at the sun, and the reference system rotates about the z axis in such a way that the x axis always contains Jupiter in circular orbit at unit distance from the sun.

Since our present interest is long-range behavior, the indirect part of the disturbing function will be neglected. With the above assumptions, the Hamiltonian f^* can be written

$$f^* = \frac{1}{2L^2} + H + \epsilon\left(\frac{1}{\Delta} - \frac{1}{r}\right) = f_0^* + f_1^* \quad , \tag{2}$$

where Δ and r are the distances asteroid-Jupiter and asteroid-sun, respectively, and $\epsilon = m_1/(m_\odot + m_1)$. Let $n_1 = 1$ be the mean motion of

Jupiter and n that of the asteroid. The near-resonance case corresponds to the relation

$$\frac{n_1}{n} \simeq \frac{p}{q} \quad , \tag{3}$$

where p and q are small relatively prime integers. For inferior asteroids $p < q$, and for superior ones $p > q$. The angle $p\lambda - q\lambda_1$, where λ is the mean longitude of the asteroid, will therefore vary slowly, and we call it the resonance argument. In other words, the quantity $(-p/L^3) + q = -pn + qn_1$ is small as compared with unity (how small it is we will later define).

The following canonical variables are now introduced:

$$\begin{aligned}
y_0 &= \ell \ , & x_0 &= L - \frac{p}{q} H \ , \\
y_1 &= p\lambda - q\lambda_1 + (q - p)\,\tilde{\omega} = p\ell + qg + qh \ , & x_1 &= \frac{H}{q} \ , \\
y_2 &= g \ , & x_2 &= L - G \ ,
\end{aligned} \tag{4}$$

where $\lambda = \ell + g + \Omega$, $h = \Omega - \lambda_1$, and $\tilde{\omega} = g + \Omega$.

The equations of motion (1) become

$$\dot{y}_j = -\frac{\partial f}{\partial x_j} \ , \ \dot{x}_j = +\frac{\partial f}{\partial y_j} \ , \ j = 0,\ 1,\ 2 \quad , \tag{5}$$

where

$$f = f_0 + f_1 = \frac{1}{2}(x_0 + px_1)^{-2} + qx_1 + f_1(x_0, x_1, x_2 ; y_0, y_1, y_2 ; \epsilon)$$

$$= f(x_0, x_1, x_2 ; y_0, y_1, y_2 ; \epsilon) \quad .$$

The first step in the solution is the reduction of the problem by one degree of freedom, by elimination of the fast variable y_0 through an averaging process. The reduced system will correspond to the Hamiltonian

$$\phi = \frac{1}{2p\pi} \int_0^{2p\pi} f \, dy_0 \Bigg|_{\substack{x=\xi \\ y=\eta}} = \frac{1}{2}(\xi_0 + p\xi_1)^{-2} + q\xi_1 + \phi_1(\xi_0, \xi_1, \xi_2; \eta_1, \eta_2; \epsilon)$$

$$= \phi_0 + \phi_1 = \phi(\xi_0, \xi_1, \xi_2; \eta_1, \eta_2; \epsilon) \quad , \tag{6}$$

where

$$\phi_1 = \frac{\epsilon}{2p\pi} \int_0^{2p\pi} \frac{1}{\Delta} dy_0 - \frac{\epsilon}{a^*} = \epsilon \left[D(\xi_0, \xi_1, \xi_2; \eta_1, \eta_2) - \frac{1}{a^*} \right] \tag{7}$$

and

$$a^* = (\xi_0 + p\xi_1)^2 = L^{*2} \quad .$$

The canonical transformation from the variables (x, y) to (ξ, η) is formally generated by a function

$$\Sigma = \Sigma(\xi_0, \xi_1, \xi_2; y_0, y_1, y_2; \epsilon)$$

such that

$$x_j = \frac{\partial \Sigma}{\partial y_j} \quad , \quad \eta_j = \frac{\partial \Sigma}{\partial \xi_j} \quad , \; j = 0, 1, 2 \quad .$$

It corresponds, with an error of $0(\epsilon^2)$, to a complete solution of the von Zeipel equation

$$f\left(\frac{\partial \Sigma}{\partial y_0}, \frac{\partial \Sigma}{\partial y_1}, \frac{\partial \Sigma}{\partial y_2}; y_0, y_1, y_2; \epsilon\right) = \phi\left(\xi_0, \xi_1, \xi_2; \frac{\partial \Sigma}{\partial \xi_1}, \frac{\partial \Sigma}{\partial \xi_2} \; ; \epsilon\right)$$

under the conditions

(a) $$\Sigma(\xi_0, \xi_1, \xi_2; y_0, y_1, y_2; 0) = \xi_0 y_0 + \xi_1 y_1 + \xi_2 y_2$$

and

(b) $$\frac{1}{2p\pi}\int_0^{2p\pi} \Sigma \, dy_0 = 0 \quad .$$

This function will not be determined, since it is not needed for the purpose of this work.

With the introduction of the Hamiltonian ϕ, the corresponding equations of motion give

$$\xi_0 = L^* - \frac{p}{q} H^* = \text{const} \tag{8}$$

and

$$\dot{\xi}_j = \frac{\partial \phi}{\partial \eta_j} \quad , \quad \dot{\eta}_j = -\frac{\partial \phi}{\partial \xi_j} \quad , \; (j = 1, 2) \quad ,$$

so that the new system has two degrees of freedom. The variable η_0 can be obtained by quadrature. For a fixed value of ϵ, the function ϕ can be evaluated numerically as a function of the five parameters $\xi_0, \xi_1, \xi_2, \eta_1$, and η_2.

In the second stage of solution, a new canonical transformation to the variables (X,Y) is introduced. It will be defined by a generating function $S(X_0, X_1, X_2; \eta_0, \eta_1, \eta_2; \epsilon)$ such that

$$\xi_j = \frac{\partial S}{\partial \eta_j}, \quad Y_j = \frac{\partial S}{\partial X_j}, \quad (j = 0, 1, 2) \quad ,$$

where

$$S(X_0, X_1, X_2; \eta_0, \eta_1, \eta_2; 0) = X_0\eta_0 + X_1\eta_1 + X_2\eta_2 = S_0 \quad .$$

Assuming further that both S and the new Hamiltonian F can be developed in power series of $\epsilon^{1/2}$, we can write

$$S = S_0 + S_{1/2} + S_1 + \ldots = S_0 + \epsilon^{1/2}\tilde{S}(X_0, X_1, X_2; \eta_1, \eta_2; \epsilon)$$

$$F = F_0 + F_{1/2} + F_1 + \ldots = F(X_0, X_1, X_2; Y_2; \epsilon) \quad ,$$

so that $X_0 = \xi_0$. The function S satisfies the von Zeipel equation

$$\phi\left(\frac{\partial S}{\partial \eta_0}, \frac{\partial S}{\partial \eta_1}, \frac{\partial S}{\partial \eta_2}; \eta_1, \eta_2; \epsilon\right) = F\left(X_0, X_1, X_2; \frac{\partial S}{\partial X_2}; \epsilon\right) \quad ,$$

where

$$F_0 = \phi_0 \Big|_{\xi = X} = \frac{1}{2}(X_0 + pX_1)^{-2} + qX_1 \quad .$$

The basic assumption for the solution of the above equation is that the derivative

$$\phi_0' = \frac{\partial \phi_0}{\partial \xi_1}\Bigg|_{\xi = X} = -p(X_0 + p X_1)^{-3} + q = q - pn^{**} \qquad (9)$$

is of the order of $\epsilon^{1/2}$ or higher. This is the width of the resonance region (Hori, 1960). The von Zeipel method gives for $S_{1/2}$ the equation

$$\phi_0' \frac{\partial S_{1/2}}{\partial \eta_1} + \frac{1}{2} \phi_0'' \left(\frac{\partial S_{1/2}}{\partial \eta_1}\right)^2 + \phi_1(X_0, X_1, X_2; \eta_1, \eta_2; \epsilon)$$

$$= F_1(X_0, X_1, X_2; \eta_2; \epsilon) \quad . \tag{10}$$

Further, since $\phi_{1/2} = 0$, $F_{1/2} = 0$.

The first-order part F_1 of the new Hamiltonian is defined by

$$F_1(X_0, X_1, X_2; Y_2; \epsilon) = \min_{\{\eta_1\}} \phi_1 \Big|_{\substack{\xi = X \\ \eta = Y}} \quad , \tag{11}$$

and $\eta_1^0 = \eta_1^0(\xi_0, \xi_1, \xi_2, \eta_2)$; that is, the point η_1^0 of minimum of ϕ_1 will, in general, be a function of $\xi_0, \xi_1, \xi_2, \eta_2$. If we now define

$$\tilde{\phi}_1 = \left(\phi_1 - \min_{\{\eta_1\}} \phi_1\right)\Big|_{\xi = X} = \tilde{\phi}_1(X_0, X_1, X_2; \eta_1, \eta_2) \quad ,$$

the function $S_{1/2}$ will satisfy the equation

$$\phi_0' \frac{\partial S_{1/2}}{\partial \eta_1} + \frac{1}{2} \phi_0'' \left(\frac{\partial S_{1/2}}{\partial \eta_{1/2}}\right)^2 + \tilde{\phi}_1(X_0, X_1, X_2; \eta_1, \eta_2) = 0 \quad ,$$

or

$$\frac{\partial S_{1/2}}{\partial \eta_1} = - \frac{\phi_0'}{\phi_0''} \pm \left[\left(\frac{\phi_0'}{\phi_0''}\right)^2 - 2 \frac{\tilde{\phi}_1}{\phi_0''}\right]^{1/2} \quad . \tag{12}$$

Since $S_{1/2}$ has to be real, the interval of variation of η_1 is defined. Moreover, the minimum of ϕ_1 with respect to η_1 is zero whatever η_2. There will be circulation or libration in η_1 if

$$\max_{\{\eta_1\}} \left(2 \frac{\phi_1}{\phi_0''} \right) \lesseqgtr \left(\frac{\phi_0'}{\phi_0''} \right)^2$$

for each value of η_2 and of the parameters X_0, X_1, X_2. Certainly, the function $\tilde{\phi}_1$ does not contain terms independent of η_1 in the sense that its Fourier representation will be

$$\tilde{\phi}_1 = \sum_{k_1 \neq 0} \sum_{k_2} a_{k_1, k_2} (X_0, X_1, X_2) \exp \left[\sqrt{-1} \left(k_1 \frac{\eta_1}{q} + k_2 \eta_2 \right) \right] .$$

In the circulation case, equation (12), with the choice of only one of the signs, defines $S_{1/2}$. In the libration case, $S_{1/2}$ is a two-valued function of η_1, the sign changing at every end point of the libration interval.

With an error of the order of $\epsilon^{3/2}$, the new Hamiltonian is

$$F = F_0 (X_0, X_1) + F_1 (X_0, X_1, X_2; Y_2; \epsilon) \quad . \tag{13}$$

Along any solution of the differential system generated by the original Hamiltonian, F differs from a constant by a quantity of the order of $\epsilon^{3/2}$ and generates the one-dimensional dynamical system

$$\dot{X}_2 = \frac{\partial F}{\partial Y_2} \quad , \quad \dot{Y}_2 = - \frac{\partial F}{\partial X_2} \quad . \tag{14}$$

On the other hand,

$$X_1 = \frac{H^{**}}{q} = \text{const} \tag{15}$$

and

$$X_0 = \xi_0 = L^{**} - \frac{p}{q} H^{**} = L^{*} - \frac{p}{q} H^{*} = \text{const} \quad . \tag{16}$$

It follows that H^{**} and L^{**} are constant, or in terms of Keplerian "mean mean elements,"

$$a^{**} = \text{const} \quad , \tag{17}$$

$$(1 - e^{**2})^{1/2} \cos I^{**} = C = \text{const} \quad . \tag{18}$$

The definitions of a^{**}, e^{**}, and I^{**} are

$$a^{**} = L^{**2} = (X_0 + p X_1)^2 \tag{19}$$

$$n^{**2} \, a^{**3} = 1$$

$$(1 - e^{**2}) \, a^{**} = G^{**2} = (X_0 + p X_1 - X_2)^2$$

$$\cos I^{**} = \frac{H^{**}}{G^{**}} = \frac{q X_1}{X_0 + p X_1 - X_2} \quad . \tag{20}$$

3. CHARACTERISTICS OF SECULAR MOTION

With an error of $O(\epsilon)$, we are able to develop the general features of the secular motion as follows. We have

$$L^* = \xi_0 + p\,\xi_1 = \xi_0 + p\left(X_1 + \frac{\partial S_{1/2}}{\partial \eta_1}\right) + O(\epsilon)$$

$$= \xi_0 + pX_1 + p\frac{\partial S_{1/2}}{\partial \eta_1} + O(\epsilon) = L^{**} + p\frac{\partial S_{1/2}}{\partial \eta_1} + O(\epsilon) \quad ,$$

so that

$$a^* = L^{*2} = \left(a^{**1/2} + p\frac{\partial S_{1/2}}{\partial \eta_1}\right)^2 + O(\epsilon)$$

$$a^* = a^{**} + 2pa^{**1/2}\frac{\partial S_{1/2}}{\partial \eta_1} + O(\epsilon) \quad . \tag{21}$$

Making use of equation (19), we have

$$\phi_0' = -\,pn^{**} + q = -\,pa^{**-3/2} + q$$

and

$$\phi_0'' = 3p^2\,(X_0 + pX_1)^{-4} = \frac{3p^2}{a^{**2}} \quad .$$

Equation (21) and the definition of $S_{1/2}$ give

$$a^* = a_0^* \pm \Delta a^* \quad , \tag{22}$$

where

$$a_0^* = \frac{5}{3} a^{**} \left(1 - \frac{2q}{5p} a^{**3/2}\right) \tag{23}$$

and

$$\Delta a^* = 2pa^{**1/2} \left[\frac{a^{**4}}{9p^4} (pa^{**-3/2} - q)^2 - \frac{**2}{3\,p^2} \tilde{\Phi}_1 (X_0, X_1, X_2; Y_1, Y_2) \right]^{1/2} . \tag{24}$$

It follows that in the libration case the mean semimajor axis (averaged over short-period perturbations) will oscillate around the value a_0^*. Note that if $n^{**} = q/p$, the value of a_0^* is equal to a^{**}, which is the mean mean semimajor axis corresponding to exact resonance. Further, the value of a_0^* can never be zero and will always be larger than the maximum value of Δa^*. On the other hand, by definition $\tilde{\Phi}_1$ is always nonnegative, so that the maximum value of Δa^* corresponds to $Y_1 = \eta_1^0(X_0, X_1, X_2; Y_2)$, which gives $\tilde{\phi}_1 = 0$. Therefore,

$$\max \Delta a^* = \frac{2a^{**5/2}}{3p} (pn^{**} - q) = O(\epsilon^{1/2}) \quad . \tag{25}$$

We conclude that long-period perturbations on the semimajor axis are of the order of $\epsilon^{1/2}$, larger than the values expected in the nonresonance case. We also see that a^* is affected by two very different periods associated with Y_1 and Y_2. From the equations

$$\dot{Y}_1 = -\frac{\partial F}{\partial X_1} = pn^{**} - q + O(\epsilon) = O(\epsilon^{1/2}) \tag{26}$$

and

$$\dot{Y}_2 = -\frac{\partial F}{\partial X_2} = O(\epsilon) \quad , \tag{26}$$

it follows that the period corresponding to Y_2 is larger than that corresponding to Y_1; that is,

$$T_2 = O(\epsilon^{-1}) > T_1 = O(\epsilon^{-1/2}) \quad .$$

The amplitude Δa^* is associated with T_1, since the maximum of Δa^* is reached when $Y_1 = \eta_1^0$ (libration case).

By definition, if the angle Y_1 undergoes a libration process, Δa^* will be zero at the end points of this libration. The end points correspond to the maximum and minimum values Y_1 can reach in order to result in a real $S_{1/2}$.

If $\overline{Y}_1$ is the mean value of Y_1 and δ is the semiamplitude of libration, then Δa^* will be zero at $\overline{Y}_1 \pm \delta$. It can be expected that if the influence of Y_2 in η_1^0 is not very strong, then $\overline{Y}_1 = \eta_1^0$ approximately. When Y_1 is maximum or minimum, Δa^* is zero; therefore, there will be a constant phase shift between the oscillations of Y_1 and a^* in time.

With respect to e^{**} and I^{**}, as a consequence of equation (18) we see that when e^{**} increases, I^{**} decreases, and vice versa. Since these two elements are affected by the long period T_2, in general their secular motions will have such a period. It is also possible to show that the perturbations on a are larger than those on e and I. In fact,

$$x_0 = X_0 + \frac{\partial \Sigma}{\partial y_0} = X_0 + O(\epsilon)$$

$$x_1 = X_1 + \frac{\partial \Sigma}{\partial y_1} + \frac{\partial S_{1/2}}{\partial \eta_1} = X_1 + O(\epsilon^{1/2})$$

$$x_2 = X_2 + \frac{\partial \Sigma}{\partial y_2} + \frac{\partial S_{1/2}}{\partial \eta_2} = X_2 + O(\epsilon^{1/2}) \quad ,$$

so that

$$L - \frac{p}{q}H = L^{**} - \frac{p}{q}H^{**} + O(\epsilon)$$

$$H = H^{**} + O(\epsilon^{1/2})$$

$$G - H = G^{**} - H^{**} + O(\epsilon^{1/2})$$

or

$$\dot{L} - \frac{p}{q}\dot{H} = O(\epsilon)$$

$$\frac{p}{q}\dot{H} = O(\epsilon^{1/2})$$

$$\dot{G} - \dot{H} = \dot{G}^{**} + O(\epsilon^{1/2}) = O(\epsilon^{1/2}) \quad ;$$

finally, $\dot{a}$ is $O(\epsilon^{1/2})$ and $\dot{e}$, $\dot{I}$ are $O(\epsilon)$. We conclude that the perturbations in the eccentricity and inclination are relatively smaller than are the perturbations in the semimajor axis. If perturbations of $O(\epsilon)$ are neglected as compared with those of $O(\epsilon^{1/2})$, we obtain

$$Y_0 = n^{**} t + Y_{00}$$

$$Y_1 = (pn^{**} - q) t + Y_{10}$$

$$Y_2 = Y_{20} \quad , \tag{27}$$

and X_0, X_1, X_2 are constant. The mean elements (averaged over short-period perturbations, which are of $O(\epsilon)$) will be given by

$$\xi_0 = X_0, \; \xi_1 = X_1 + \frac{\partial S_{1/2}}{\partial \eta_1}, \; \xi_2 = X_2 + \frac{\partial S_{1/2}}{\partial \eta_2} \quad ,$$

$$\eta_0 = n^{**} t + Y_{00} - \frac{\partial S_{1/2}}{\partial X_0} \quad ,$$

$$\eta_1 = (pn^{**} - q)t + Y_{10} - \frac{\partial S_{1/2}}{\partial X_1} \quad ,$$

$$\eta_2 = Y_{20} - \frac{\partial S_{1/2}}{\partial X_2} \quad , \tag{28}$$

where in the right-hand members the variables η_1, η_2 can be substituted by Y_1, Y_2. This is the complete solution, with an error of $O(\epsilon)$, since $S_{1/2}$ is a known function. In the circulation case it can be defined as

$$S_{1/2} = \int_0^{\eta_1} \frac{\partial S_{1/2}}{\partial \eta_1} \, d\eta_1 \quad ; \tag{29}$$

and in the libration case,

$$S_{1/2} = \int_{\eta_1^0}^{\eta_1} \frac{\partial S_{1/2}}{\partial \eta_1} \, d\eta_1 \quad , \tag{30}$$

where η_1^0 is a function of X_0, X_1, X_2, and η_2. The choice of a plus or a minus sign in equation (12) depends on the variable η_1 being in the interval $\overline{Y}_1 - \delta = \eta_1^0 < \eta_1 \leq \overline{Y}_1 + \delta$ or $\overline{Y}_1 - \delta \leq \eta_1 \leq \eta_1^0 = \overline{Y}_1 + \delta$, respectively.

4. MOTION OF PERIHELION

The final stage of solution corresponds to the analysis of the one-dimensional system generated by the Hamiltonian as defined by equation (12); that is,

$$F = F_0(X_0, X_1) + F_1(X_0, X_1, X_2; Y_2; \epsilon) + O(\epsilon^{3/2}) \quad .$$

Since X_0 and X_1 are constants, it follows that, neglecting terms of $O(\epsilon^{3/2})$, we have F_1 = const or, according to equations (6) and (11),

$$\int_0^{2p\pi} \frac{1}{\Delta} dy_0 \Bigg|_{\substack{x = X \\ y_1 = \eta_{10}(X; Y_2) \\ y_2 = Y_2}} = D^* = \text{const} \quad , \tag{31}$$

where x and X stand for (x_0, x_1, x_2) and (X_0, X_1, X_2), respectively. Moreover, X_0 and X_1 are constants. The value $y_1 = \eta_1^0 (X_0, X_1, X_2; Y_2)$ is defined by the minimum point of D with respect to η_1 for every value of η_2, ξ_0, ξ_1, ξ_2 or, within our precision, with respect to Y_1 for every value of Y_2, X_0, X_1, X_2. Both η_{10} and D^* can be determined numerically, and the final outcome for fixed values of X_0 and X_1 will be the function $D^* = D^* (X_2, Y_2)$, which is independent of the particular value of ϵ. A plot of D^* = const in the plane (X_2, Y_2) will therefore show the long-range behavior of perihelion and eccentricity. For a fixed value of a^{**}, the parameters we are left with are e^{**} and I^{**}. Since these elements are related by equation (17), fixing the value of C will produce curves of D^* as functions of $Y_2 = \omega^{**}$ with the only parameter e^{**}. From this one-parameter family of curves, we can construct D^* = const curves in the plane (ω^{**}, e^{**}). Such a plot immediately gives the libration or circulation character of ω^{**}, which appears to be independent of ϵ.

The scaling of the mathematical model with the actual motion of an asteroid depends essentially on a set of observed values during a time not shorter then the period T_1. Both the libration (or circulation) characteristics of Y_1 and the amplitude of oscillation of a^*, Δa^*, will allow the determination of a^{**}. The constant C and a pair of values (e^{**}, ω^{**}) will identify the particular $D^* = \text{const}$ curve, that is, the libration or circulation processes in Y_2 together with the ranges of variation of e^{**} and I^{**}. With the value of a^{**}, the more important part $(pn^{**} - q)$ of the mean motion of Y_1 can be found, that is, its period, which should be compared with the observed value. In order to evaluate the period of Y_2, we can use the equation

$$\dot{X}_2 = \frac{\partial F}{\partial Y_2} = \frac{\partial F_1}{\partial Y_2} = \epsilon \frac{\partial D^*}{\partial Y_2}(X_0, X_1, X_2; Y_2) \quad . \tag{32}$$

If we construct a curve of $1/\epsilon\ (\partial D^*/\partial Y_2)^{-1}$ versus X_2 from $X_2(\text{min})$ to $X_2(\text{max})$, the area under this curve will immediately give half the period in Y_2. Of course, in the construction of the right-hand member of equation (32), the relation between Y_2 and X_2 must be obtained from the corresponding $D^* = \text{const}$ curve, while X_0 and X_1 are kept constant.

5. THE TROJAN GROUP

When $p = q = 1$ (exact resonance) and $I = e = 0$, the corresponding solutions are the Lagrangian triangular equilibrium points. The general problem of totality of motions in the vicinity of this 1/1 resonance case has been chosen as an example of the general theory described in the previous sections.

For $a = 1$, the disturbing function $1/\Delta$ (equation (2)) was averaged numerically with the use of the parameters C, e, y_1, and y_2 in the following ranges:

$$C = 0.1\ (0.1)\ 0.9$$

$$e = 0.01\ (0.01)\ 0.99$$

$$y_1 = 0^\circ\ (15^\circ)\ 180^\circ$$

$$y_2 = 0^\circ\ (15^\circ)\ 180^\circ \quad .$$

The result is the function $D(\xi_0, \xi_1, \xi_2; \eta_1, \eta_2)$, given by

$$D = \frac{1}{2\pi} \int_0^{2\pi} \frac{1}{\Delta}\, dy_0$$

according to equation (7). With the use of C, e, and y_2 as parameters, the function D has been plotted versus η_1, as shown in Figures 1 through 36. The function D is related to ϕ_1 by equation (7). These figures show that whatever the values of the parameters, the variable η_1 undergoes a libration process. The amplitude of libration depends strongly on the values of C, e, and y_2. It must be noted that since a^* is not a constant at this stage, the function D is not constant through the motion. Within the precision of the theory, the constant Hamiltonian is the complete function ϕ by equation (6).

The second stage of solution is the determination of F_1 (equation (11)), which we do by inspection, determining the minimum value of D for every value of C, e, and y_2 with respect to η_1 and the point of minimum η_1^0 (C, e, y_2). From Figures 1 to 36 we see that for small eccentricities the minimum is attained close to $\eta_1 = 60°$. As the eccentricity increases, the minimum shifts to or near $\eta_1 = 0°$. Therefore, the maximum deviation of the mean semimajor axis a^* from the mean value a_0^* is reached around $\eta_1 = 60°$ for orbits of small eccentricity and around $\eta_1 = 0°$ for highly eccentric orbits. Moreover, since η_1 measures the mean elongation between Jupiter and the asteroid, for $\eta_1 = 0$ and $e = 0$ the disturbing function is discontinuous, while for $\eta_1 = 60°$ and $e = 0$ the minimum is at exactly 60°, which defines the Lagrangian equilibrium points ($\eta_1 = 60°$ or $60° + 180°$).

Once we have the minimum of ϕ_1 for every C, e, and y_2, we can produce a plot of F_1 (equation (11)), or actually of the minimum D^* of D, since at this stage a^{**} is constant. The basic parameter for this plot is C from 0.1 to 0.9 by steps of 0.1. Figures 37 to 45 show the function D^* plotted against Y_2 for every C by use of e as a parameter. Furthermore, since D^* is constant because a^{**} is constant, any line in these graphs drawn parallel to the Y_2 axis will define the variation of e as a function of ω along an orbit.

In order to make evident the character of motion of the perihelion, we redrew the previous graphs, using C as the main parameter and plotting curves $D^* =$ const in the plane (ω, e). Figures 46 to 54 show such isoenergetic curves. In the interval (0, π) of y_2, we find a libration center and a saddle point for every value of C from 0.1 to 0.9. The libration center remains close to $\omega = 135°$, and the corresponding eccentricity increases from 0.29 to 0.40 as C increases from 0.1 to 0.9, while the "energy" constant D^* decreases from 0.722 to 0.670 and then increases again to 0.744. The location of the saddle point is always around $\omega = 30°$, and the corresponding eccentricity increases from 0 to 0.40. When the constant C goes above the value 0.7, there is a shift of the saddle point that reaches $\omega = 90°$ at $C = 0.9$. The energy constant D^* decreases from 0.632 to 0.551 and then increases to 0.727.

However, for C larger than 0.2 and smaller than 0.8 another pair of libration center and saddle point appears in the picture. This new libration center is at $\omega = 90°$ and corresponds to highly eccentric orbits. For such centers the eccentricity decreases from 0.94 to 0.71 as C increases from 0.3 to 0.7. The corresponding energy constant D^* decreases from 0.214 to 0.172 and then increases to 0.212 for $C = 0.7$. The overall mechanism appears to be a shifting of stable points into unstable ones, which goes through a complex phase space configuration for intermediate values of C. We note, however, that all numbers shown are only approximate, so that a very fine structure of the system may be completely missing. In any event, the two parallel lines at $e = 0$ and $e = e_{max}$ (which is defined by C) always correspond to asymptotic motion from or toward unstable configurations. Moreover, for all values of C, according to the value of the energy constant D^*, which is defined by a pair (ω, e), the variable ω may undergo libration or circulation.

Table 1 shows the above description in a condensed form. The position of an actual situation in the described totality of motions requires a certain amount of information from observations or numerical integration. Such information should cover a time at least equal to the period of libration in y_1. If we know the actual value of the ratio $(\max \Delta a^*)/a_0^*$, this will allow the computation of the integration constant a^{**} by equations (23) and (25). An approximate value can be obtained by interpolation. Table 2 shows the relation between n^{**} and $(\max \Delta a^*)/a_0^*$ within the region of resonance for $\epsilon = 10^{-3}$, that is, for $|n^{**} - 1| \le \epsilon^{1/2} \simeq 0.035$.

The value of a^{**} thus found determines the mean mean motion n^{**} of the asteroid. We note, however, that, as seen from Table 2, for one value of $\Delta a^* / a_0^*$ there are two values of n^{**} (or a^{**}) satisfying that value. Such a double determination must be eliminated by a reference once more to the observed secular trend of Y_0 or Y_1 (direct or retrograde motion). If the amplitude of libration of η_1 is known, the function $S_{1/2}$ can now be determined, as can the perturbations of long period T_1. The value of D^* that defines the evolution of e^{**} and ω^{**} along an orbit over the longest period T_2 is defined by a pair of such elements at some epoch, given by observations or numerical integration.

The last information given by the theory is the long period T_2 (of libration or circulation) of the mean mean argument of perihelion. Since the orbit in the (ω^{**}, e^{**}) plane is defined, the function $e^{**} = e^{**}(\omega^{**})$ is known together with the values of a^{**} and C. Equation (32) and the method developed there can therefore be applied.

Table 1. Location of stable and unstable points in the (ω, e) plane

C	e_{max}	ω (libration center)	D^*	e	ω (saddle point)	D^*	e	ω (additional libration center)	D^*	e
0.1	0.99	135°	0.722	0.29	30°	0.632	0	–	–	–
0.2	0.98	135°	0.701	0.29	30°	0.609	0	–	–	–
0.3	0.96	135°	0.685	0.29	27°	0.586	0	90°	0.214	0.94
0.4	0.92	130°	0.675	0.29	28°	0.566	0	90°	0.187	0.89
0.5	0.87	143°	0.670	0.32	30°	0.552	0.26	90°	0.172	0.84
0.6	0.81	140°	0.672	0.32	30°	0.551	0.31	90°	0.176	0.78
0.7	0.72	143°	0.688	0.34	30°	0.519	0.36	90°	0.212	0.71
0.8	0.61	165°	0.703	0.39	45°	0.640	0.38	–	–	–
0.9	0.44	135°	0.744	0.40	90°	0.727	0.40	–	–	–

Table 2. Maximum relative oscillation of mean mean semimajor axis

n^{**}	a^{**}	a_0^*	$\lvert \max \Delta a^* \rvert$	$\frac{\lvert \max \Delta a^* \rvert}{a_0^*}$	Orbits
0.965	1.02404	0.999275	0.0247608	0.0247788	
0.070	1.02051	0.999472	0.0210415	0.0210526	
0.075	1.01702	0.999637	0.0173850	0.0173913	($\phi_0' > 0$, retrograde)
0.080	1.01356	0.999770	0.0137899	0.0137931	
0.085	1.01013	0.999872	0.0102551	0.0102564	
0.090	1.00672	0.999943	0.00677928	0.00677966	
0.095	1.00335	0.999986	0.00336130	0.00336134	
1.000	1.000	1.000	0.000	0.000	($\phi_0' = 0$, equilibrium)
0.005	0.996680	0.999986	0.00330574	0.00330579	
0.010	0.993388	0.999945	0.00655702	0.00655738	
0.015	0.990123	0.999878	0.00975491	0.00915610	
0.020	0.986885	0.999785	0.0129005	0.0129032	($\phi_0' < 0$, direct)
0.025	0.983673	0.999668	0.0159947	0.0160000	
0.030	0.980487	0.999526	0.0190386	0.0190476	
0.035	0.977327	0.999360	0.0220331	0.0220472	

6. HIGHER ORDER SOLUTION

We are left with the question of whether or not the process of solution can be extended to higher orders of approximation. The next step would correspond to von Zeipel's equation

$$\left(\phi_0' + \phi_0'' \frac{\partial S_{1/2}}{\partial \eta_1}\right) \frac{\partial S_1}{\partial \eta_1} + \frac{1}{6} \phi_0''' \left(\frac{\partial S_{1/2}}{\partial \eta_1}\right)^3 + \frac{\partial \phi_1}{\partial X_1} \frac{\partial S_{1/2}}{\partial \eta_1} + \frac{\partial \phi_1}{\partial X_2} \frac{\partial S_{1/2}}{\partial \eta_2}$$

$$= F_{3/2}(X_0, X_1, X_2; \eta_2; \epsilon) + \frac{\partial F_1}{\partial \eta_2} \frac{\partial S_{1/2}}{\partial X_2} \quad , \qquad (33)$$

where the functions S_1 and $F_{3/2}$ have to be determined. In the first-order ($\epsilon^{1/2}$) solution, equation (10) was solved with F_1 defined as the minimum of ϕ_1 with respect to η_1; this resulted in a stable equilibrium solution at $Y_1 = \eta_1^0 (X_0, X_1, X_2; Y_2)$. For such a condition to be satisfied as the order increases to $\epsilon^{3/2}$, we should define (Hori, 1967, private communication)

$$F_{3/2} = \left[\frac{1}{6} \phi_0''' \left(\frac{\partial S_{1/2}}{\partial \eta_1}\right)^3 + \frac{\partial \phi_1}{\partial X_1} \frac{\partial S_{1/2}}{\partial \eta_1} + \frac{\partial \phi_1}{\partial X_2} \frac{\partial S_{1/2}}{\partial \eta_2} - \frac{\partial F_1}{\partial \eta_2} \frac{\partial S_{1/2}}{\partial X_2}\right]_{\eta_1 = \eta_1^0 \pm \delta} ; \qquad (34)$$

but for this definition to be consistent, we have to prove that the quantity in brackets takes the same values at the two end points of the libration in η_1. This is true, of course, for $\partial S_{1/2}/\partial \eta_1$. But for all other terms, the verification of such an hypothesis is not trivial. Assuming moderate eccentricity and inclination, since at the end points of the libration in η_1 the semimajor axis a^* is not unity, at those points we might be able to have a valid representation of the disturbing function by the classical development. Neglecting terms of the fifth order in the eccentricity and in the sine of the inclination, we have (Brouwer and Clemence, 1961):

$$\phi_1 = \epsilon a^{*2} R_2 + \frac{\epsilon^*}{a^*} \quad , \tag{35}$$

where $a^* < 1$ and

$$\begin{aligned}
R_2 = \sum_{-\infty}^{+\infty} \Bigg\{ & \Bigg[\frac{1}{2} A_j^* + \frac{1}{8} e^{*2} \left(-4 j^2 + 2\alpha^* D_{\alpha^*} + \alpha^{*2} D^2_{\alpha^*} \right) A_j^* \\
& - \frac{1}{4} \sigma^{*2} (B^*_{j-1} + B^*_{j+1}) - \frac{1}{16} e^{*2} \sigma^{*2} \quad -4j^2 + 2\alpha^* D_{\alpha^*} \\
& + \alpha^{*2} D^2_{\alpha^*} \; (B^*_{j-1} + B^*_{j+1}) + \frac{1}{128} e^{*4} \Big(16 j^4 - 9 j^2 - 8 j^2 \alpha^* D_{\alpha^*} \\
& - 8 j^2 \alpha^{*2} D^2_{\alpha^*} + 4 \alpha^{*3} D_{\alpha^{*3}} + \alpha^{*4} D^4_{\alpha^*} \Big) A_j^* \Bigg] \cos j\eta_1 \\
& + \left[\frac{1}{16} e^{*2} \sigma^{*2} \Big(4j^2 - 3j - 1 - (4j - 2) \alpha^* D_{\alpha^*} + \alpha^{*2} D^2_{\alpha^*} \Big) B_j \right] \\
& \cdot \cos \left[(j + 1) \eta_1 - 2\eta_2 \right] \Bigg\} \quad ;
\end{aligned}$$

here,

$$\sigma^{*2} = \sin^2 \frac{I^*}{2}$$

$$\alpha^* = a^*$$

$$D^n_{\alpha^*} = \frac{\partial^n}{\partial \alpha^{*n}}$$

and

$$A_j = b^j_{-1/2} (\alpha^*)$$

$$B_j = b^j_{-3/2} (\alpha^*)$$

are the usual Laplace coefficients. By use of the above expansion and its reciprocal for $a^* > 1$, it seems possible to show that, in fact, the definition contained in equation (34) is meaningful. Such a proof, nevertheless, must be considered with much care, since expression (35) is only a crude approximation for the function ϕ_1.

Even if such a proof could be achieved in its full generality, we would still wonder whether or not the process could be continued up to any order of approximation. Even then, the last question remains — are the formal series thus obtained convergent ? In part, we can answer the question of the validity of such a solution by comparing its results with observations or by numerical integration. As we have already mentioned, such verification has been very good indeed in the problem of the motion of Pluto (Hori and Giacaglia, 1965); we hope it will be equally good in the 1/1 rational case.

ACKNOWLEDGMENTS

Part of the numerical work was performed on the IBM 7040-7094 of the Yale Computer Center, supported by contracts NGR 07-004-049 from the National Aeronautics and Space Administration and NONR 609(50) from the Office of Naval Research to Yale University. The final part of the numerical study was completed on the IBM 1620D of the University of São Paulo and supported by the Office of Naval Research contract N000 14-67-C-0347. For the analysis of the numerical results, I am indebted to Dr. Eric Guy de Montille and Mr. Felix Wąckrat of the Observatory of the University of São Paulo.

REFERENCES

ARNOLD, V. I.

1963. Stability and instability in classical mechanics. Usp. Math. Nauk U.S.S.R., vol. 18, no. 5, pp. 13-40; no. 6, pp. 91-192.

BROUWER, D. and CLEMENCE, G. H.

1961. Methods of Celestial Mechanics. Academic Press, New York, 598 pp.

COHEN, C. J. and HUBBARD, E. C.

1965. Libration of the close approaches of Pluto to Neptune. Astron. Journ., vol. 70, pp. 10-13.

COHEN, C. J., HUBBARD, E. C., and OESTERWINTER, C.

1967. New orbit for Pluto and analysis of differential corrections. Astron. Journ., vol. 72, pp. 973-988.

GIACAGLIA, G. E. O.

1967. Sistemas dinâmicos não integráveis. Publ. Inst. Astron. Geophys. Univ. São Paulo, no. 4, 171 pp., São Paulo, Brazil.

HORI, G.

1960. The motion of an artificial satellite in the vicinity of the critical inclination. Astron. Journ., vol. 65, pp. 291-300.

HORI, G. and GIACAGLIA, G. E. O.

1965. Secular perturbations of Pluto (unpublished).

MOSER, J.

1967. Convergent series expansions for quasi-periodic motions. Math. Ann., vol. 169, pp. 136-176.

SZEBEHELY, V.

1967. Theory of Orbits — The Restricted Problem of Three Bodies. Academic Press, New York, 668 pp.

Figures 1-36.

Averaged disturbing function over short-periodic perturbations.

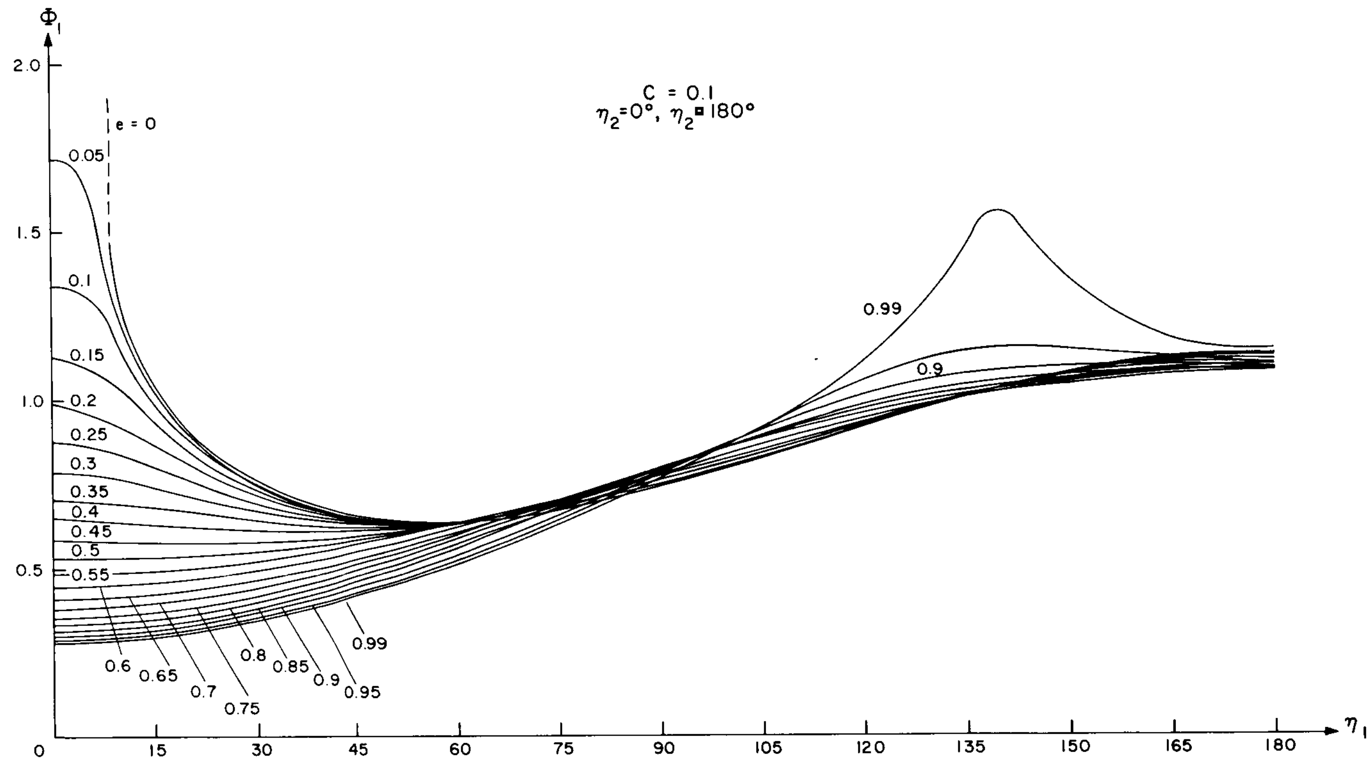

Figure 1.

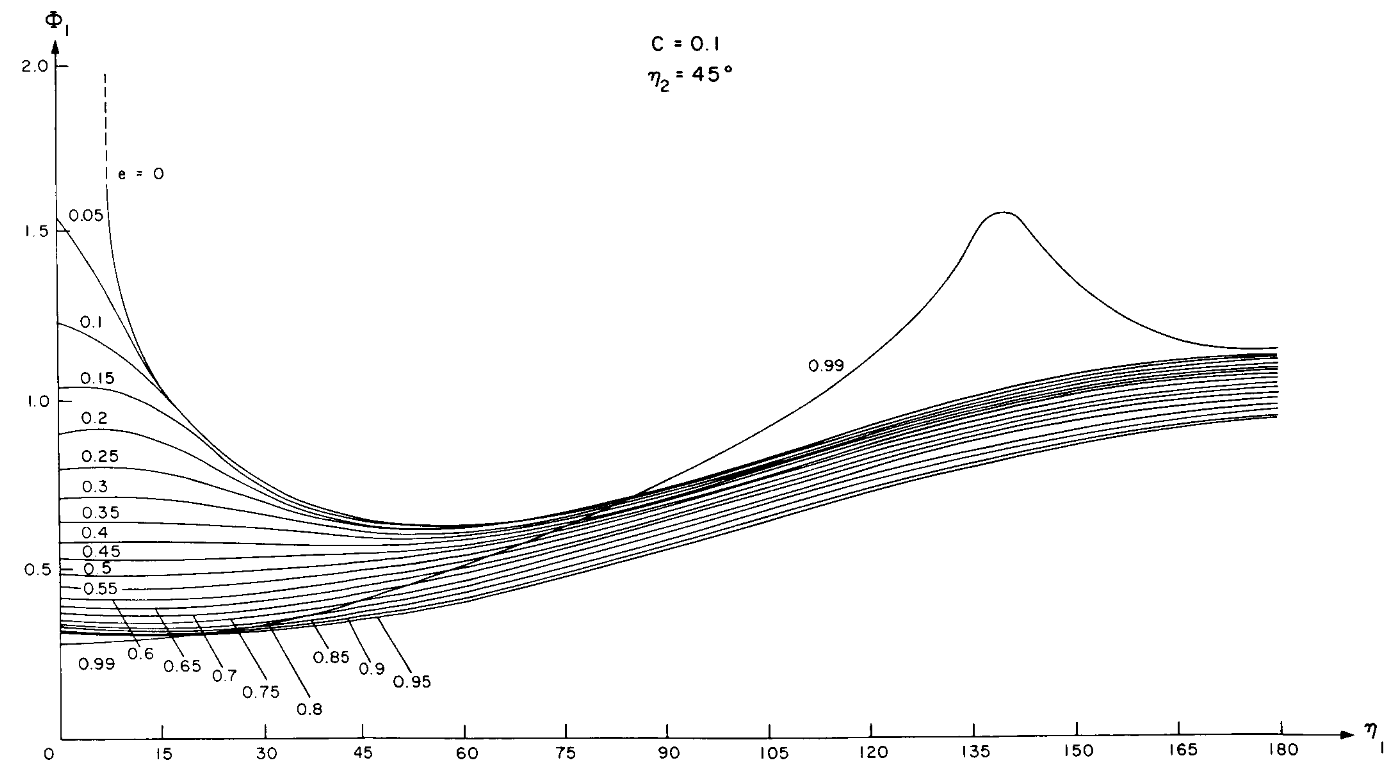

Figure 2.

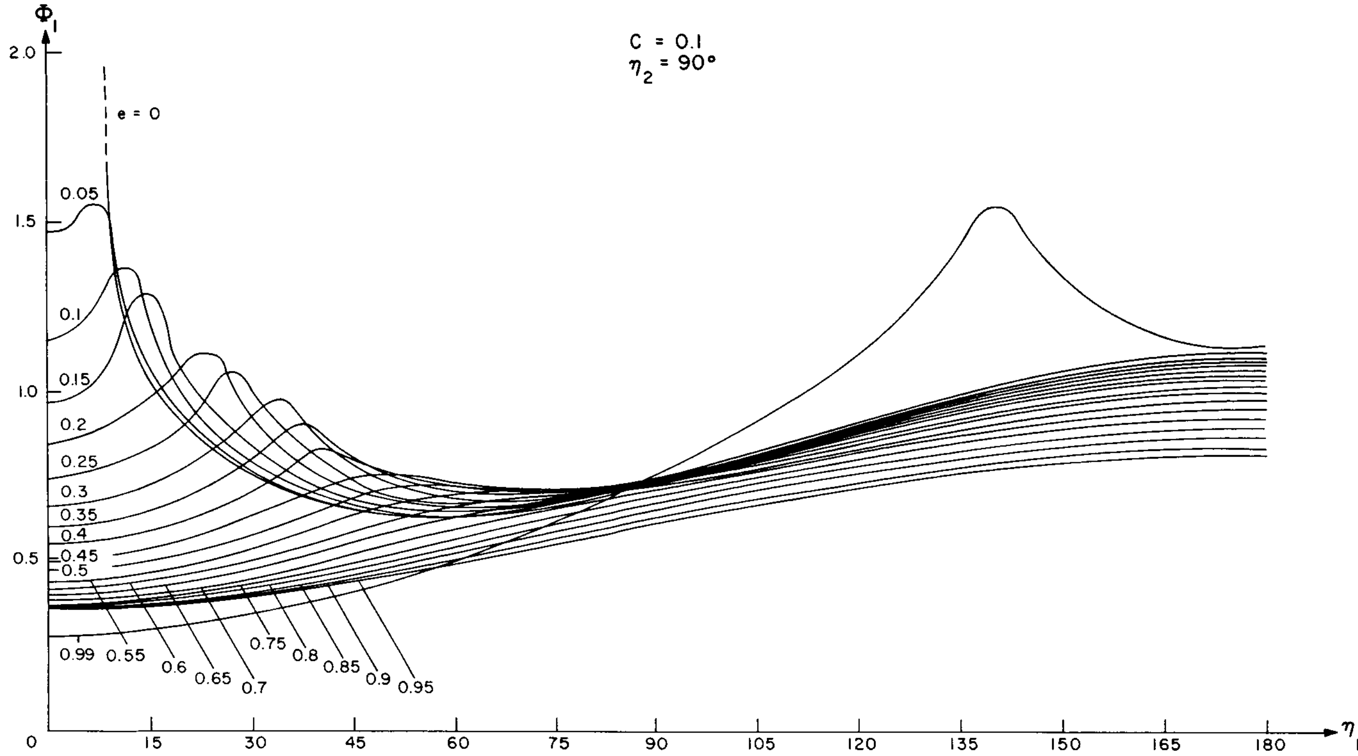

Figure 3.

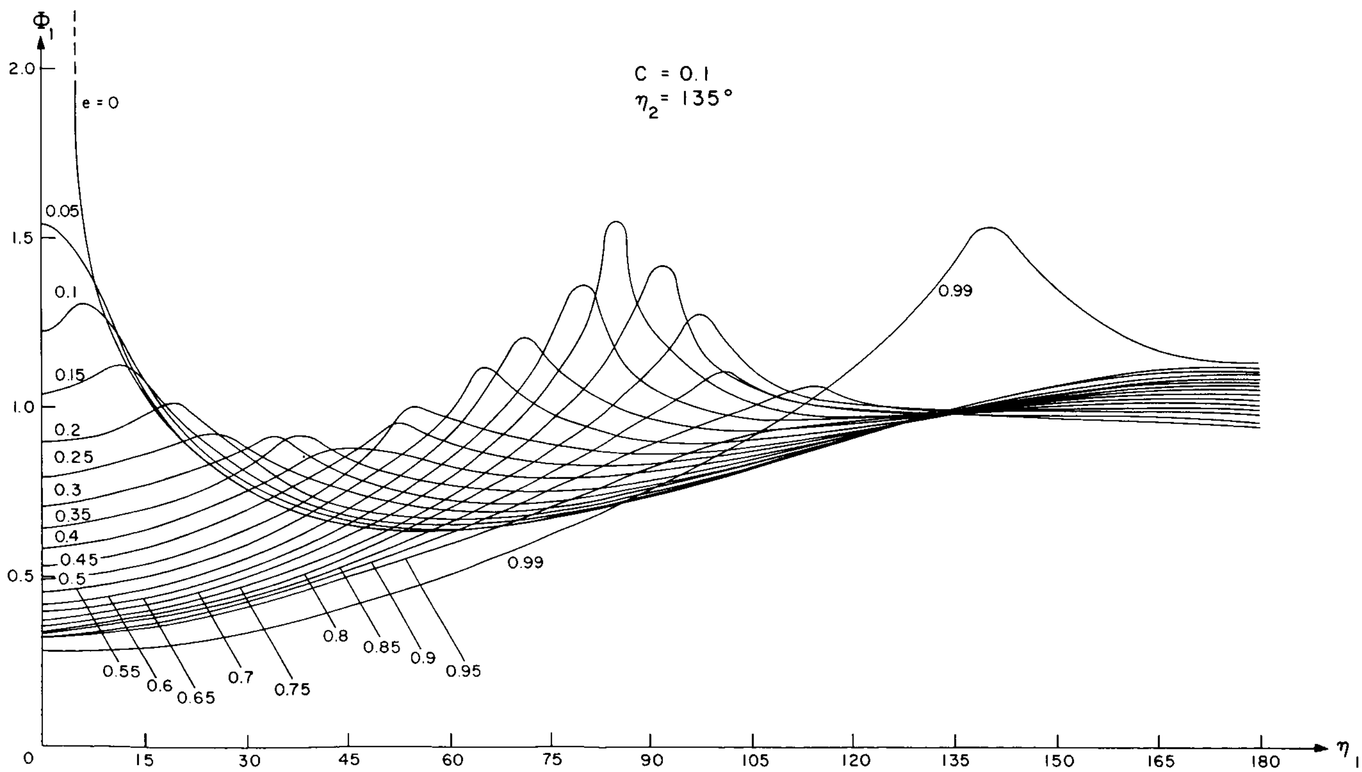

Figure 4.

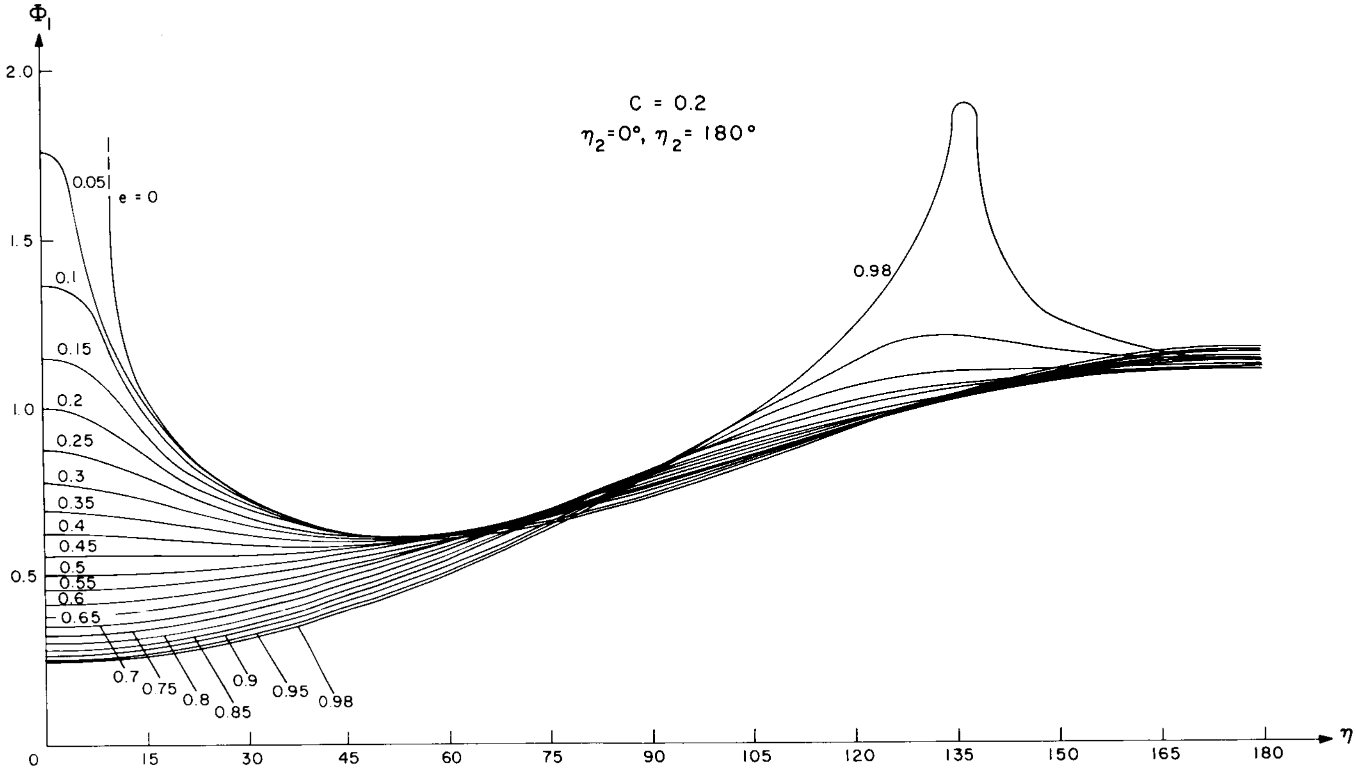

Figure 5.

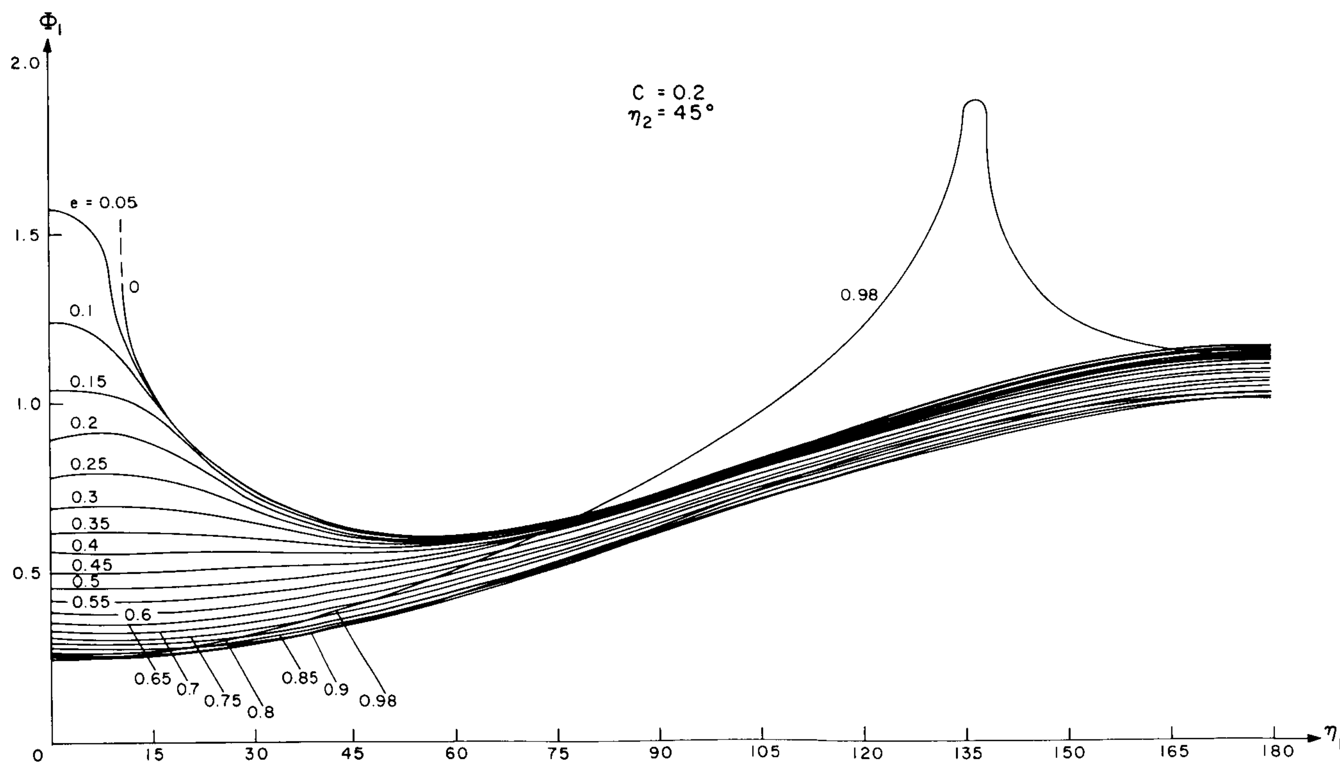

Figure 6.

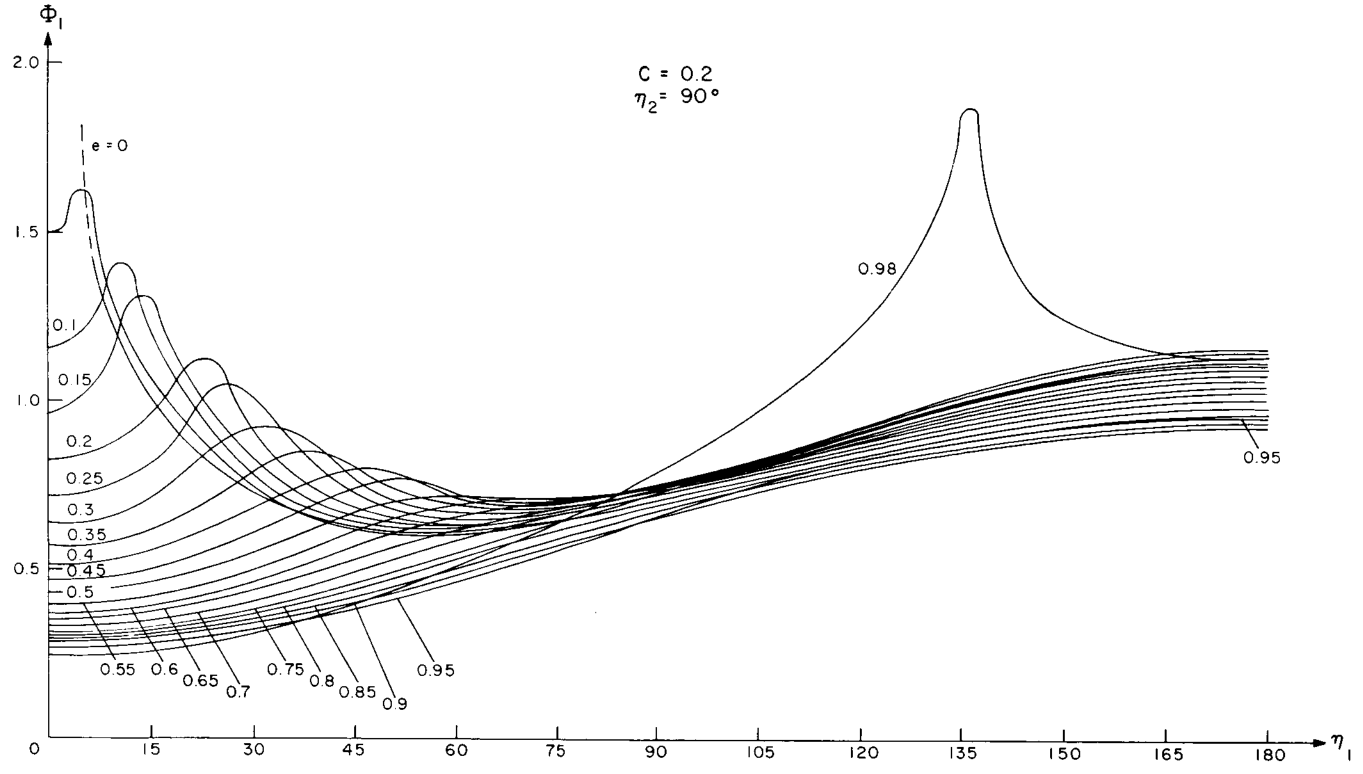

Figure 7.

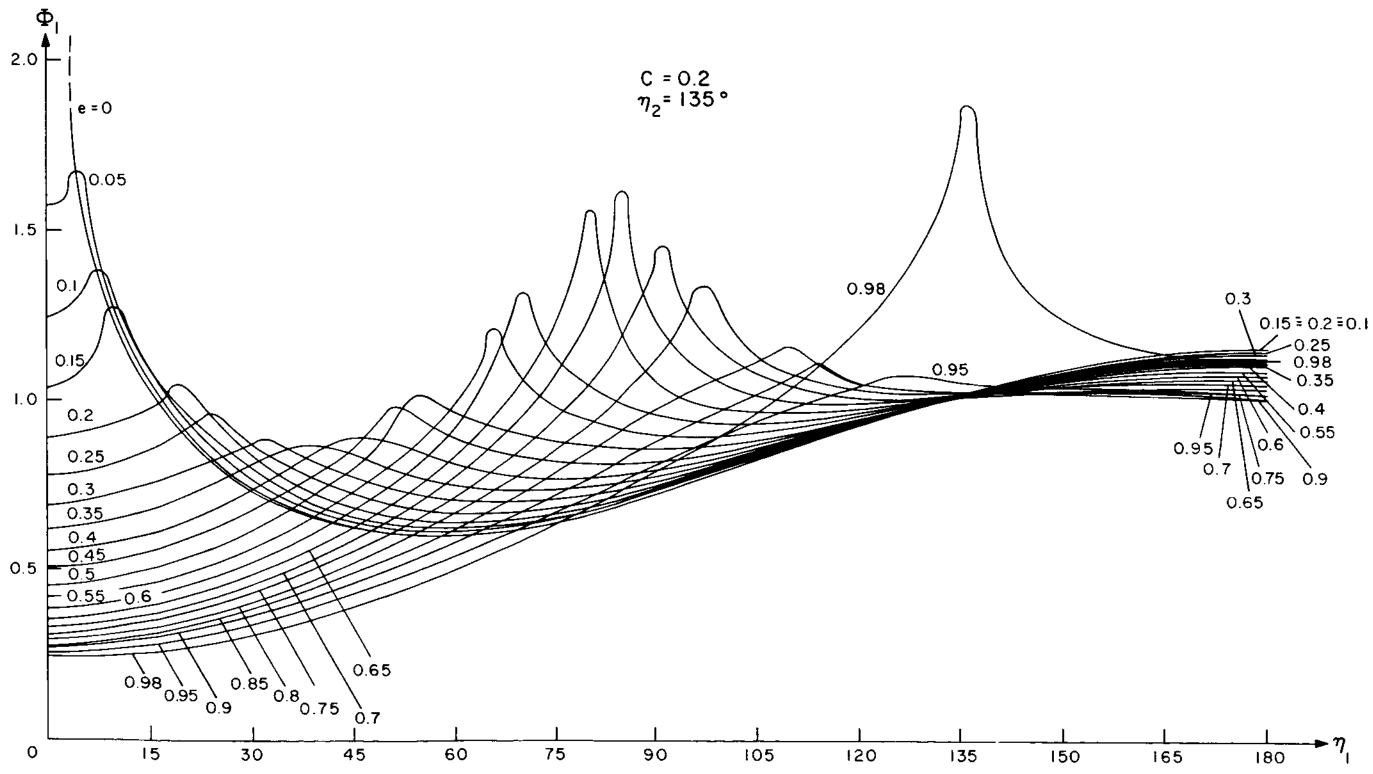

Figure 8.

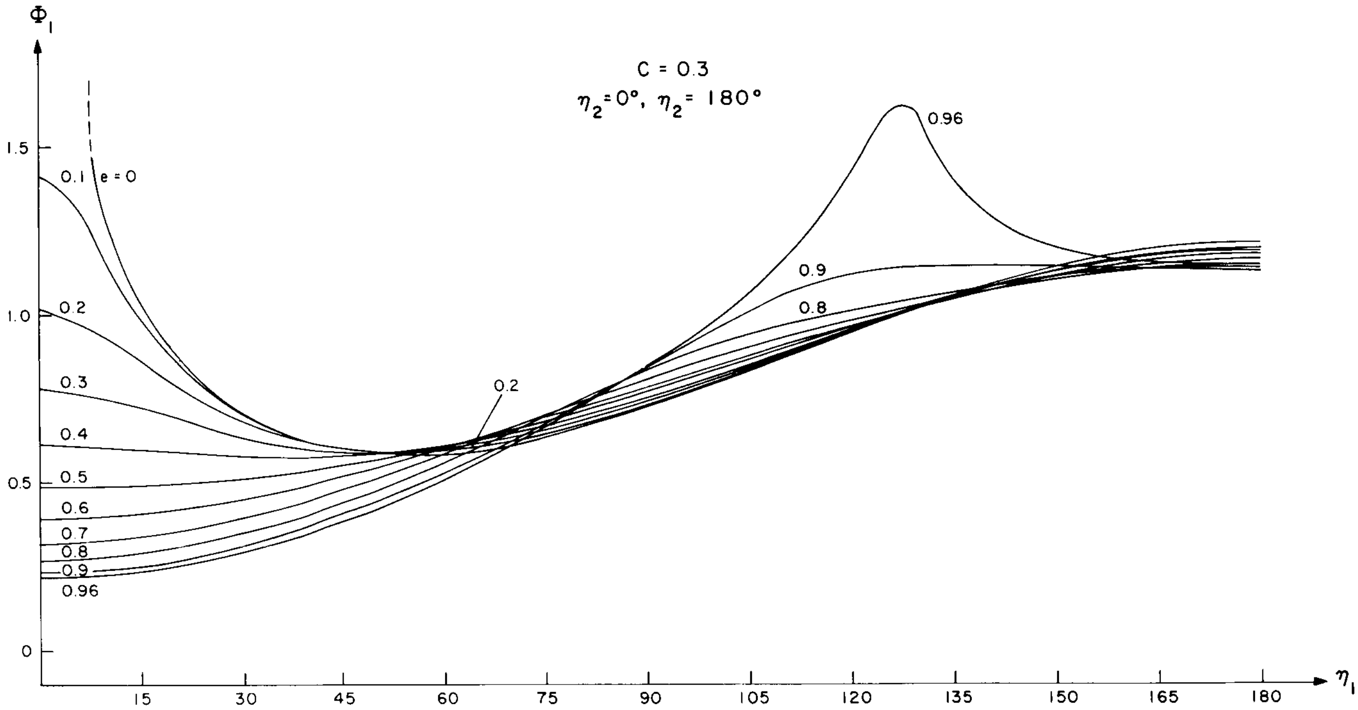

Figure 9.

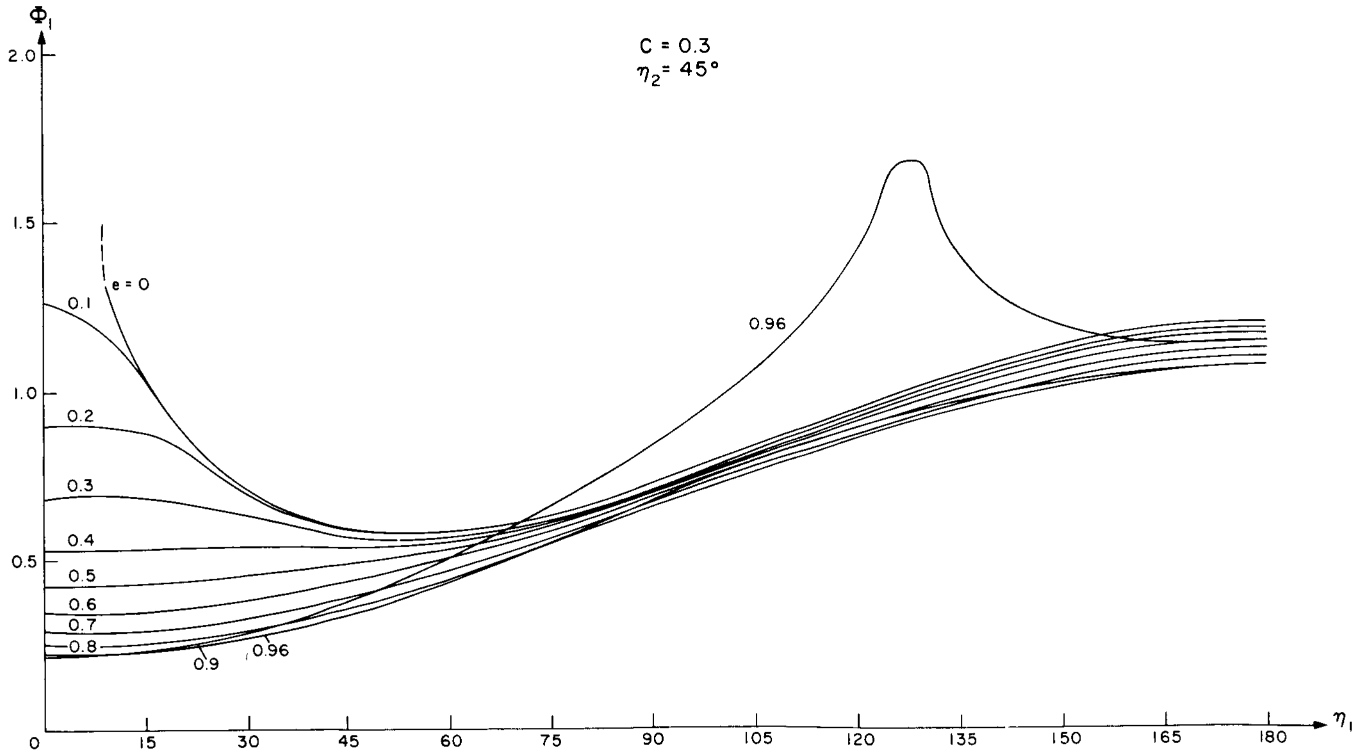

Figure 10.

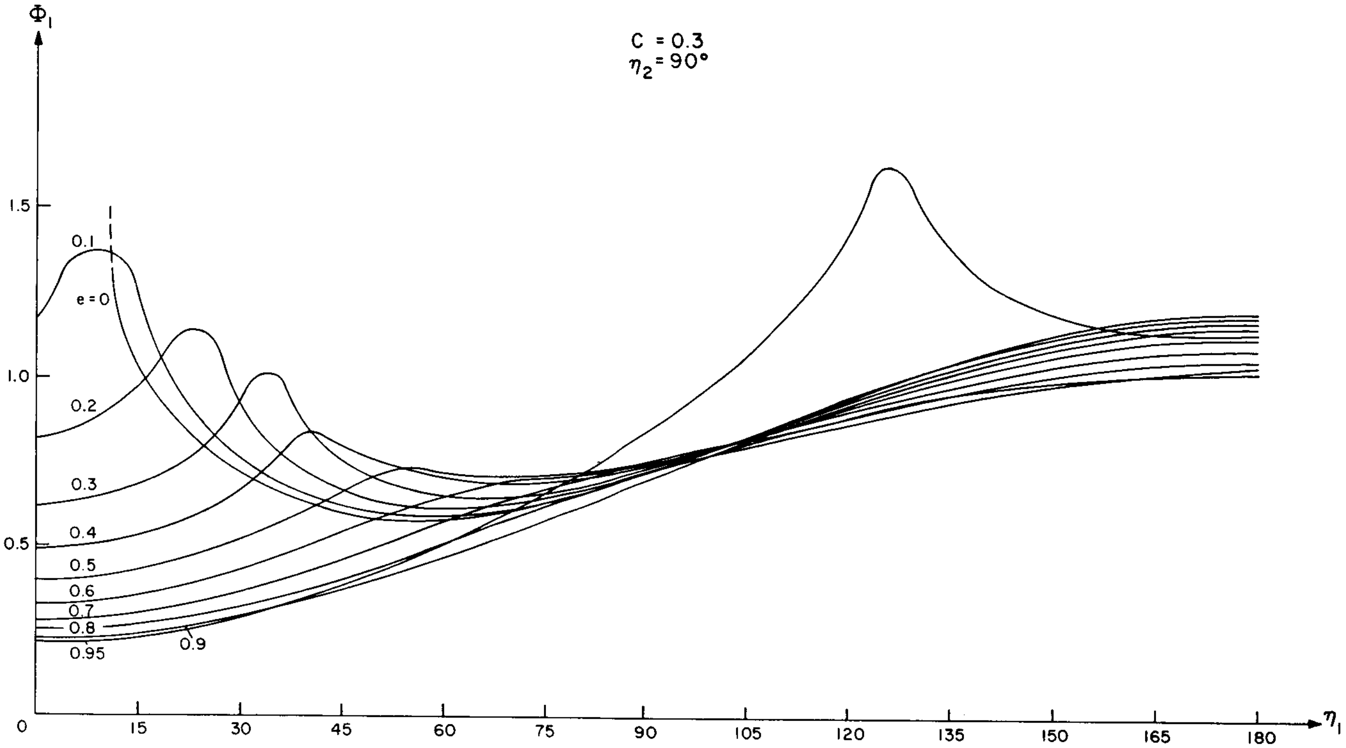

Figure 11.

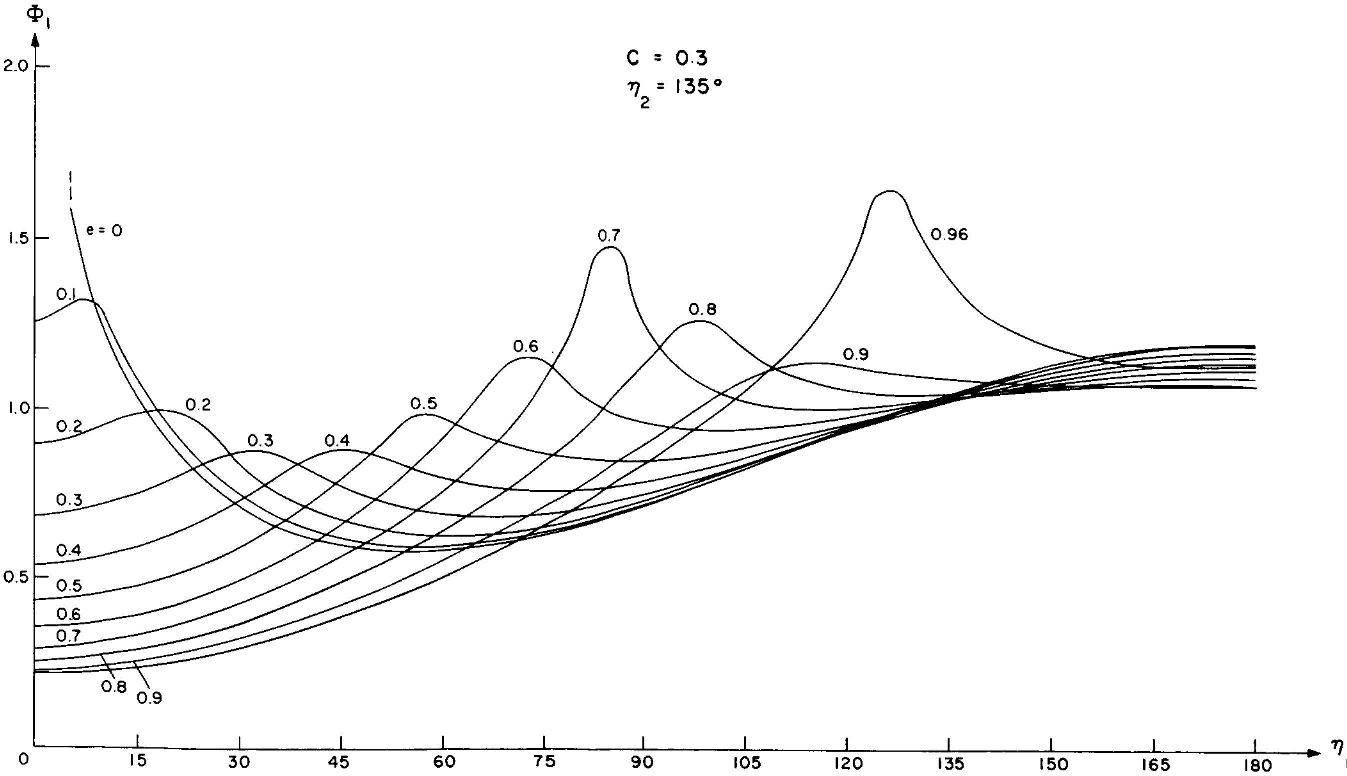

Figure 12.

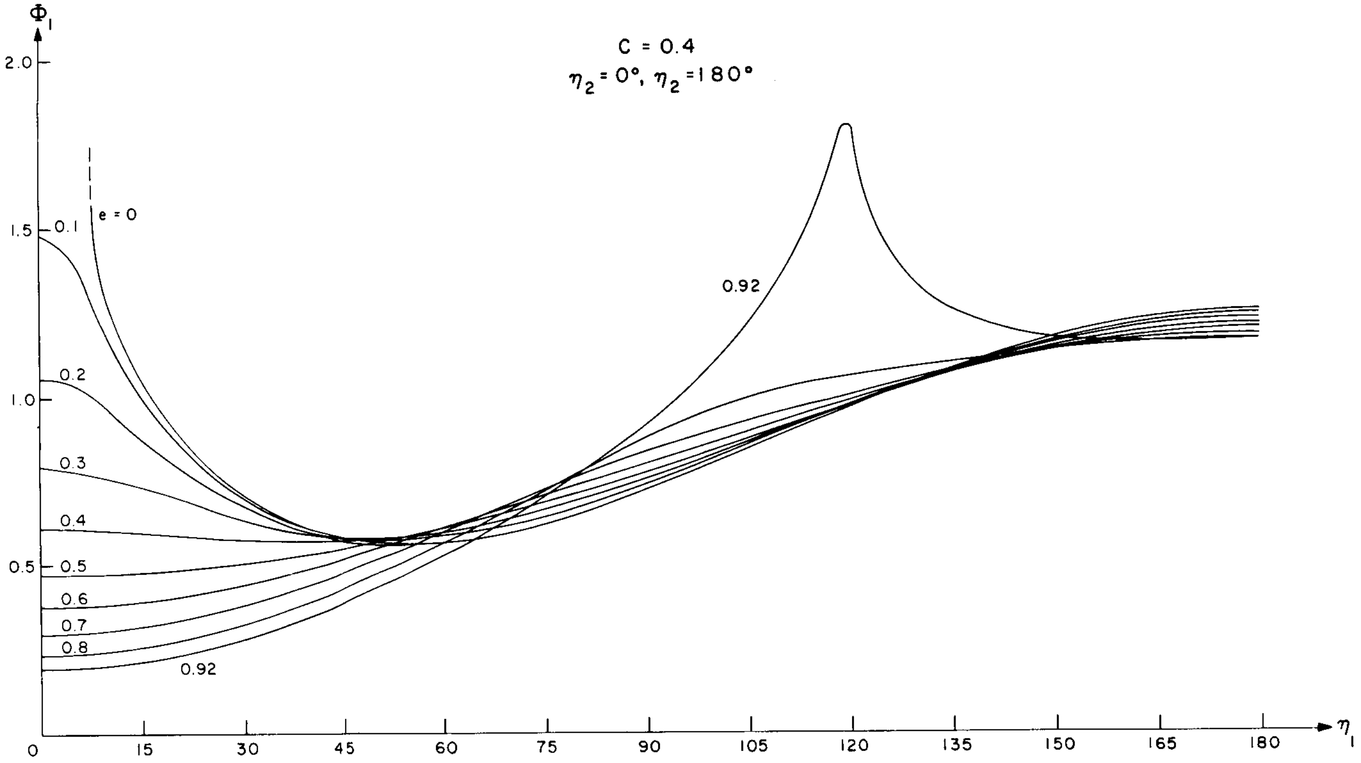

Figure 13.

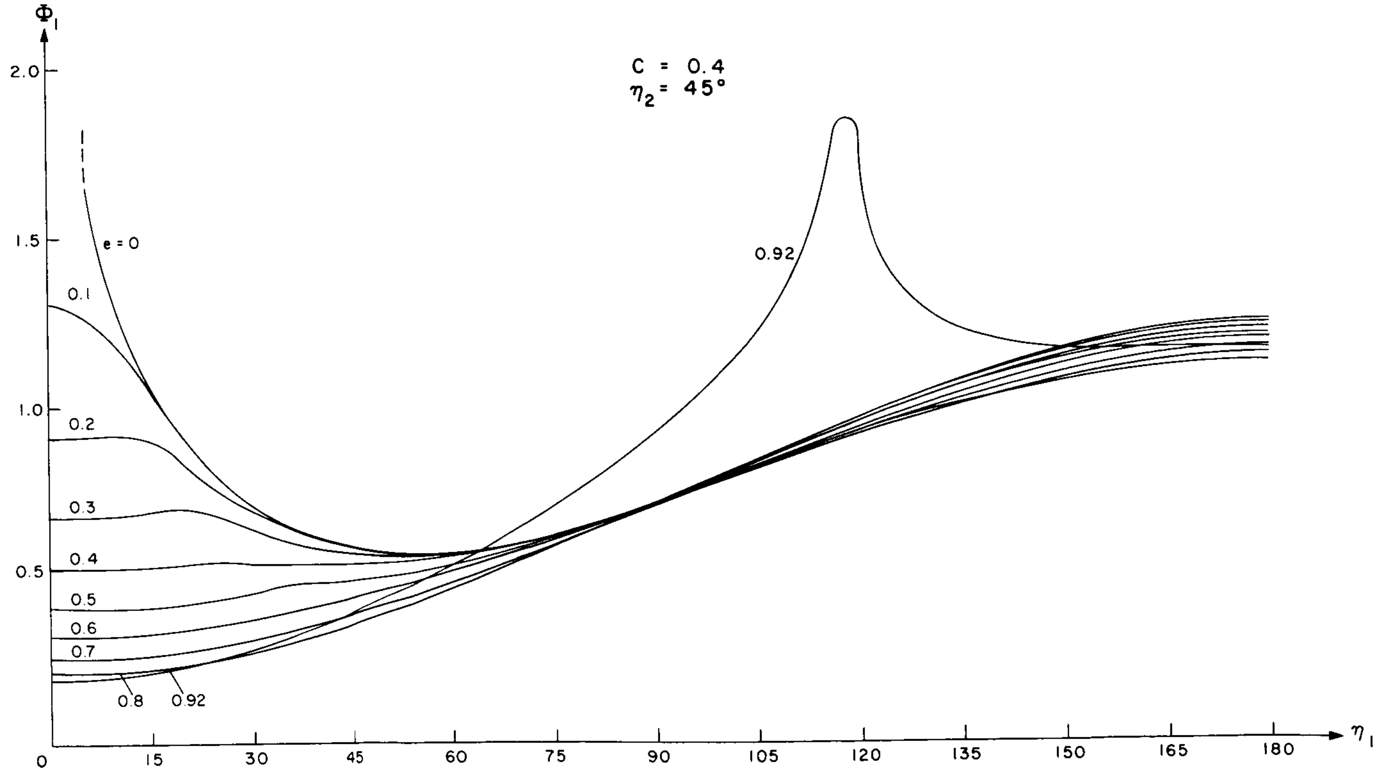

Figure 14.

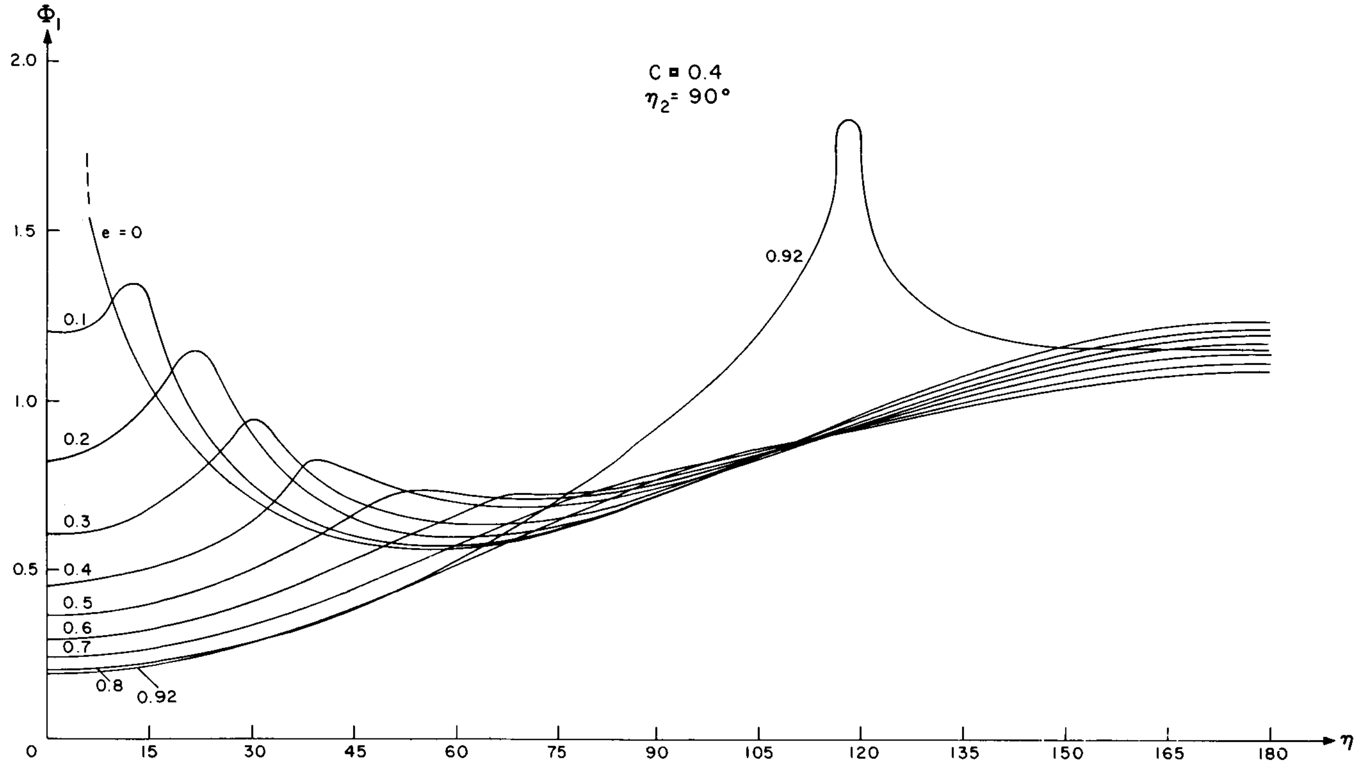

Figure 15.

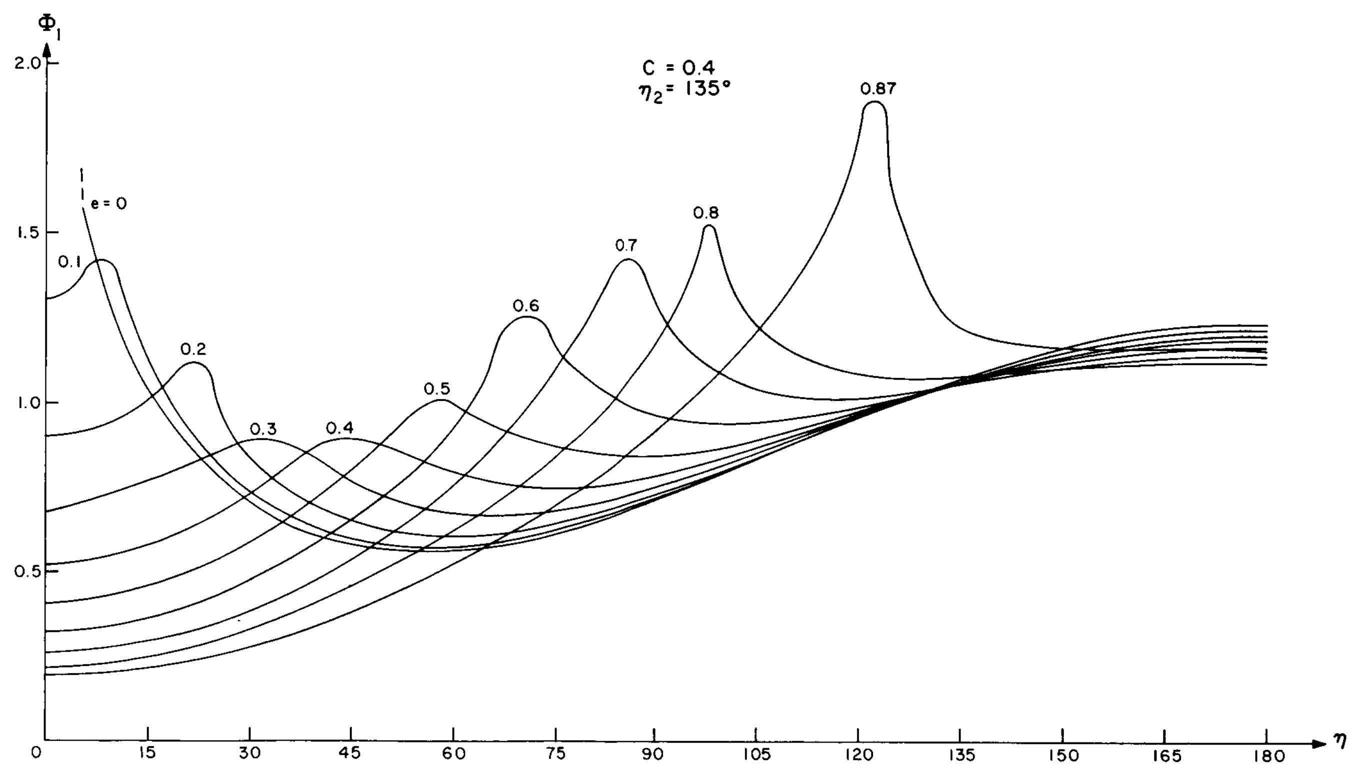

Figure 16.

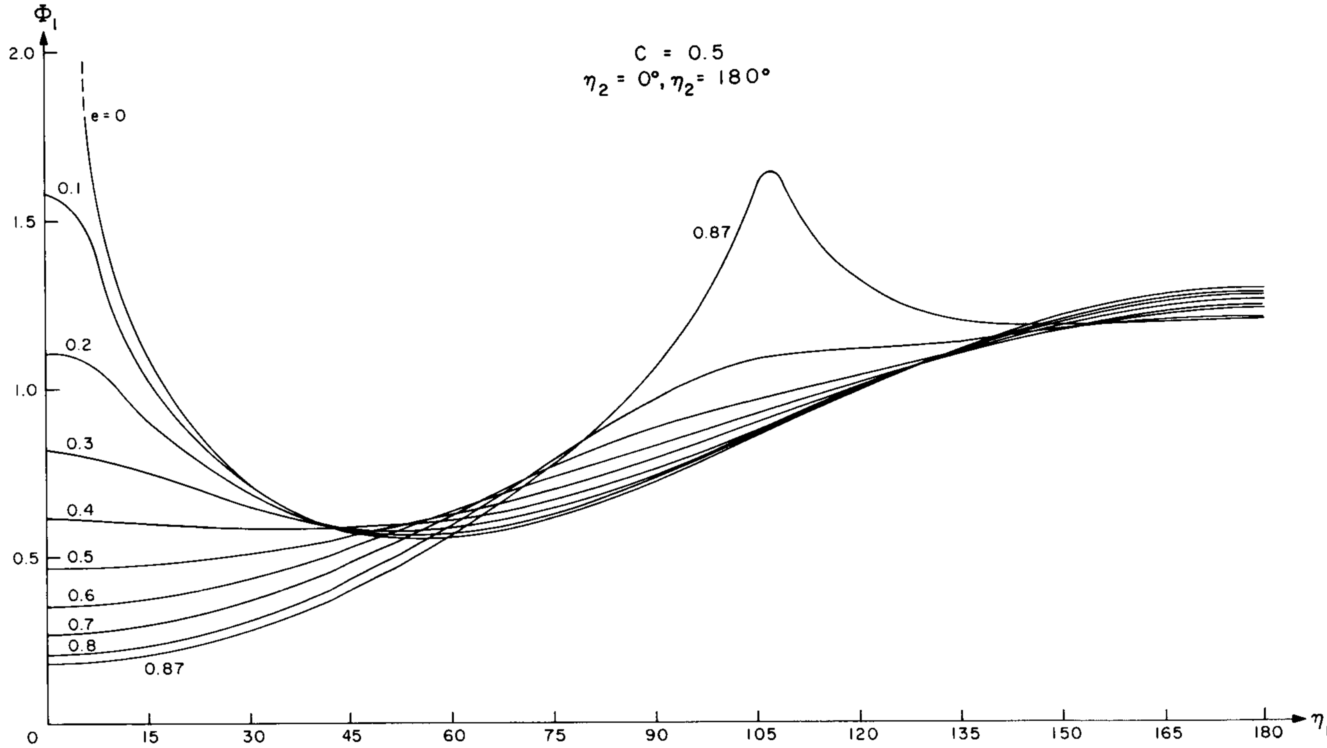

Figure 17.

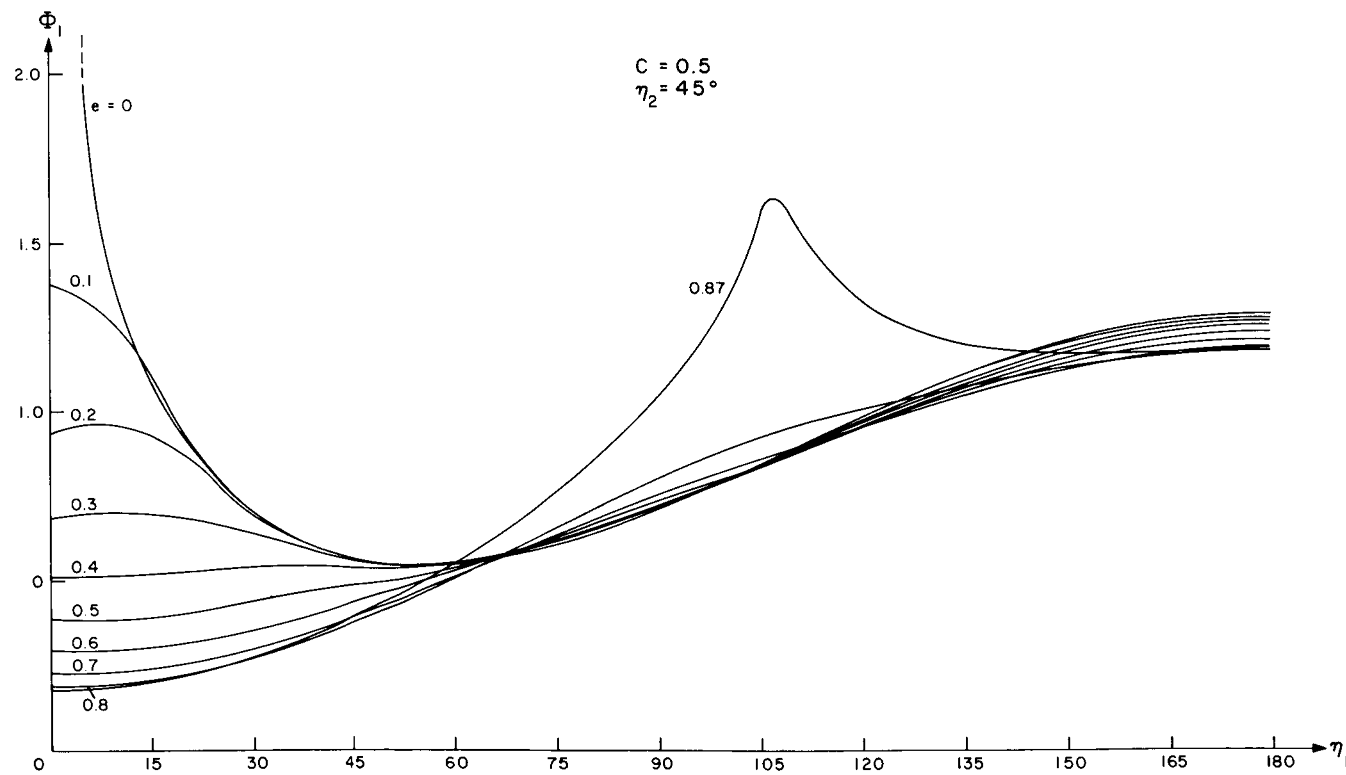

Figure 18.

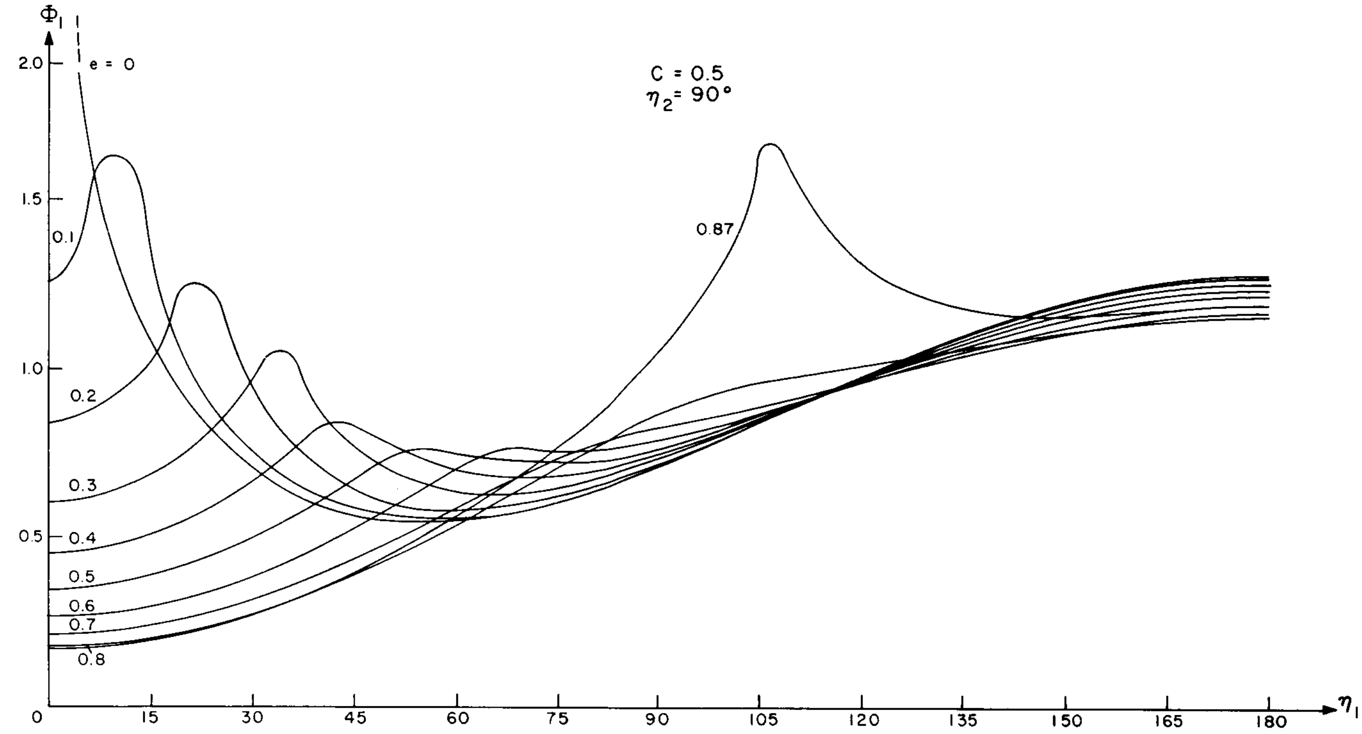

Figure 19.

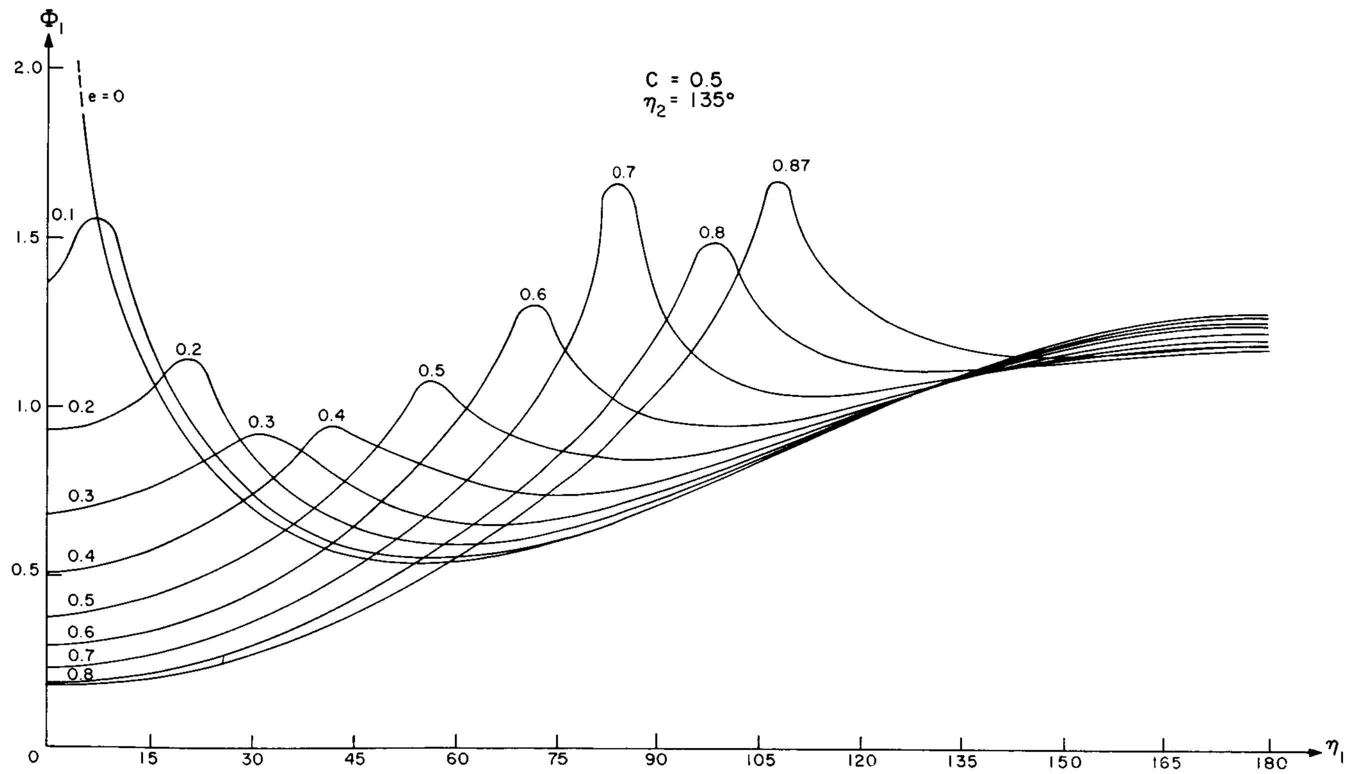

Figure 20.

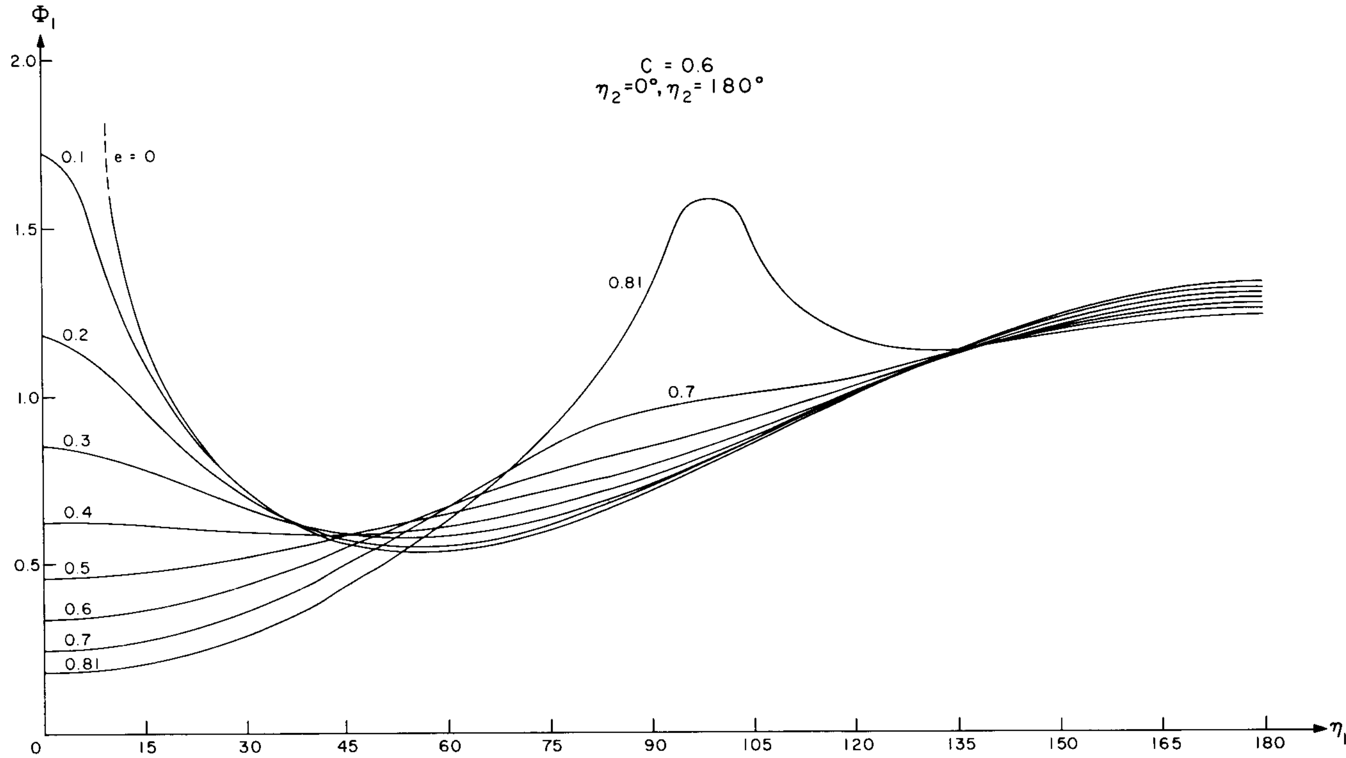

Figure 21.

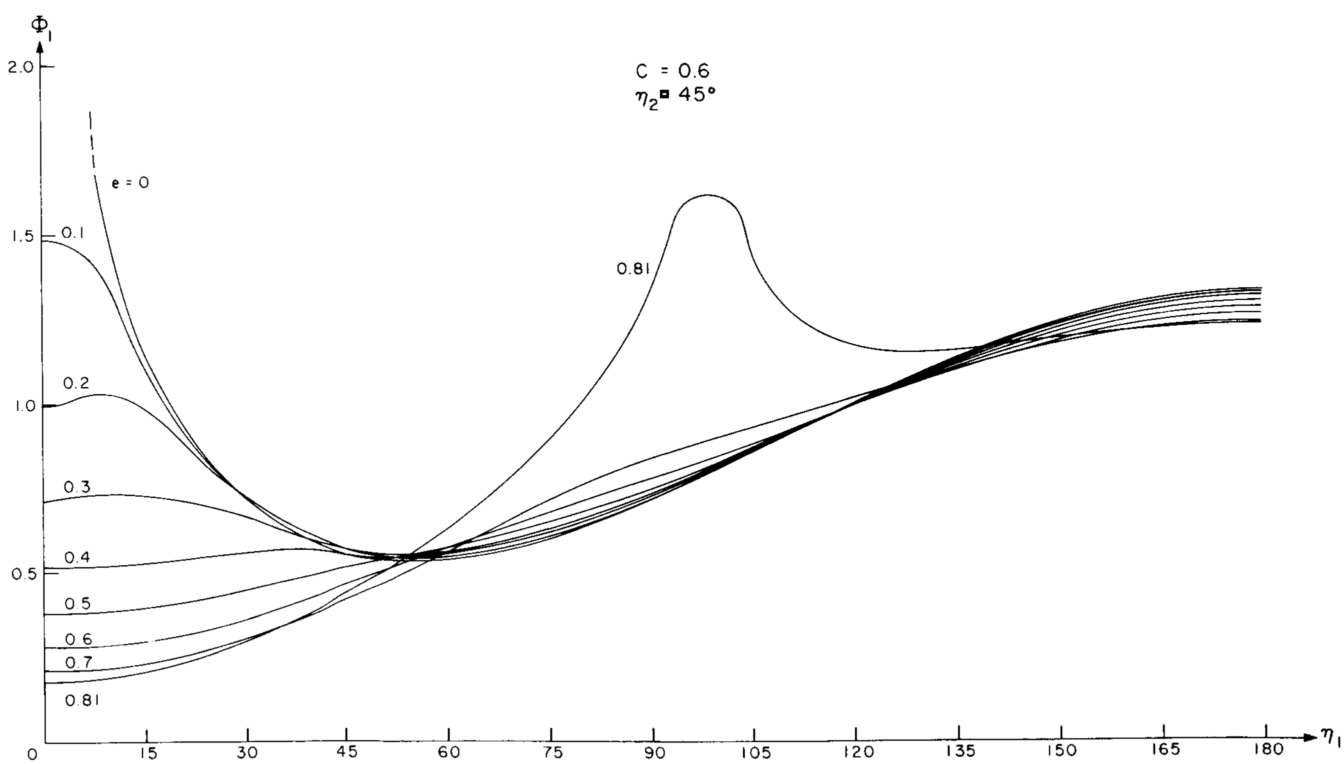

Figure 22.

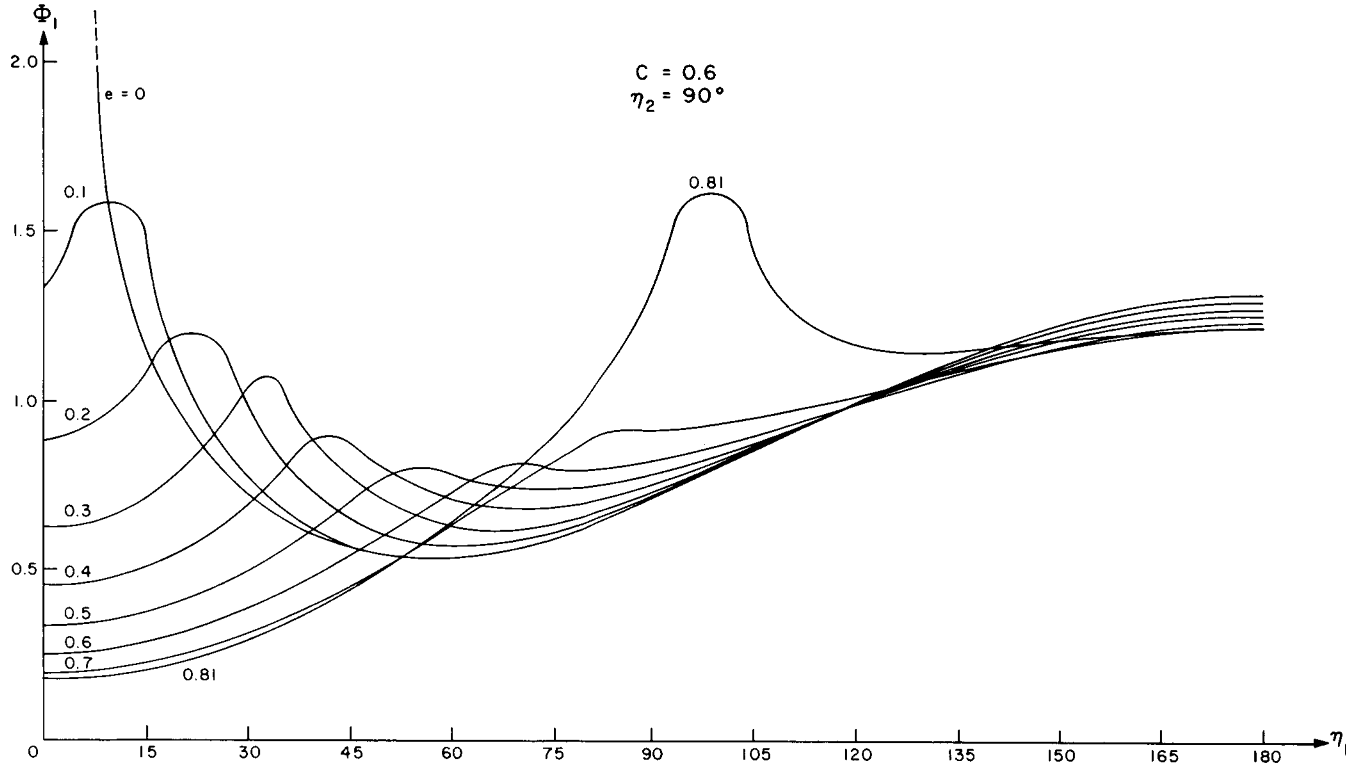

Figure 23.

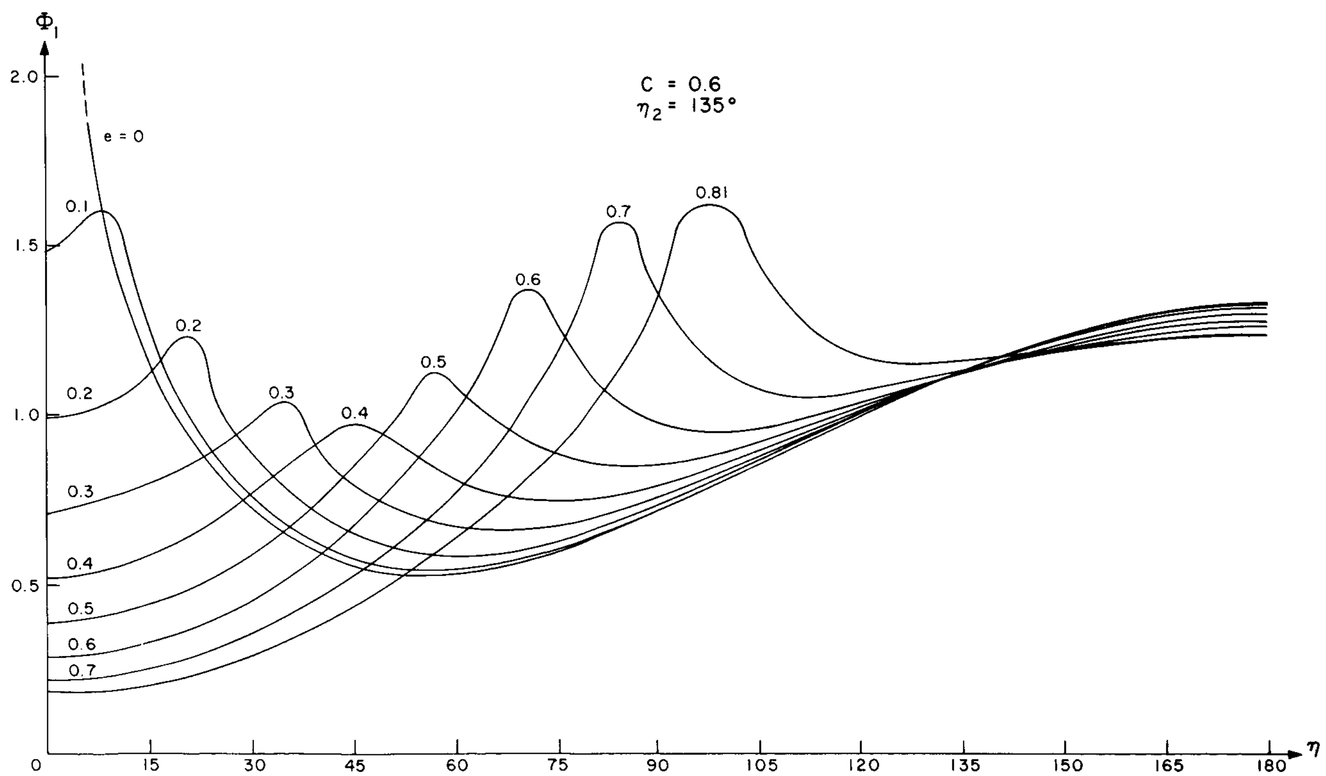

Figure 24.

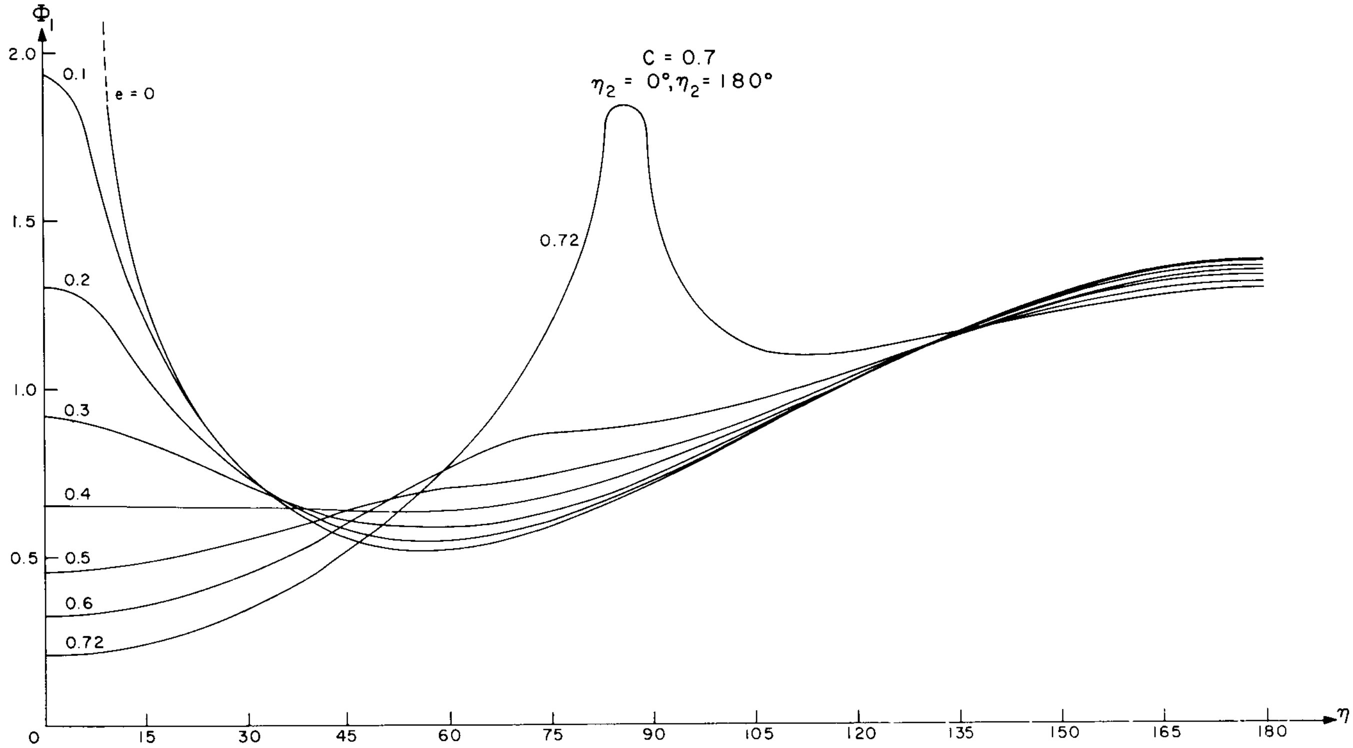

Figure 25.

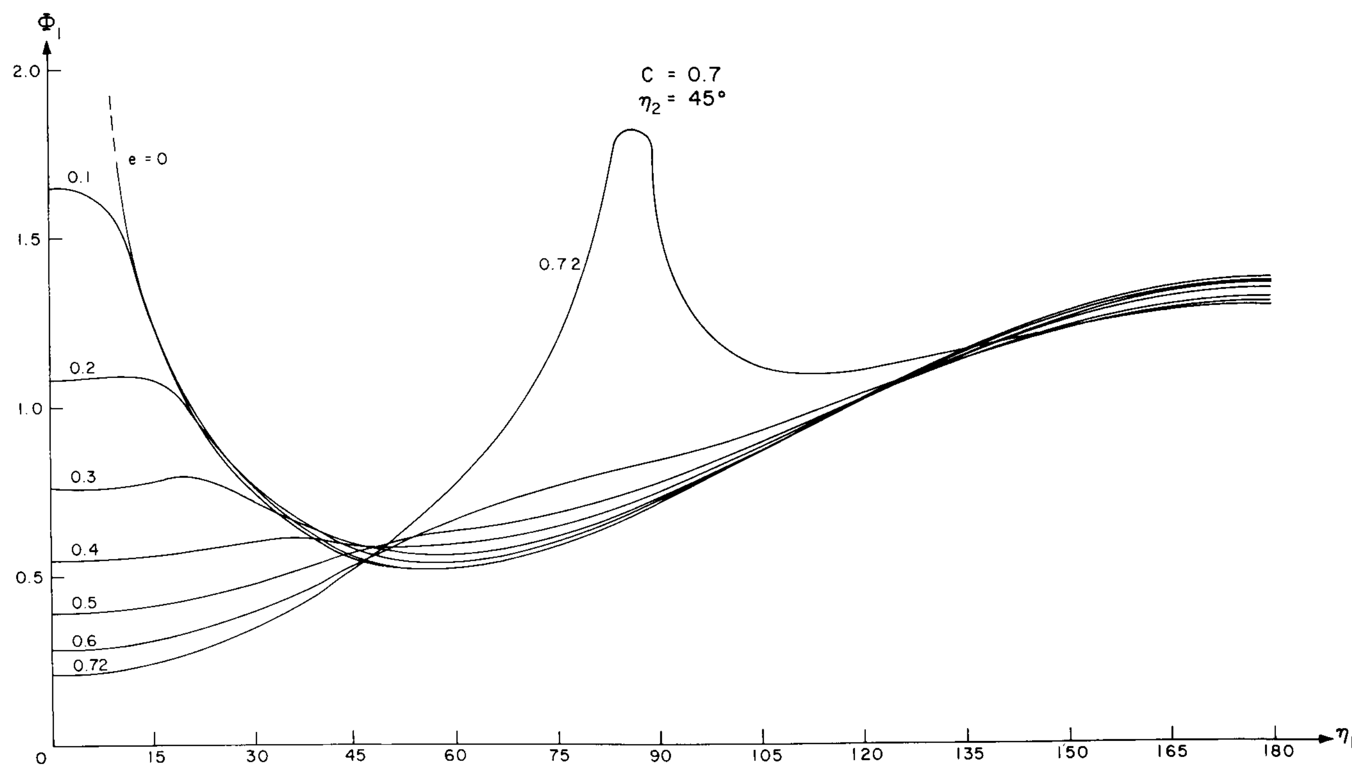

Figure 26.

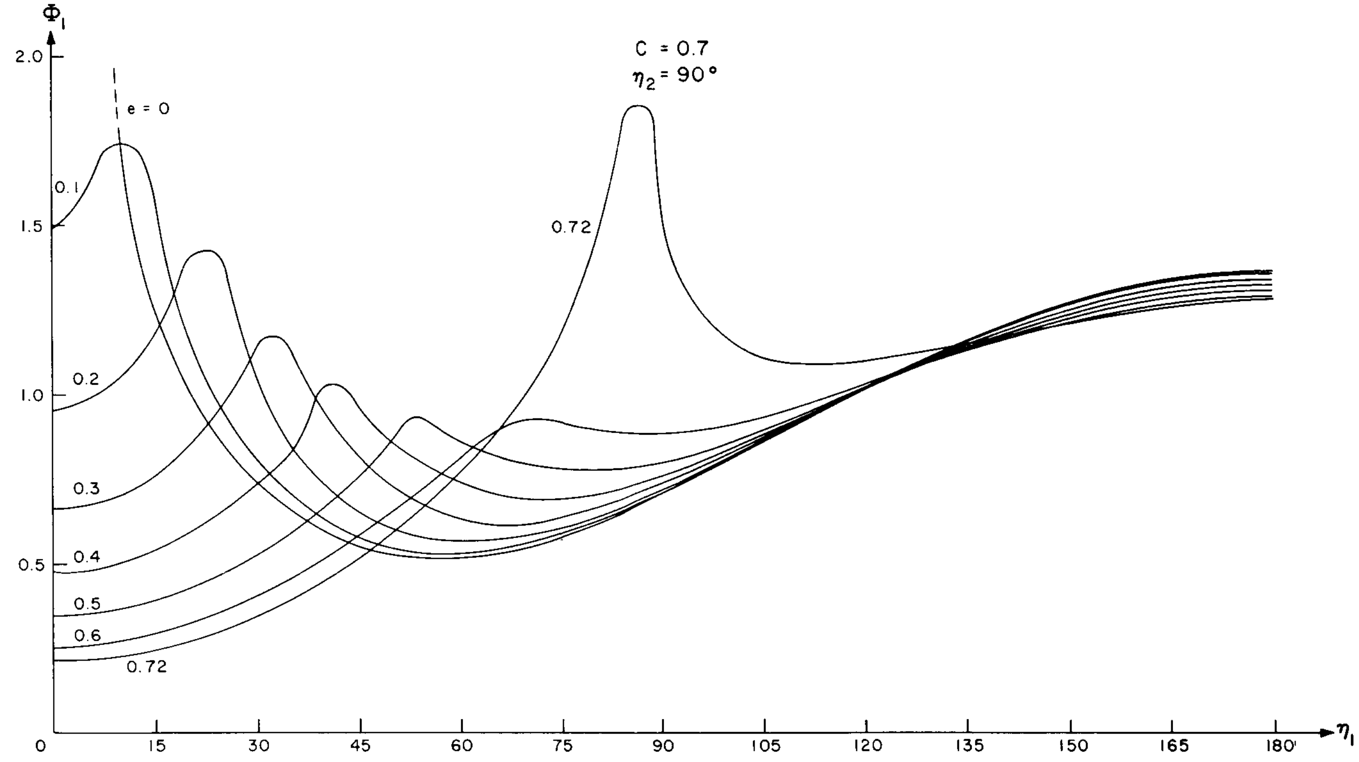

Figure 27.

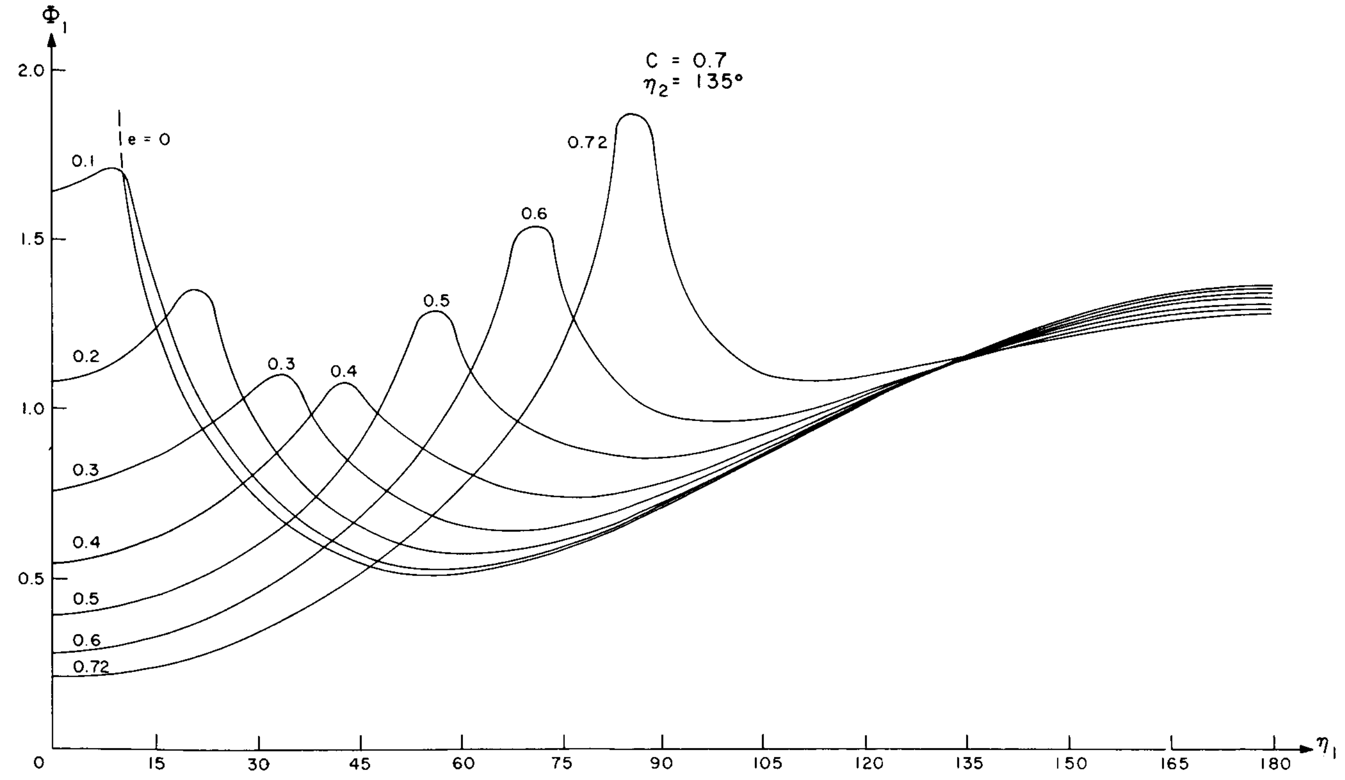

Figure 28.

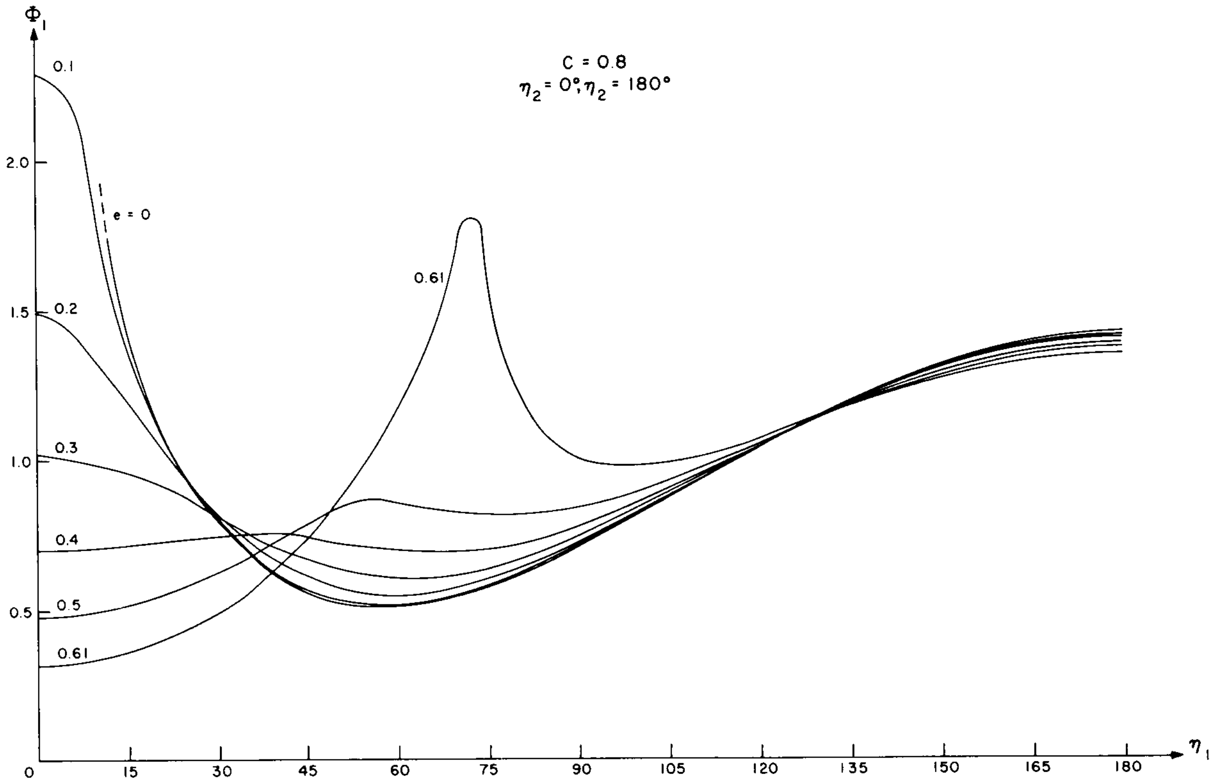

Figure 29.

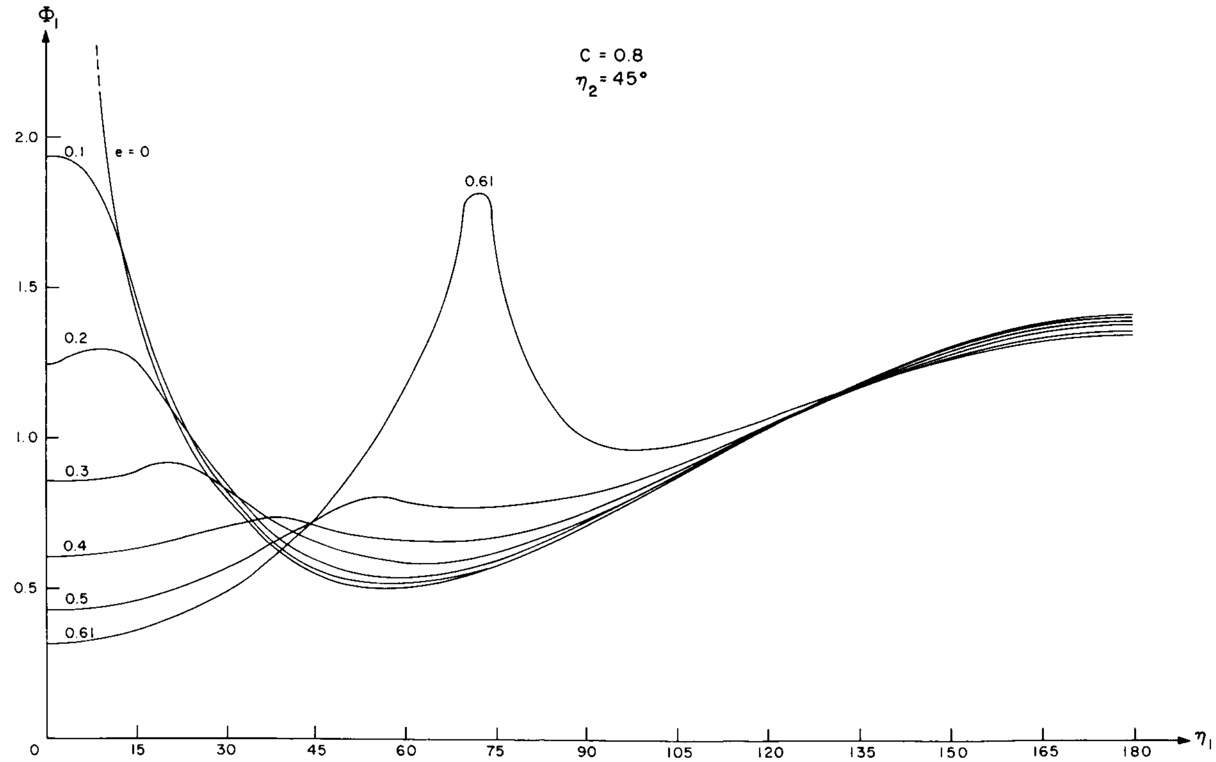

Figure 30.

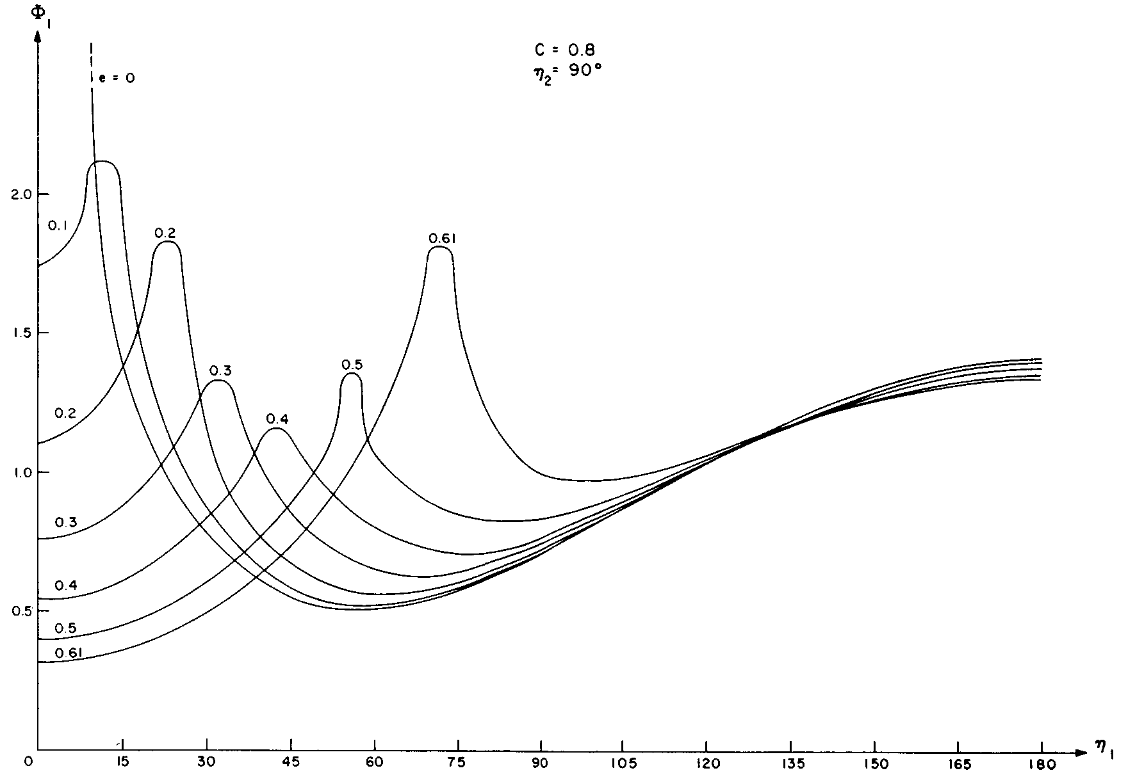

Figure 31.

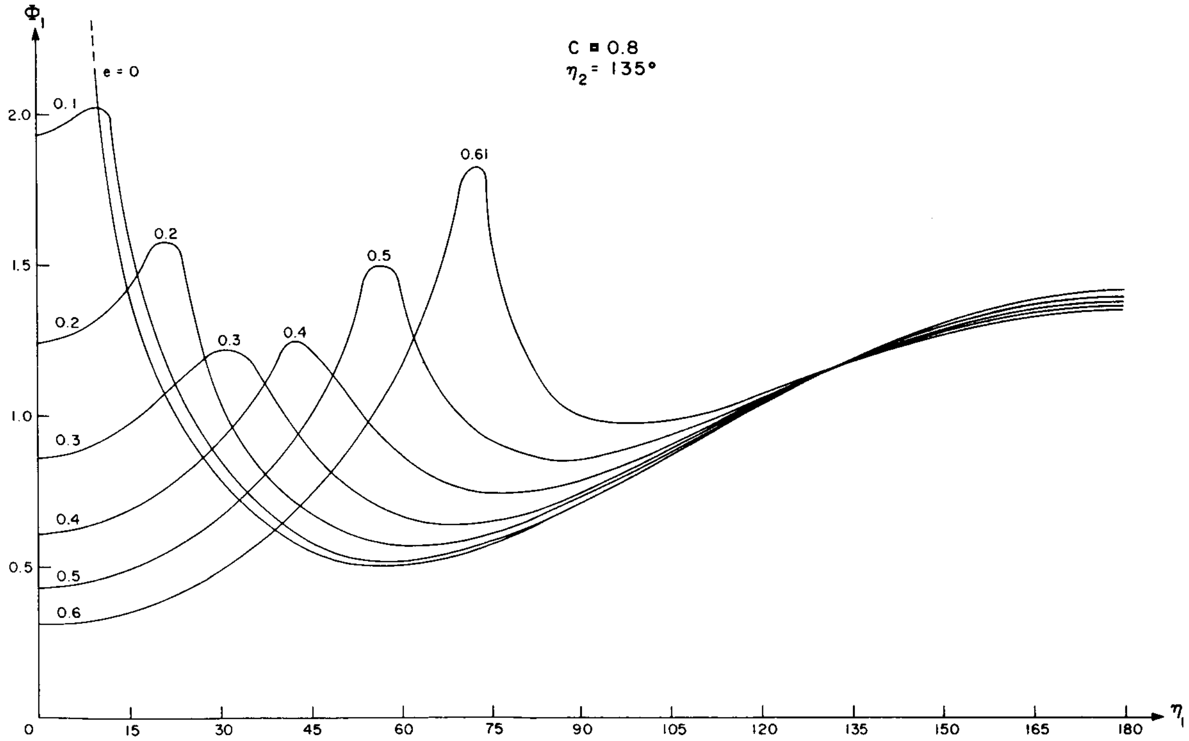

Figure 32.

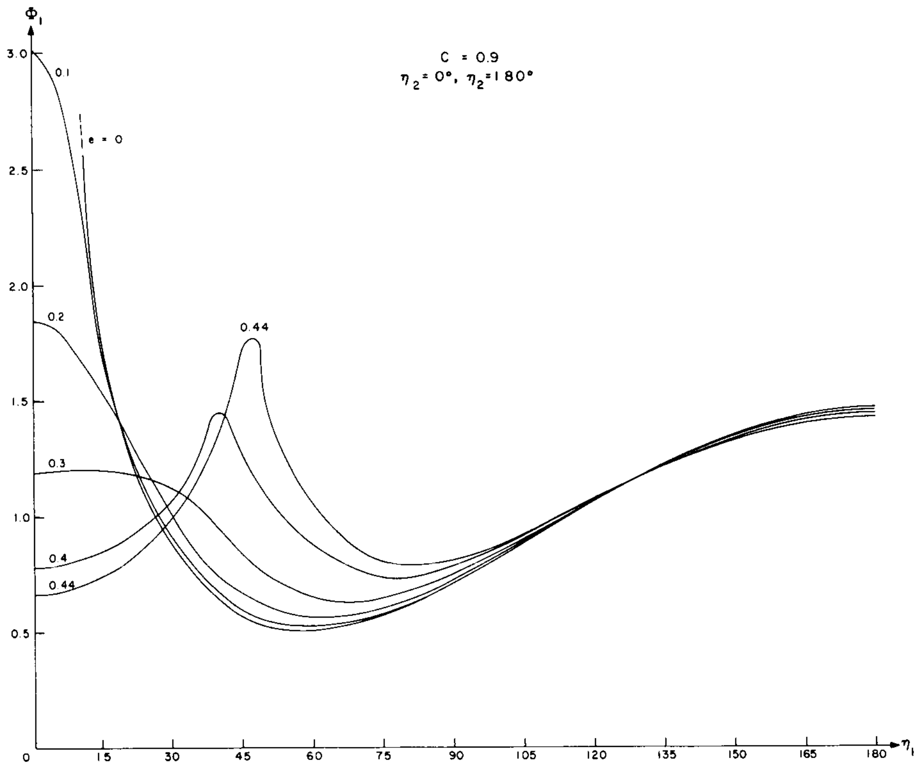

Figure 33.

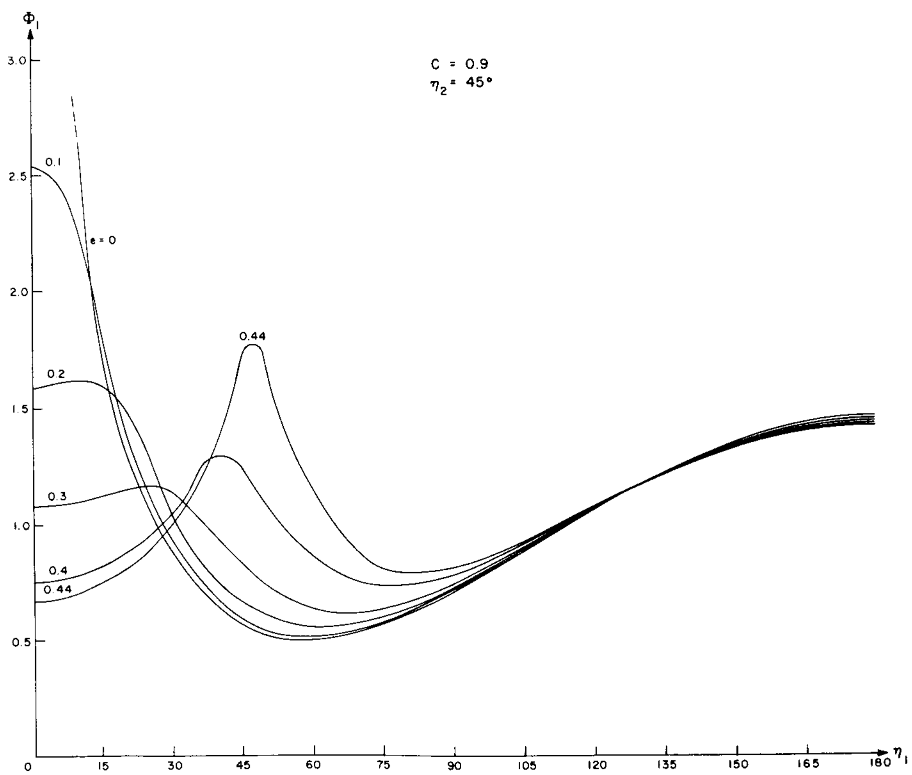

Figure 34.

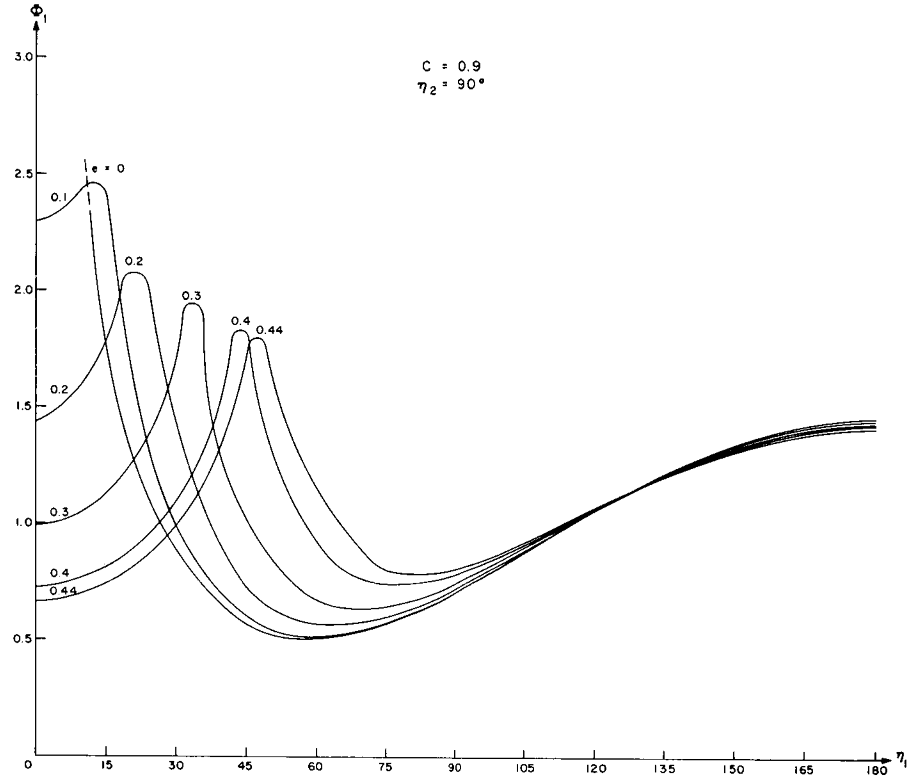

Figure 35.

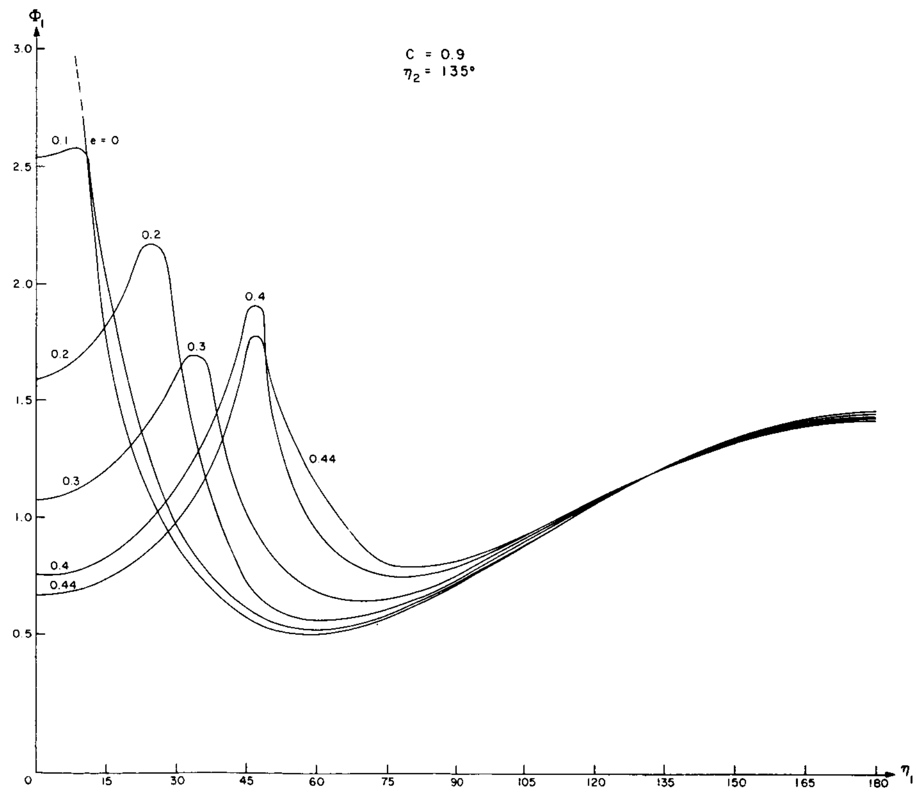

Figure 36.

Figures 37-45.

Minimum energy curves for long-periodic perturbations.

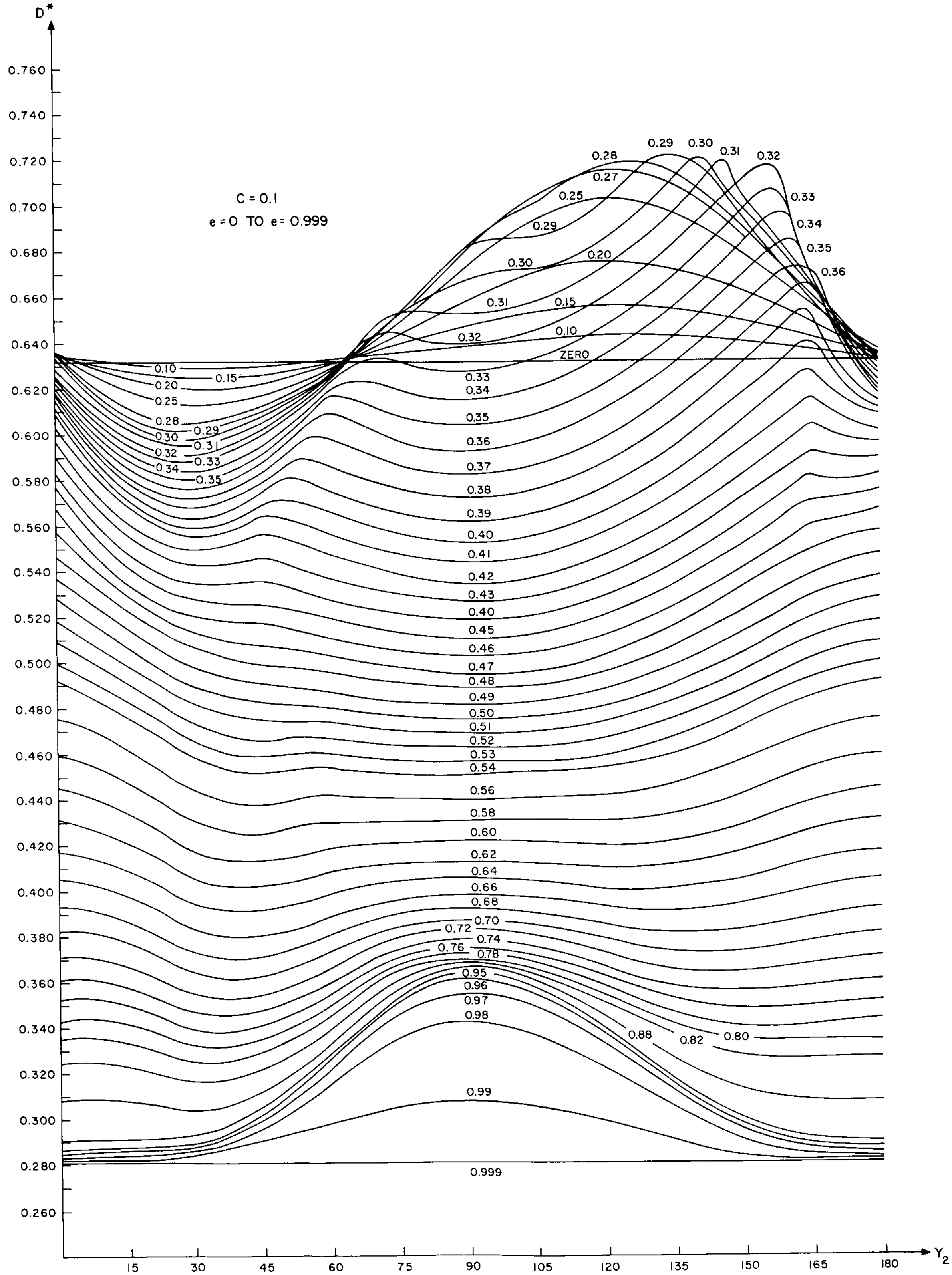

Figure 37.

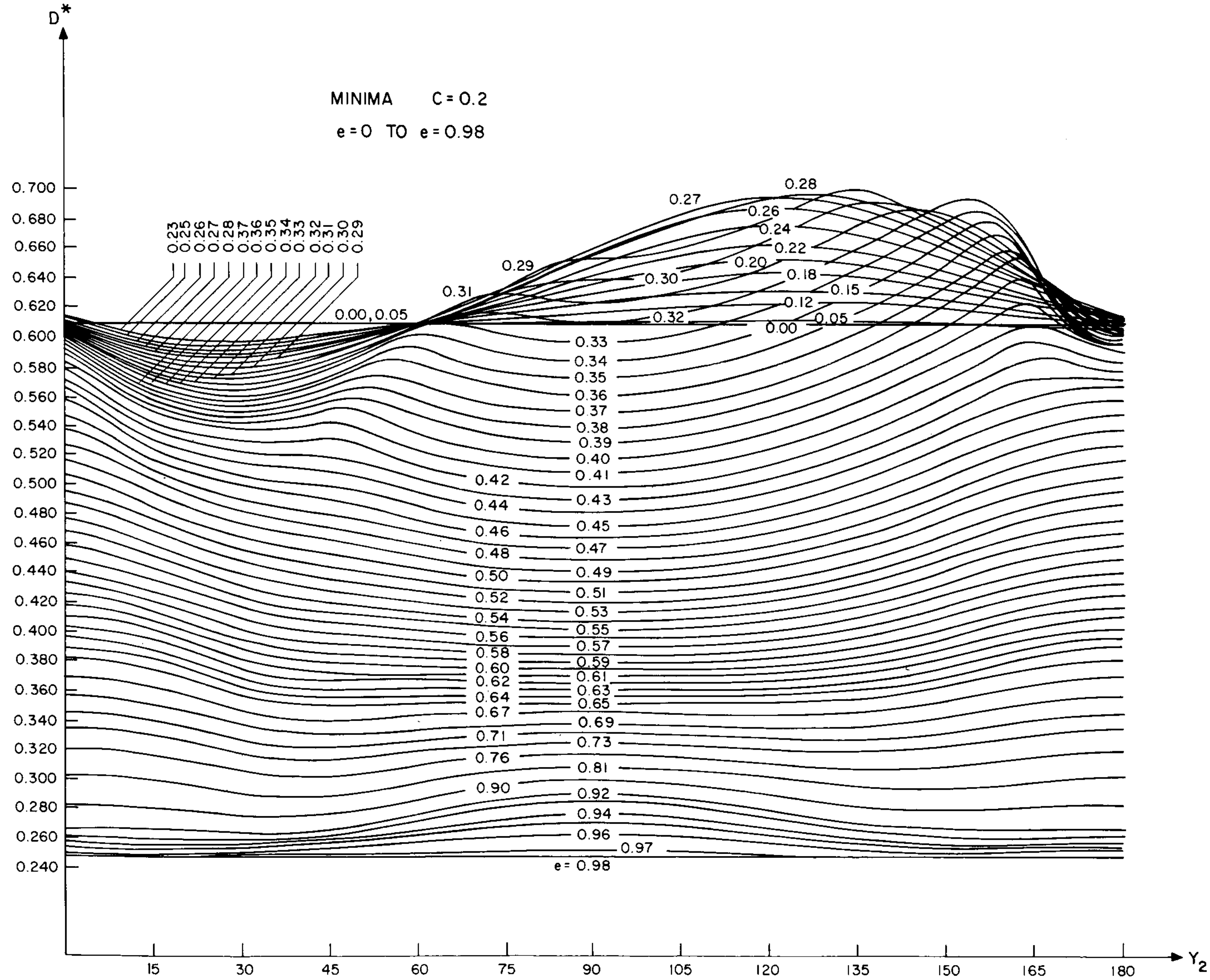

D*
MINIMA C = 0.2
e = 0 TO e = 0.98
0.700
0.680
0.660
0.640
0.620
0.600
0.580
0.560
0.540
0.520
0.500
0.480
0.460
0.440
0.420
0.400
0.380
0.360
0.340
0.320
0.300
0.280
0.260
0.240
0.23 0.25 0.26 0.27 0.28 0.37 0.36 0.35 0.34 0.33 0.32 0.31 0.30 0.29
0.00, 0.05
0.31
0.29
0.27
0.28
0.26
0.24
0.22
0.20
0.30
0.18
0.15
0.12
0.32
0.05
0.00
0.33
0.34
0.35
0.36
0.37
0.38
0.39
0.40
0.41
0.42
0.43
0.44
0.45
0.46
0.47
0.48
0.49
0.50
0.51
0.52
0.53
0.54
0.55
0.56
0.57
0.58
0.59
0.60
0.61
0.62
0.63
0.64
0.65
0.67
0.69
0.71
0.73
0.76
0.81
0.90
0.92
0.94
0.96
0.97
e = 0.98
15
30
45
60
75
90
105
120
135
150
165
180
Y_2

Figure 38.

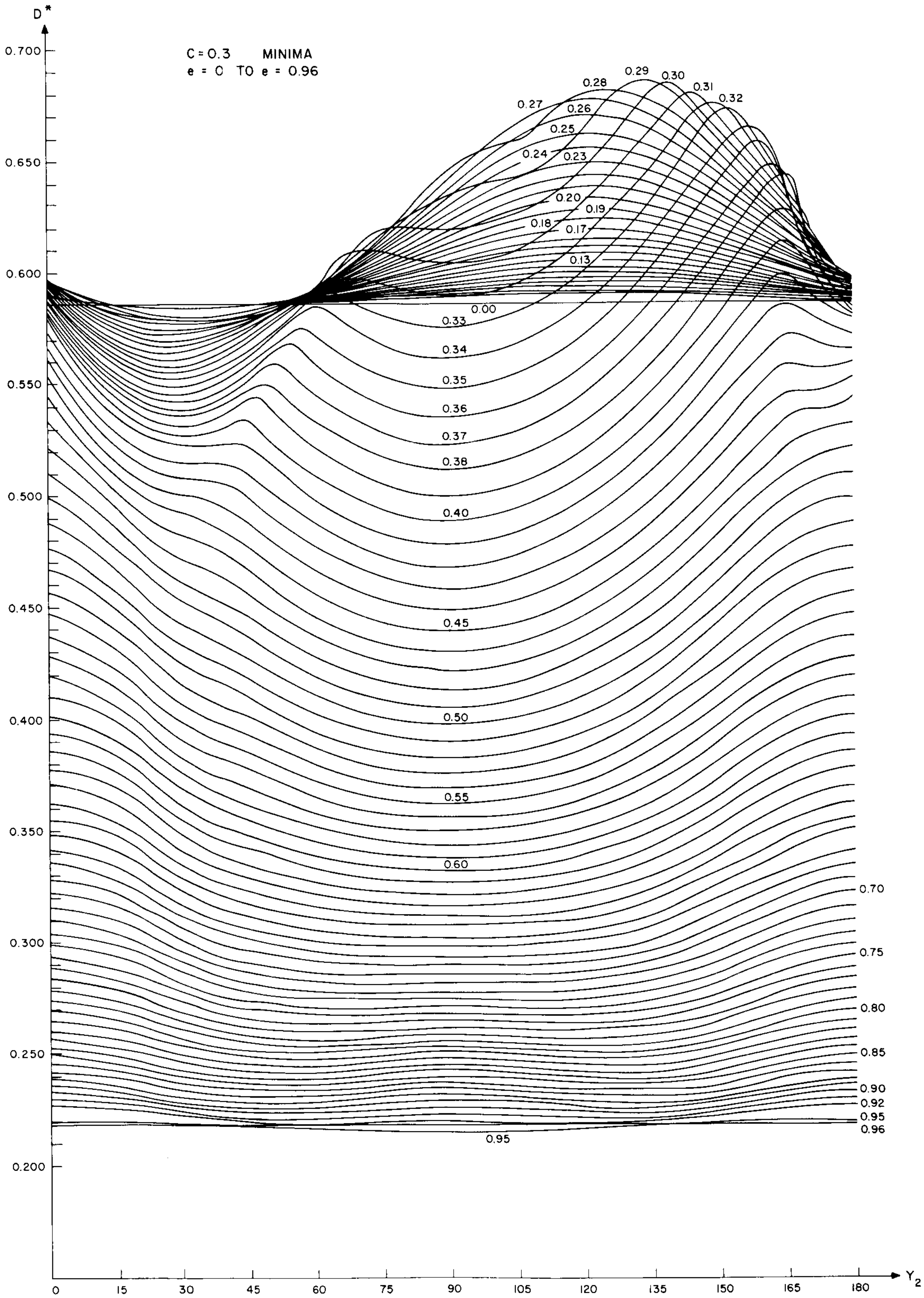

D*
C = 0.3 MINIMA
e = 0 TO e = 0.96
0.700
0.650
0.600
0.550
0.500
0.450
0.400
0.350
0.300
0.250
0.200
0.29
0.30
0.28
0.31
0.32
0.27
0.26
0.25
0.24
0.23
0.20
0.19
0.18
0.17
0.13
0.00
0.33
0.34
0.35
0.36
0.37
0.38
0.40
0.45
0.50
0.55
0.60
0.70
0.75
0.80
0.85
0.90
0.92
0.95
0.96
0.95
0
15
30
45
60
75
90
105
120
135
150
165
180
Y_2

Figure 39.

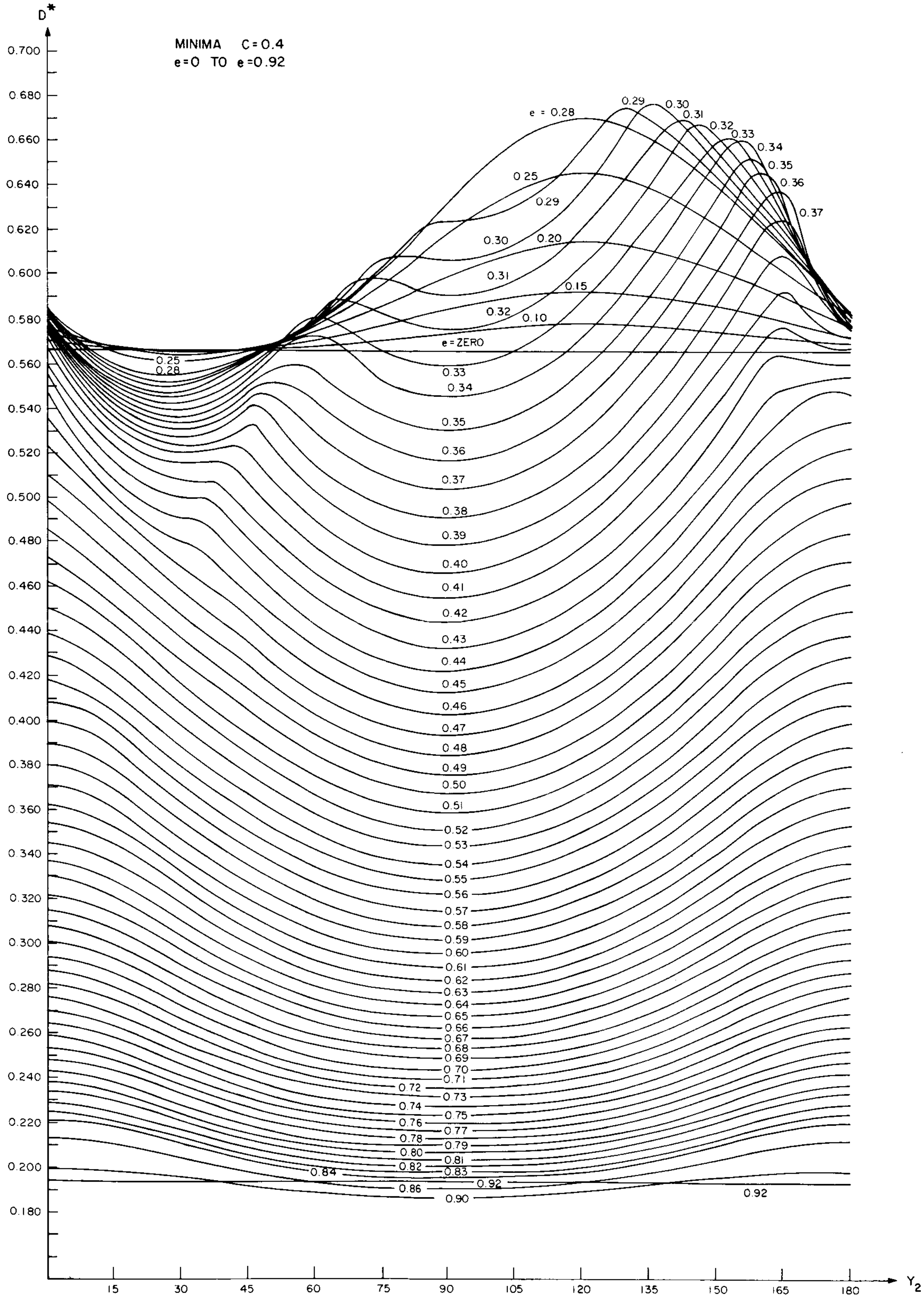
D*
MINIMA C = 0.4
e=0 TO e=0.92
0.700
0.680
0.660
0.640
0.620
0.600
0.580
0.560
0.540
0.520
0.500
0.480
0.460
0.440
0.420
0.400
0.380
0.360
0.340
0.320
0.300
0.280
0.260
0.240
0.220
0.200
0.180
15
30
45
60
75
90
105
120
135
150
165
180
Y_2
e = 0.28
e = ZERO

Figure 40.

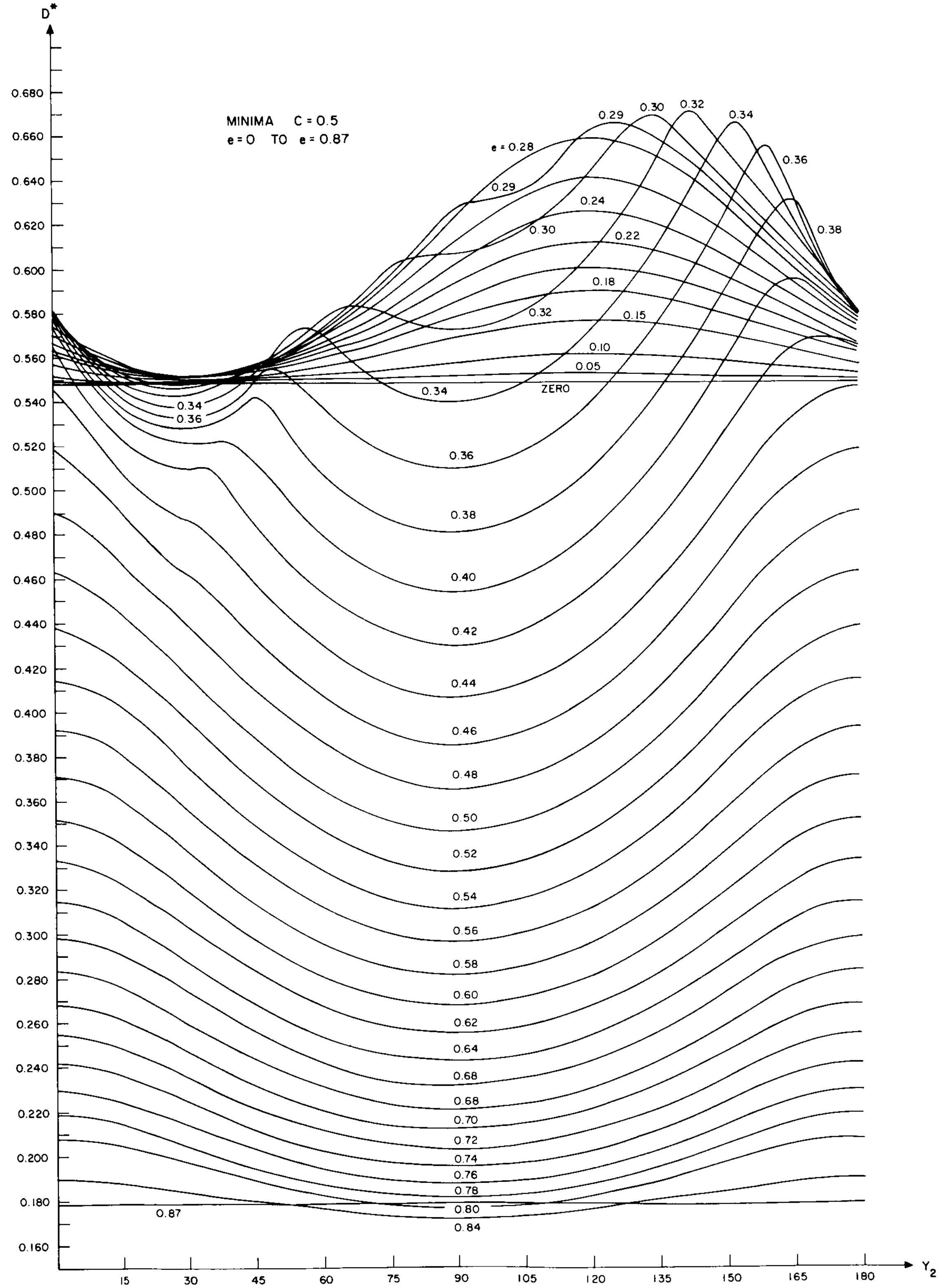
D*
MINIMA C = 0.5
e = 0 TO e = 0.87
e = 0.28
0.29
0.30
0.32
0.34
0.36
0.38
0.24
0.22
0.18
0.15
0.10
0.05
ZERO
0.40
0.42
0.44
0.46
0.48
0.50
0.52
0.54
0.56
0.58
0.60
0.62
0.64
0.68
0.68
0.70
0.72
0.74
0.76
0.78
0.80
0.84
0.87
0.680
0.660
0.640
0.620
0.600
0.580
0.560
0.540
0.520
0.500
0.480
0.460
0.440
0.420
0.400
0.380
0.360
0.340
0.320
0.300
0.280
0.260
0.240
0.220
0.200
0.180
0.160
15
30
45
60
75
90
105
120
135
150
165
180
Y_2

Figure 41.

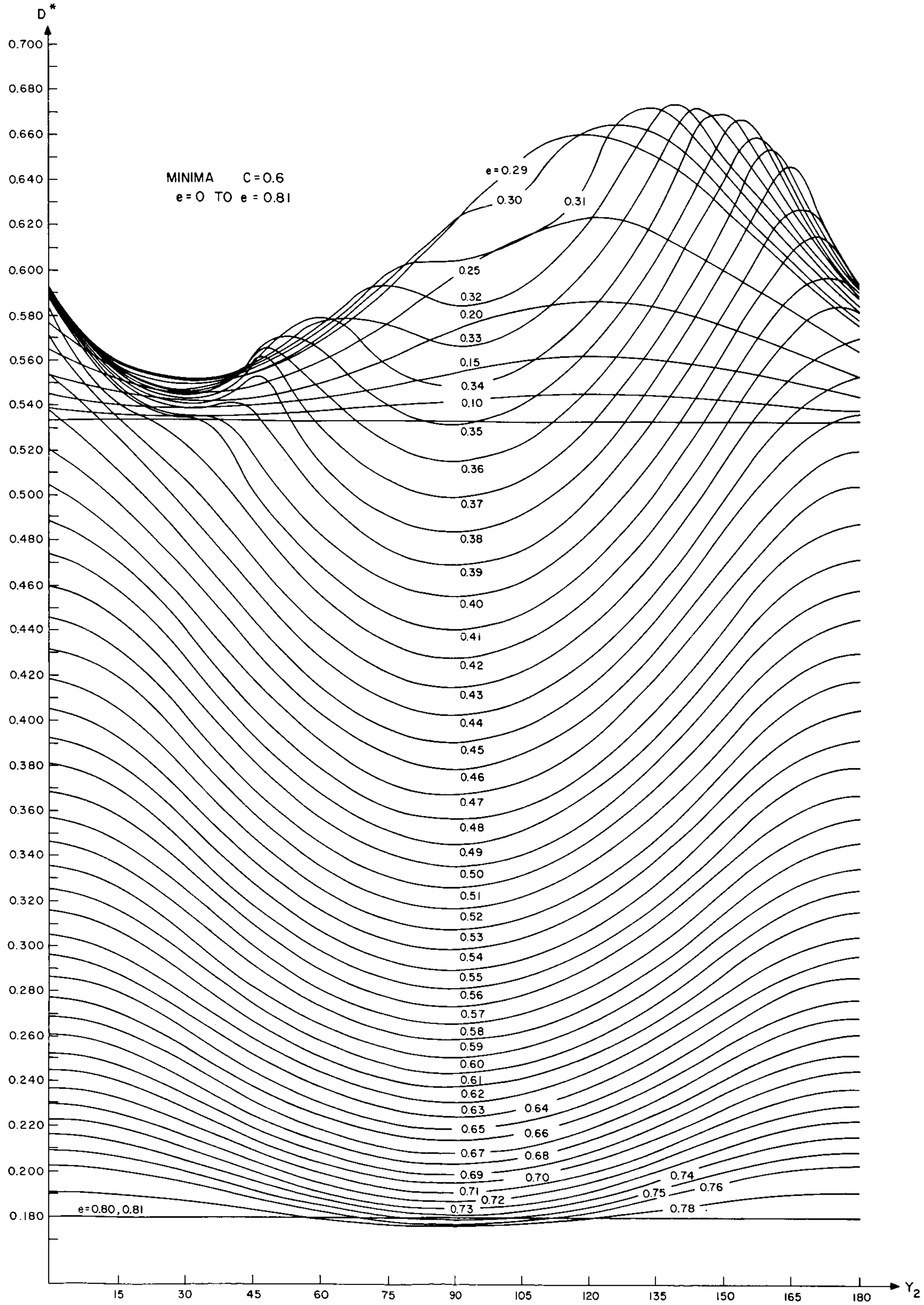
D*
MINIMA C=0.6
e=0 TO e=0.81
e=0.29
0.30
0.31
0.25
0.32
0.20
0.33
0.15
0.34
0.10
0.35
0.36
0.37
0.38
0.39
0.40
0.41
0.42
0.43
0.44
0.45
0.46
0.47
0.48
0.49
0.50
0.51
0.52
0.53
0.54
0.55
0.56
0.57
0.58
0.59
0.60
0.61
0.62
0.63
0.64
0.65
0.66
0.67
0.68
0.69
0.70
0.71
0.72
0.73
0.74
0.75
0.76
0.78
e=0.80, 0.81
Y2

Figure 42.

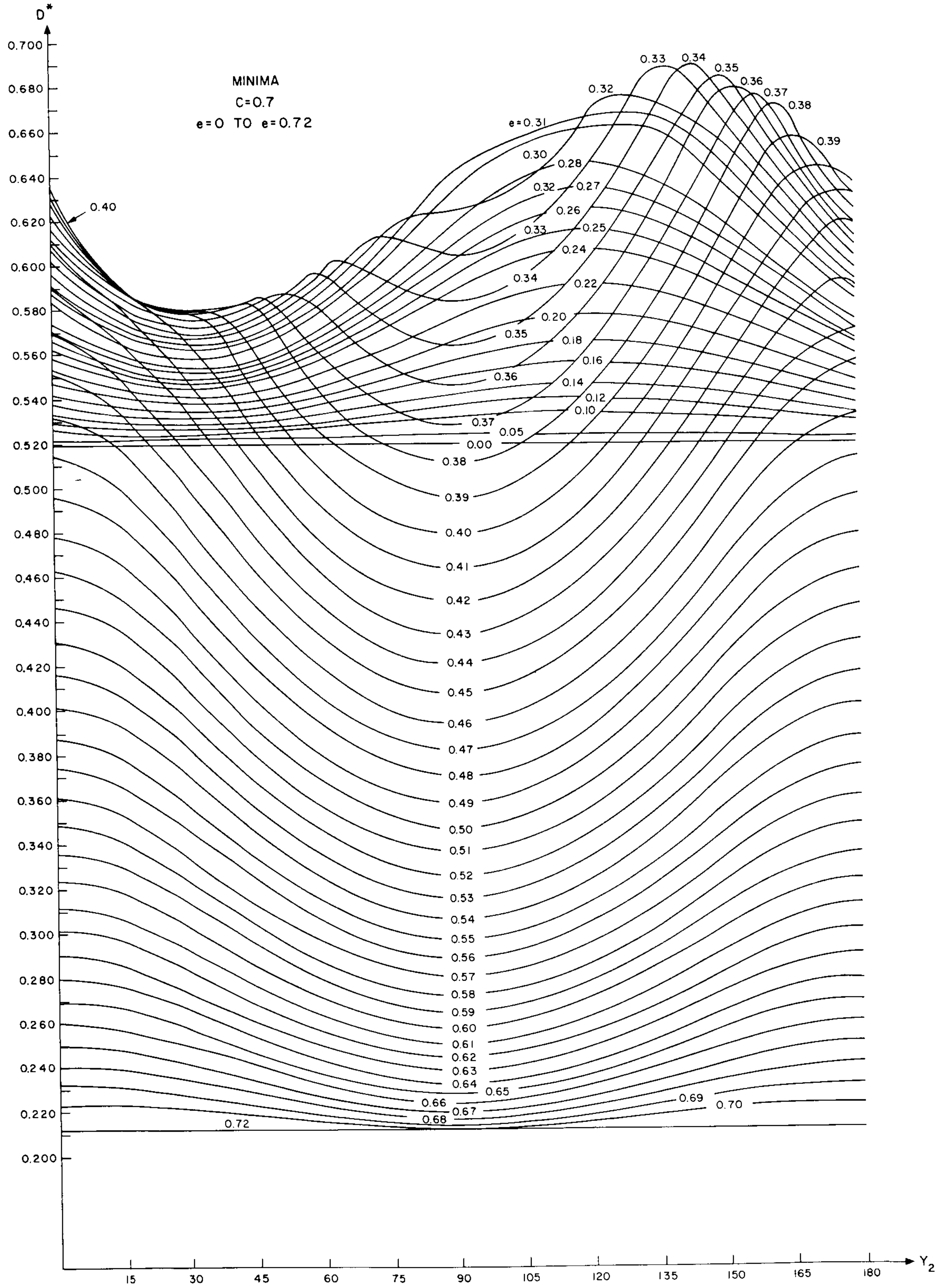

D*
MINIMA
C=0.7
e=0 TO e=0.72
0.700
0.680
0.660
0.640
0.620
0.600
0.580
0.560
0.540
0.520
0.500
0.480
0.460
0.440
0.420
0.400
0.380
0.360
0.340
0.320
0.300
0.280
0.260
0.240
0.220
0.200
15
30
45
60
75
90
105
120
135
150
165
180
Y2

Figure 43.

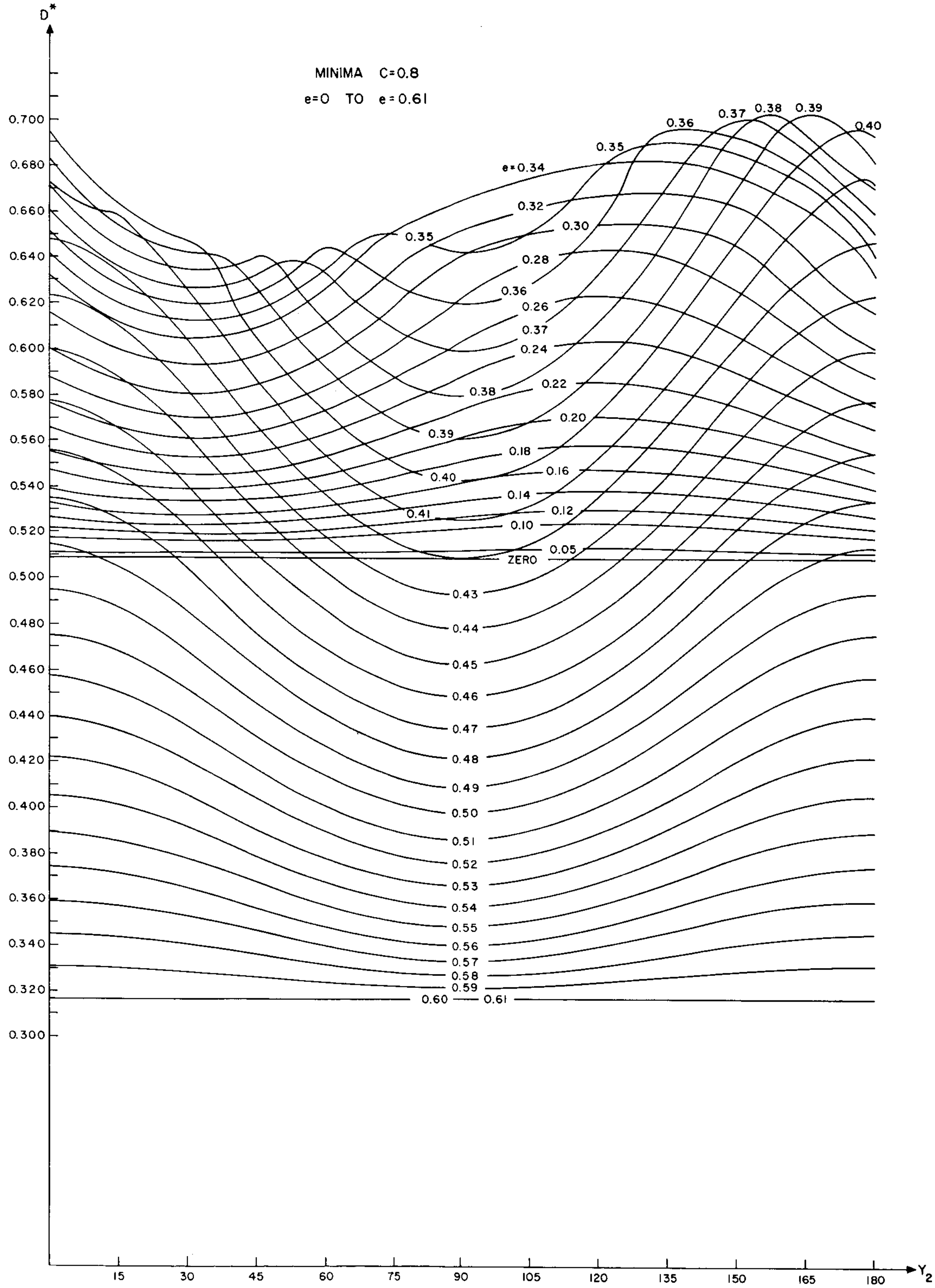

D*
MINIMA C=0.8
e=0 TO e=0.61
0.700
0.680
0.660
0.640
0.620
0.600
0.580
0.560
0.540
0.520
0.500
0.480
0.460
0.440
0.420
0.400
0.380
0.360
0.340
0.320
0.300
e=0.34
0.32
0.30
0.28
0.26
0.24
0.22
0.20
0.18
0.16
0.14
0.12
0.10
0.05
ZERO
0.35
0.36
0.37
0.38
0.39
0.40
0.41
0.43
0.44
0.45
0.46
0.47
0.48
0.49
0.50
0.51
0.52
0.53
0.54
0.55
0.56
0.57
0.58
0.59
0.60
0.61
15
30
45
60
75
90
105
120
135
150
165
180
Y_2

Figure 44.

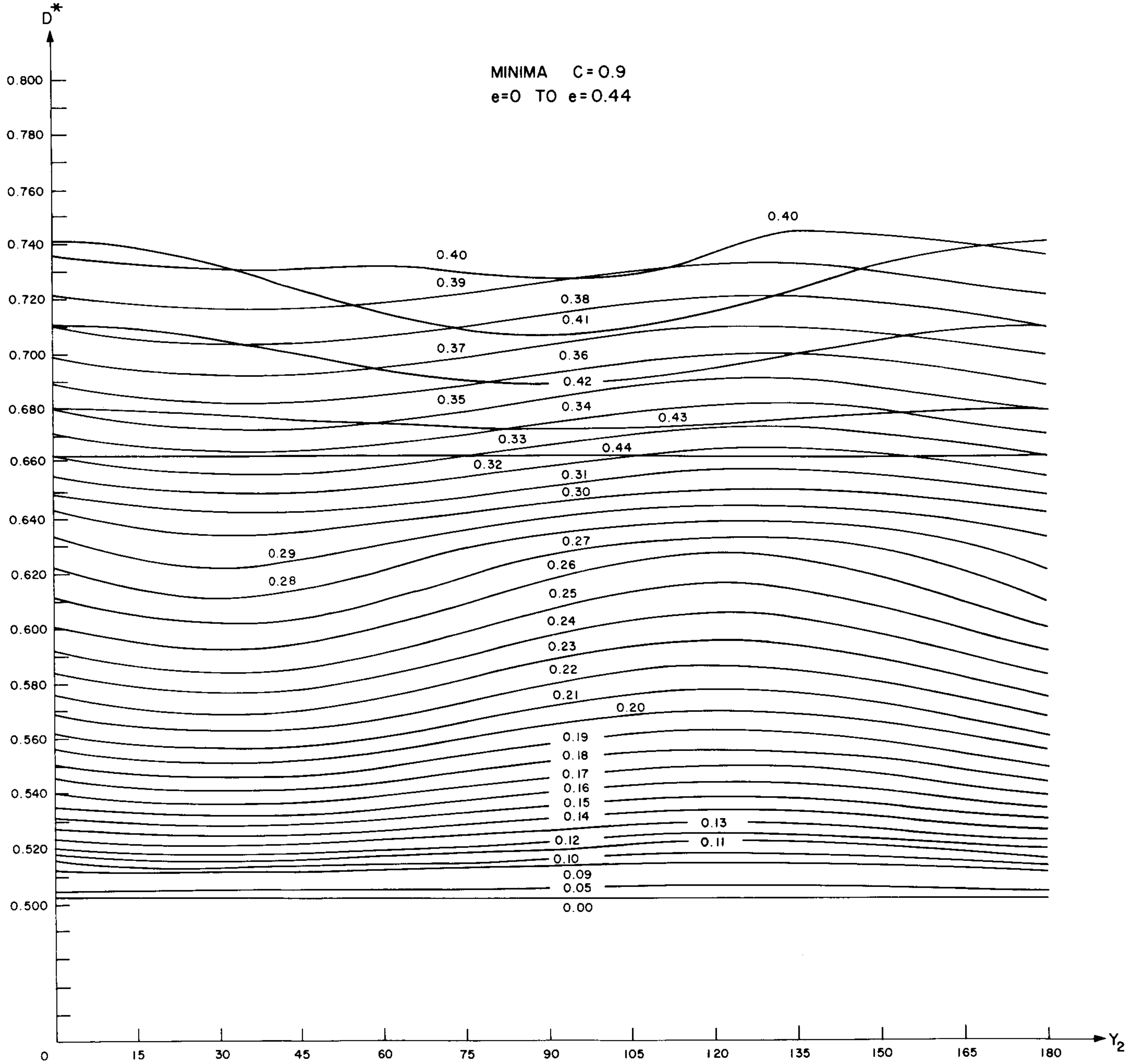

D*
MINIMA C = 0.9
e=0 TO e=0.44
0.800
0.780
0.760
0.740
0.720
0.700
0.680
0.660
0.640
0.620
0.600
0.580
0.560
0.540
0.520
0.500
0.40
0.40
0.39
0.38
0.41
0.37
0.36
0.42
0.35
0.34
0.43
0.33
0.44
0.32
0.31
0.30
0.29
0.27
0.28
0.26
0.25
0.24
0.23
0.22
0.21
0.20
0.19
0.18
0.17
0.16
0.15
0.14
0.13
0.12
0.11
0.10
0.09
0.05
0.00
0
15
30
45
60
75
90
105
120
135
150
165
180
Y_2

Figure 45.

Figures 46-54.

Isoenergetic curves for the long-periodic motion of perihelion.

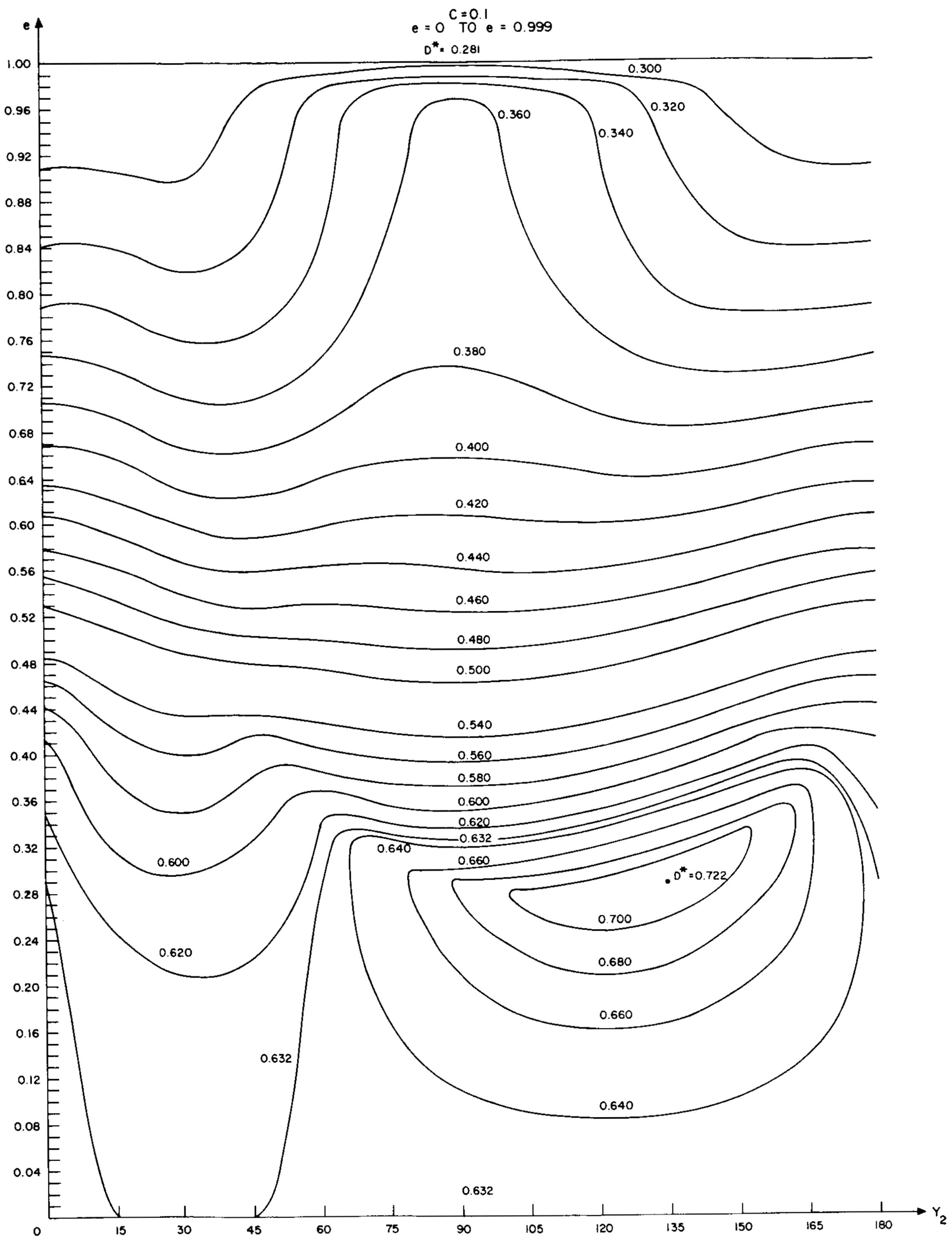
C = 0.1
e = 0 TO e = 0.999
D* = 0.281
0.300
0.320
0.340
0.360
0.380
0.400
0.420
0.440
0.460
0.480
0.500
0.540
0.560
0.580
0.600
0.620
0.632
0.640
0.660
D* = 0.722
0.700
0.680
0.660
0.640
0.632
0.600
0.620
0.632
e
1.00
0.96
0.92
0.88
0.84
0.80
0.76
0.72
0.68
0.64
0.60
0.56
0.52
0.48
0.44
0.40
0.36
0.32
0.28
0.24
0.20
0.16
0.12
0.08
0.04
0
15
30
45
60
75
90
105
120
135
150
165
180
Y_2

Figure 46.

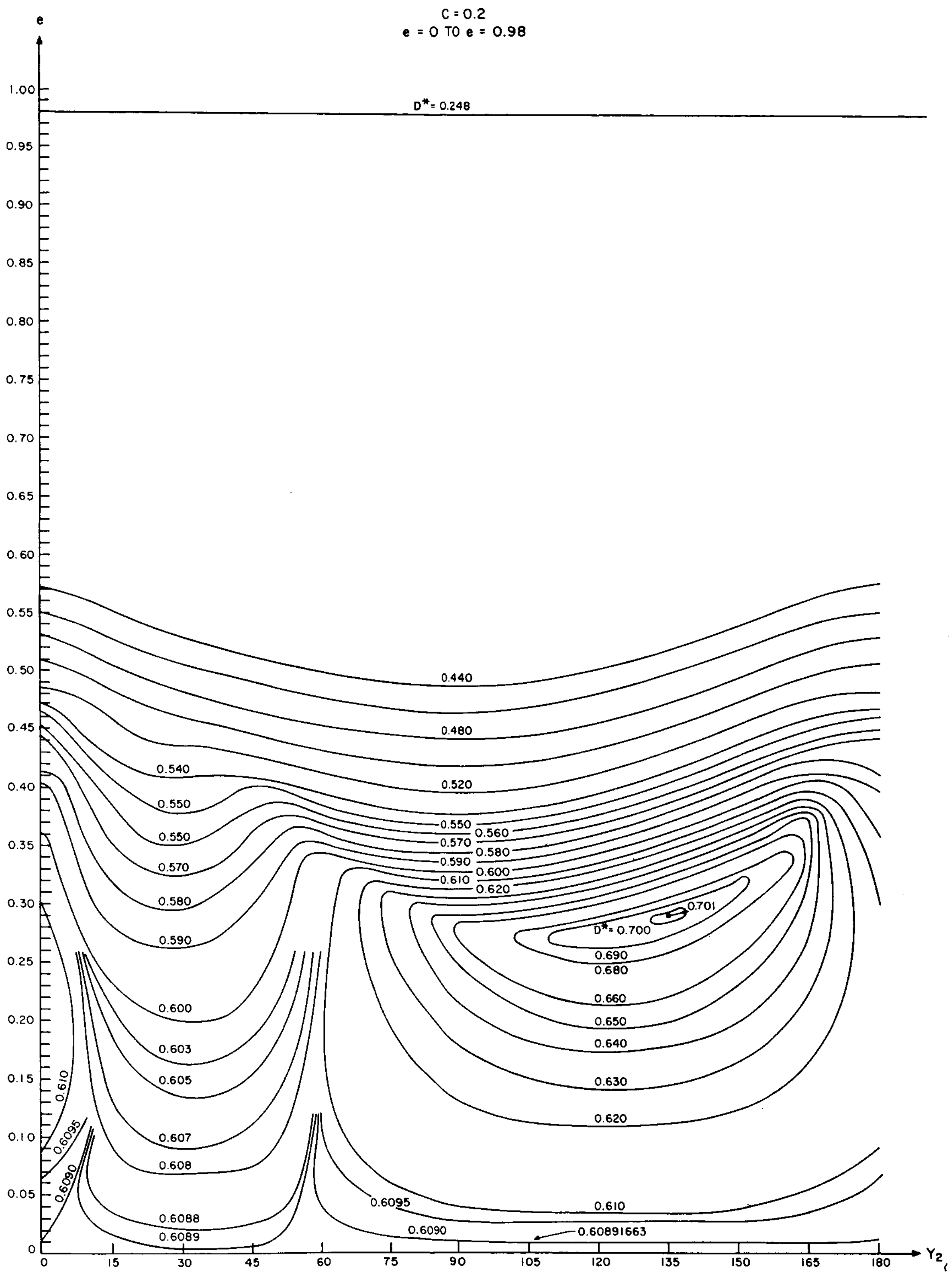

C = 0.2
e = 0 TO e = 0.98
e
1.00
0.95
0.90
0.85
0.80
0.75
0.70
0.65
0.60
0.55
0.50
0.45
0.40
0.35
0.30
0.25
0.20
0.15
0.10
0.05
0
D* = 0.248
0.440
0.480
0.520
0.540
0.550
0.550
0.570
0.580
0.590
0.600
0.603
0.605
0.607
0.608
0.6088
0.6089
0.610
0.6095
0.6090
0.550
0.560
0.570
0.580
0.590
0.600
0.610
0.620
0.701
D* = 0.700
0.690
0.680
0.660
0.650
0.640
0.630
0.620
0.610
0.6095
0.6090
0.60891663
0
15
30
45
60
75
90
105
120
135
150
165
180
Y_2

Figure 47.

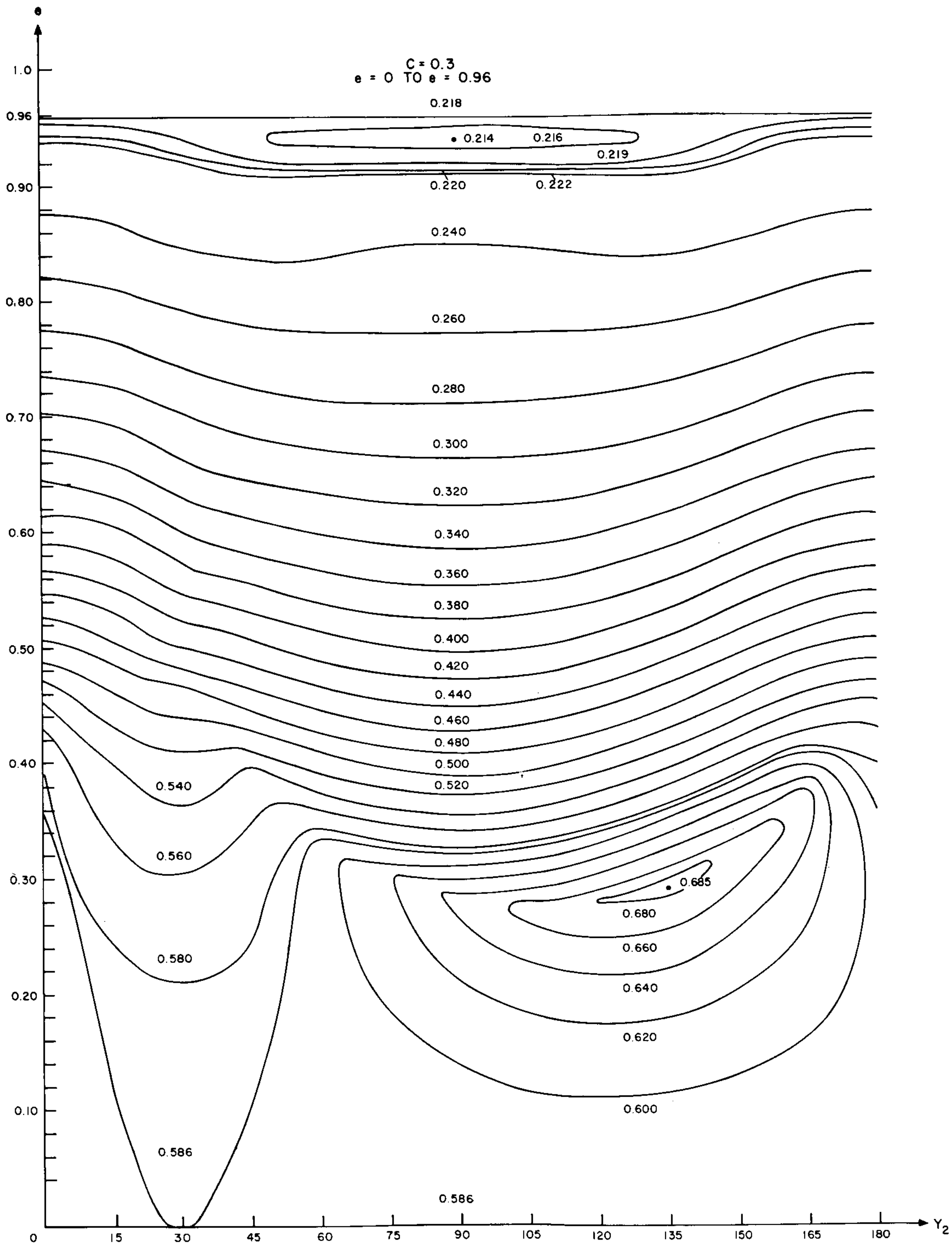

C = 0.3
e = 0 TO e = 0.96
e
1.0
0.96
0.90
0.80
0.70
0.60
0.50
0.40
0.30
0.20
0.10
0
15
30
45
60
75
90
105
120
135
150
165
180
Y_2
0.218
0.214
0.216
0.219
0.220
0.222
0.240
0.260
0.280
0.300
0.320
0.340
0.360
0.380
0.400
0.420
0.440
0.460
0.480
0.500
0.520
0.540
0.560
0.580
0.586
0.586
0.600
0.620
0.640
0.660
0.680
0.685

Figure 48.

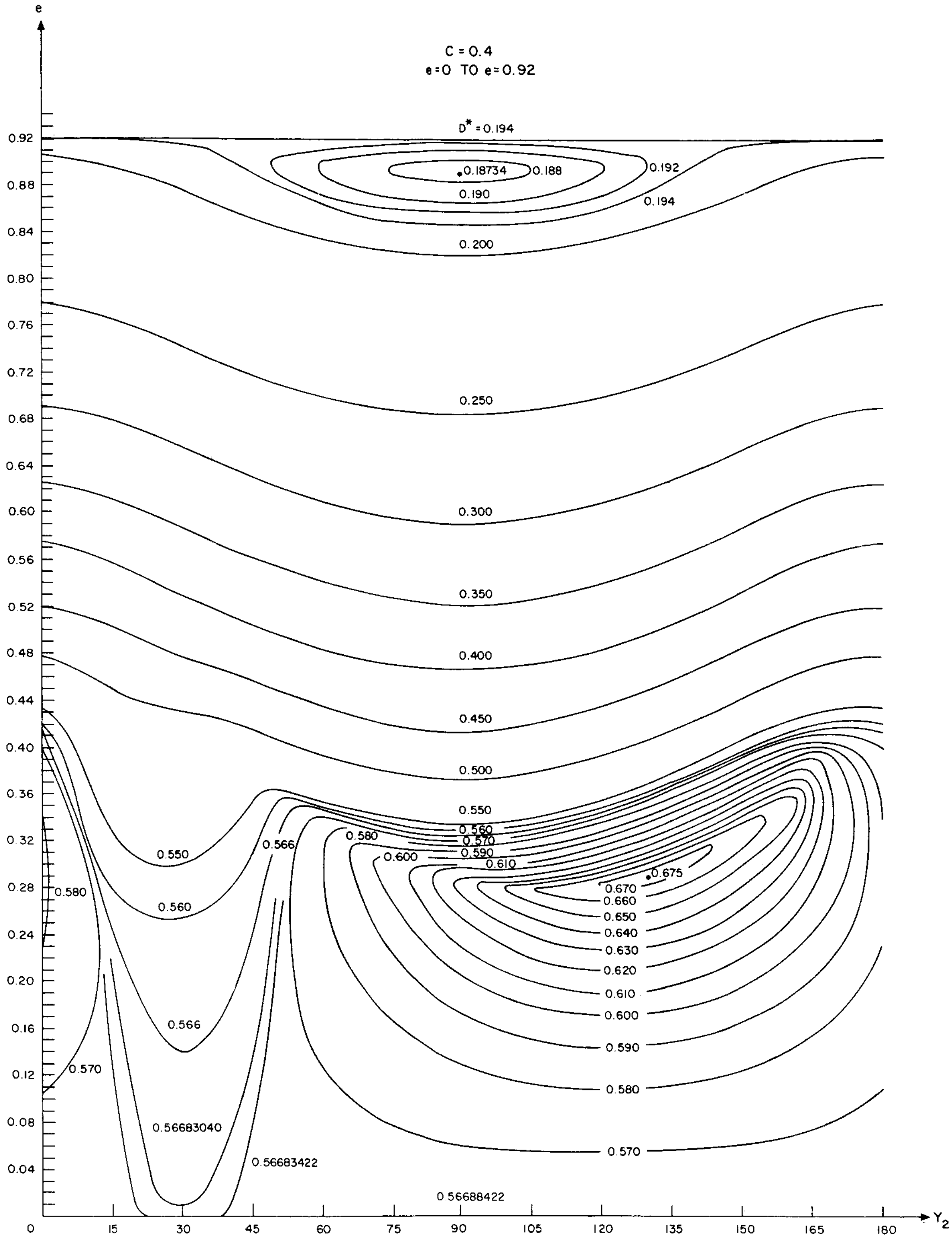
C = 0.4
e=0 TO e=0.92
D* = 0.194
0.18734
0.188
0.190
0.192
0.194
0.200
0.250
0.300
0.350
0.400
0.450
0.500
0.550
0.560
0.566
0.570
0.580
0.590
0.600
0.610
0.620
0.630
0.640
0.650
0.660
0.670
0.675
0.56683040
0.56683422
0.56688422
e
Y2
0.92
0.88
0.84
0.80
0.76
0.72
0.68
0.64
0.60
0.56
0.52
0.48
0.44
0.40
0.36
0.32
0.28
0.24
0.20
0.16
0.12
0.08
0.04
0
15
30
45
60
75
90
105
120
135
150
165
180

Figure 49.

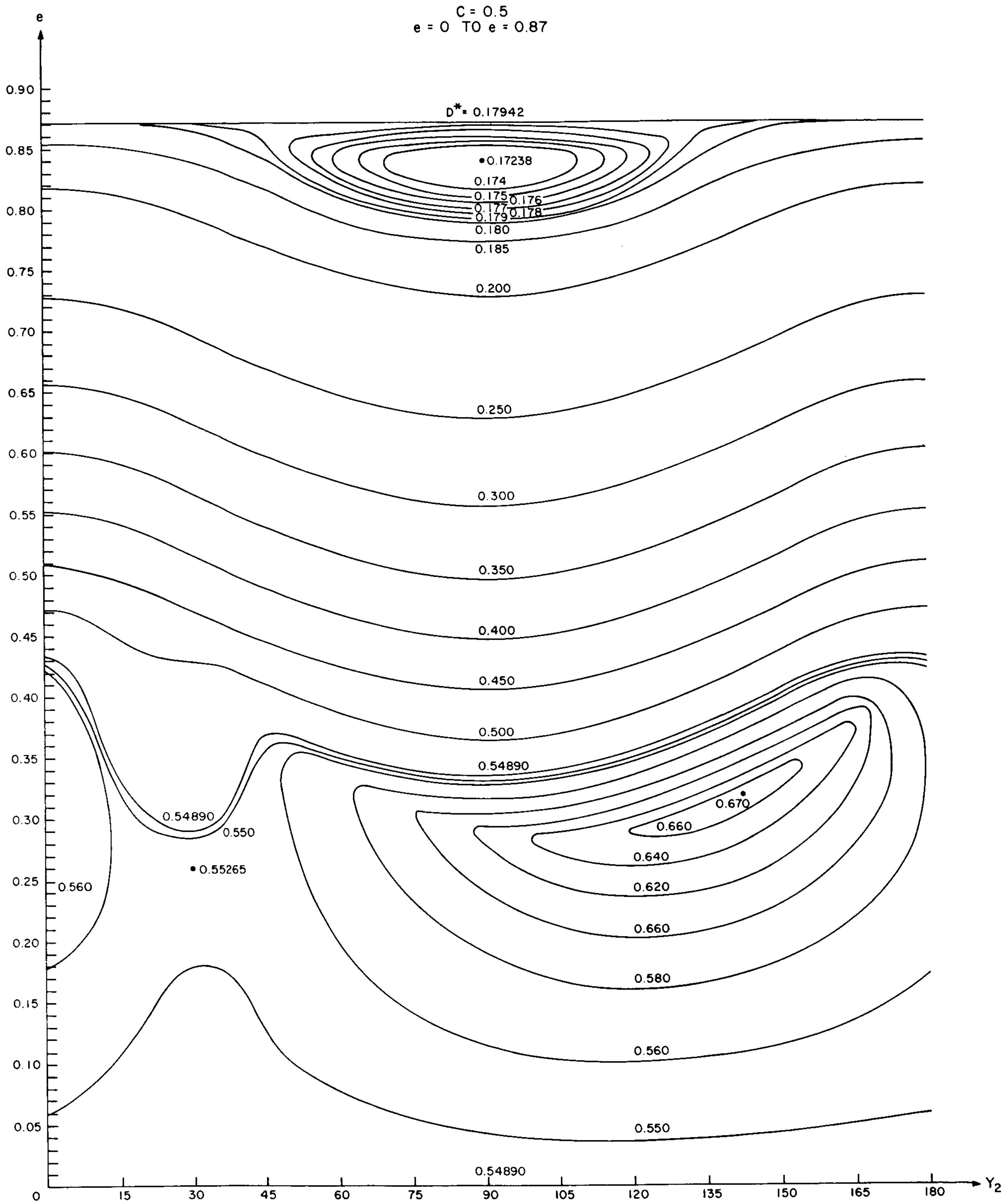

C = 0.5
e = 0 TO e = 0.87
e
D* = 0.17942
0.17238
0.174
0.175
0.176
0.177
0.178
0.179
0.180
0.185
0.200
0.250
0.300
0.350
0.400
0.450
0.500
0.54890
0.54890
0.550
0.55265
0.560
0.670
0.660
0.640
0.620
0.660
0.580
0.560
0.550
0.54890
0.90
0.85
0.80
0.75
0.70
0.65
0.60
0.55
0.50
0.45
0.40
0.35
0.30
0.25
0.20
0.15
0.10
0.05
0
15
30
45
60
75
90
105
120
135
150
165
180
Y_2

Figure 50.

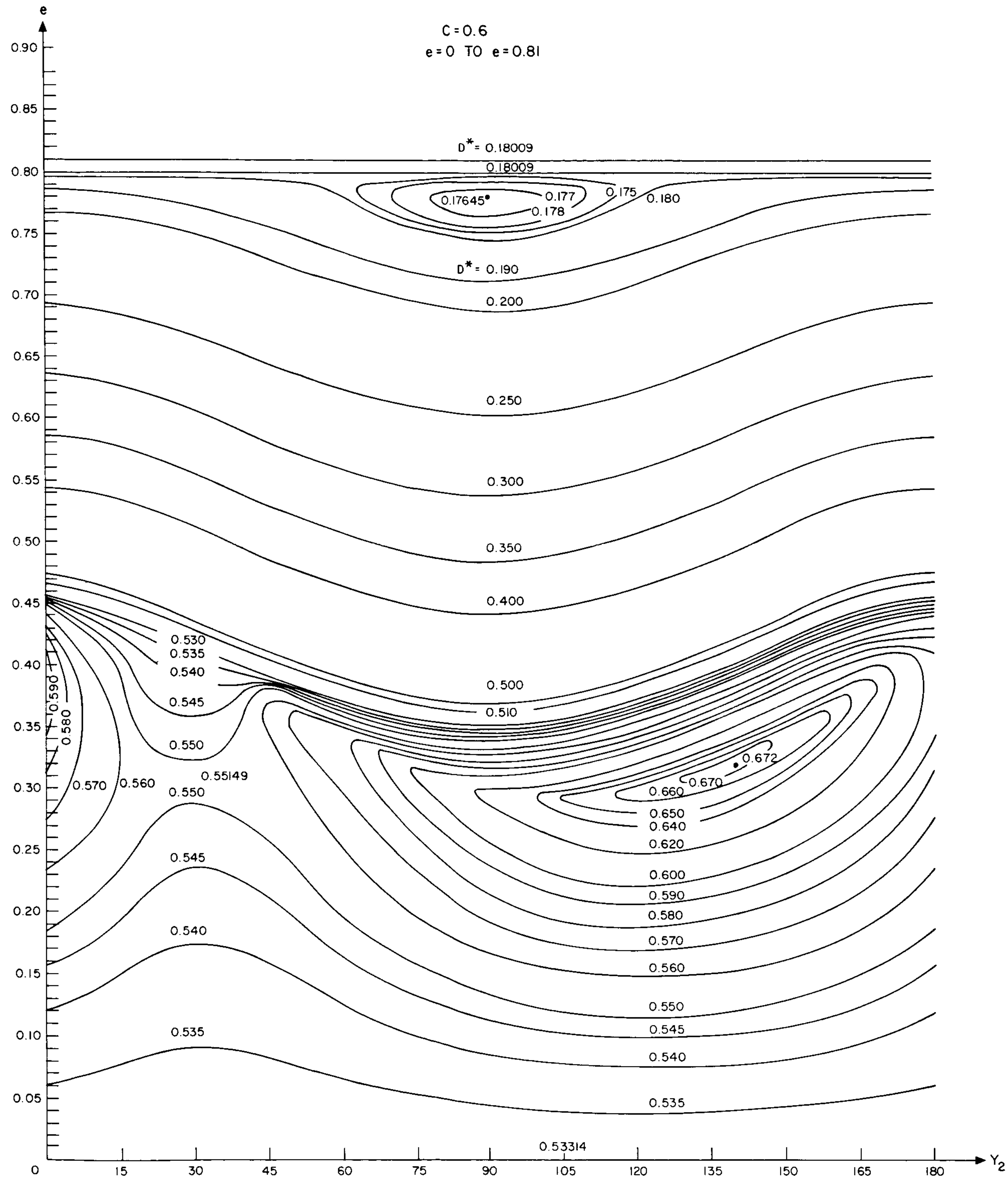
C = 0.6
e = 0 TO e = 0.81
e
Y_2
D* = 0.18009
0.18009
0.17645
0.177
0.178
0.175
0.180
D* = 0.190
0.200
0.250
0.300
0.350
0.400
0.500
0.510
0.530
0.535
0.540
0.545
0.550
0.55149
0.590
0.580
0.570
0.560
0.672
0.670
0.660
0.650
0.640
0.620
0.600
0.53314

Figure 51.

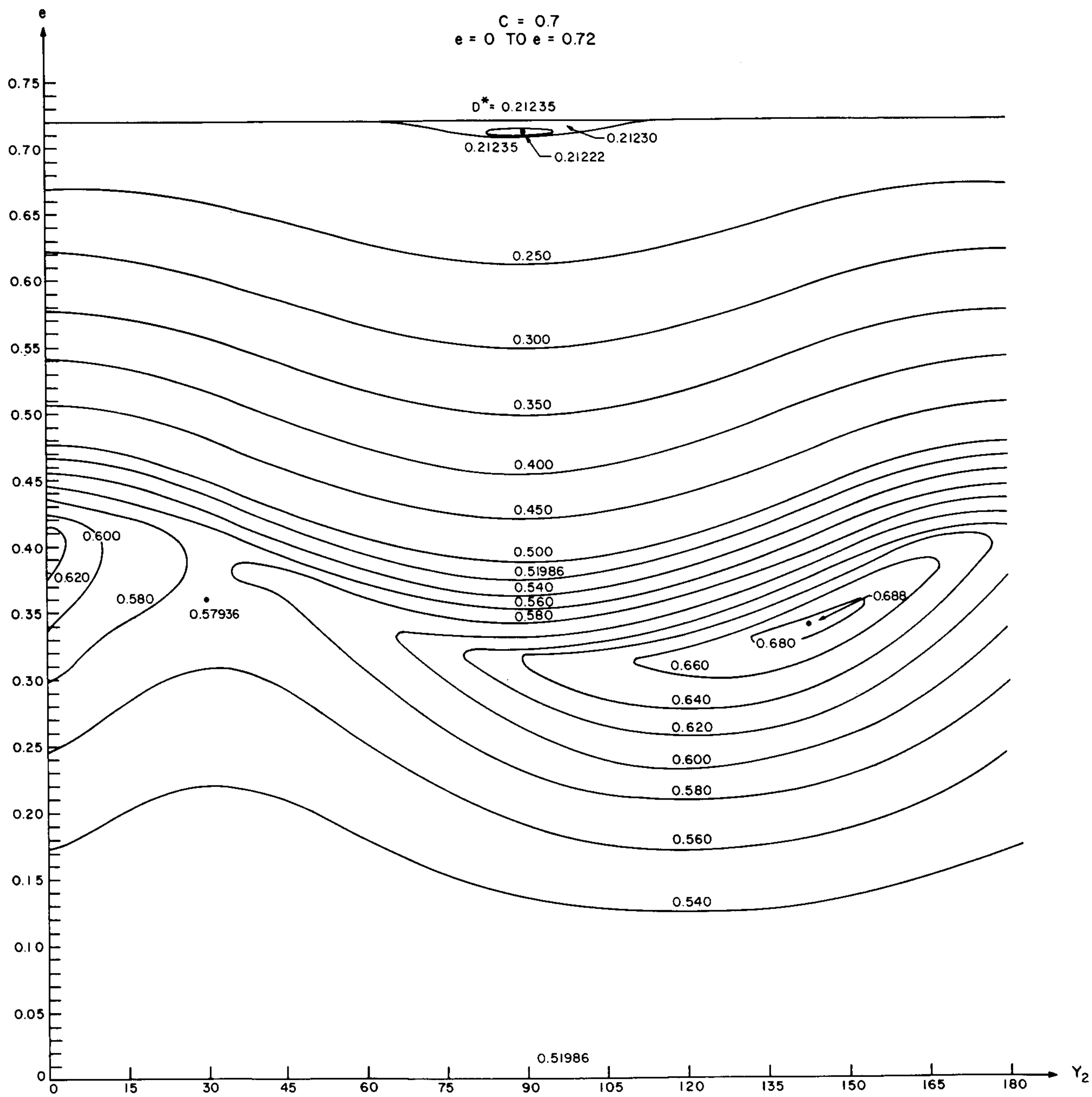

C = 0.7
e = 0 TO e = 0.72
e
$D^* = 0.21235$
0.21235
0.21222
0.21230
0.250
0.300
0.350
0.400
0.450
0.500
0.51986
0.540
0.560
0.580
0.600
0.620
0.580
0.57936
0.688
0.680
0.660
0.640
0.620
0.600
0.580
0.560
0.540
0.51986
Y_2
0.75
0.70
0.65
0.60
0.55
0.50
0.45
0.40
0.35
0.30
0.25
0.20
0.15
0.10
0.05
0
0
15
30
45
60
75
90
105
120
135
150
165
180

Figure 52.

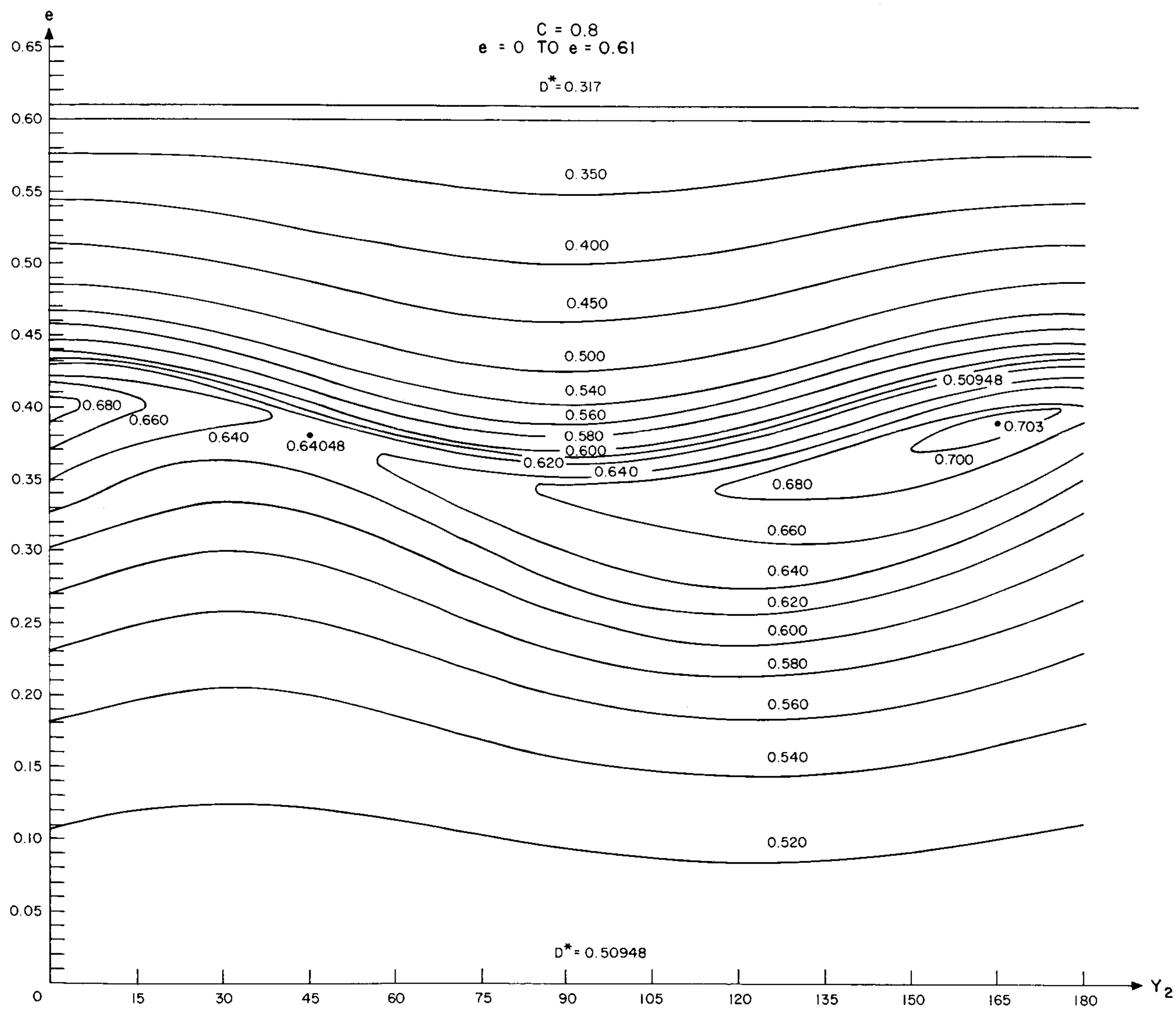
C = 0.8
e = 0 TO e = 0.61
D* = 0.317
0.350
0.400
0.450
0.500
0.540
0.560
0.580
0.600
0.620
0.640
0.50948
0.703
0.700
0.680
0.660
0.640
0.620
0.600
0.580
0.560
0.540
0.520
0.680
0.660
0.640
0.64048
D* = 0.50948
e
0.65
0.60
0.55
0.50
0.45
0.40
0.35
0.30
0.25
0.20
0.15
0.10
0.05
0
15
30
45
60
75
90
105
120
135
150
165
180
Y_2

Figure 53.

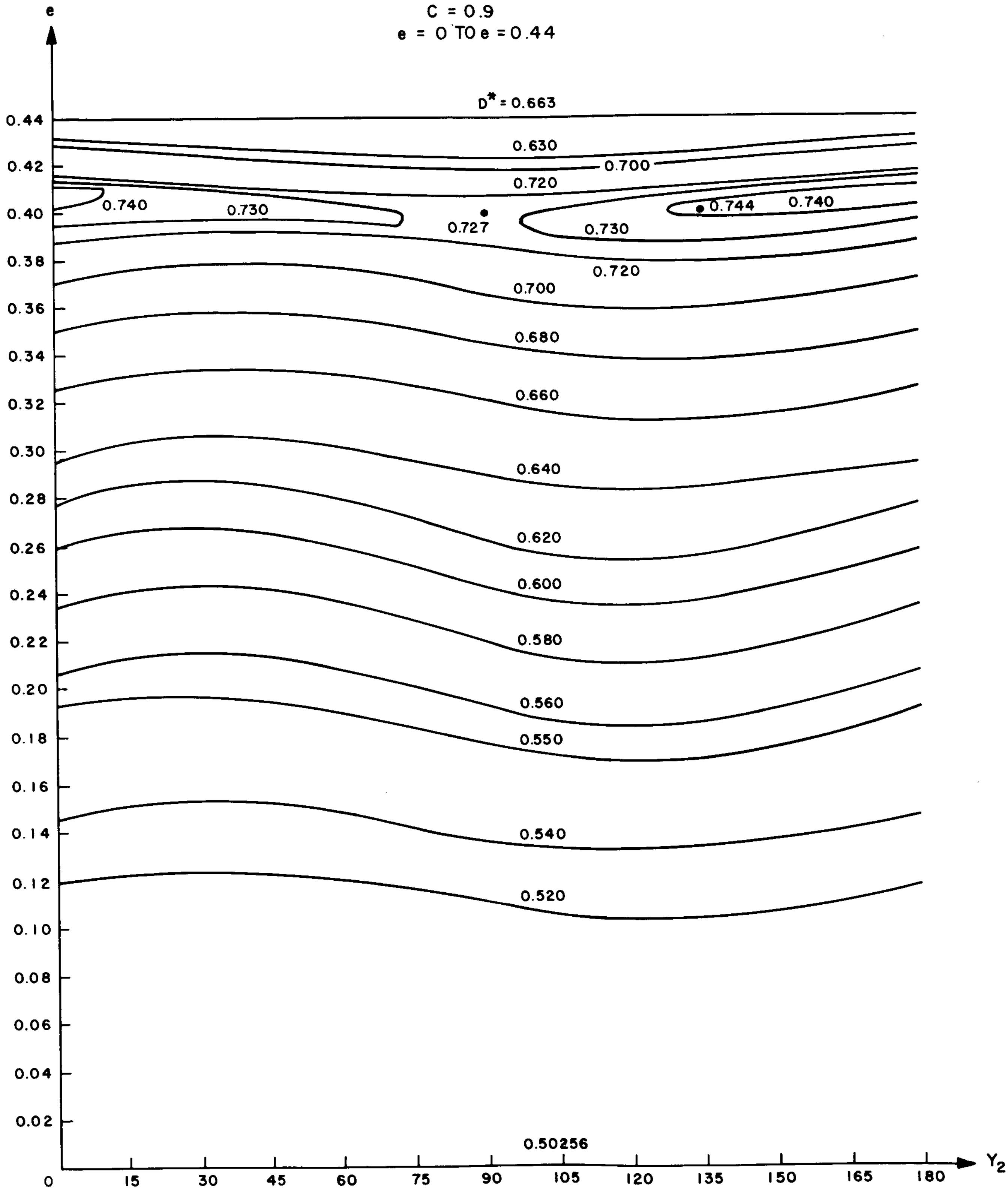

e
C = 0.9
e = 0 TO e = 0.44
D* = 0.663
0.630
0.700
0.720
0.740
0.730
0.727
0.730
0.744
0.740
0.720
0.700
0.680
0.660
0.640
0.620
0.600
0.580
0.560
0.550
0.540
0.520
0.50256
0.44
0.42
0.40
0.38
0.36
0.34
0.32
0.30
0.28
0.26
0.24
0.22
0.20
0.18
0.16
0.14
0.12
0.10
0.08
0.06
0.04
0.02
0
15
30
45
60
75
90
105
120
135
150
165
180
Y_2

Figure 54.

BIOGRAPHICAL NOTE

GIORGIO E. O. GIACAGLIA received his B.S. in physics from the Faculty of Sciences of the University of São Paulo in 1958. He attended the Polytechnical School of the University from 1954 to 1960, where he earned the degree of Senior Engineer. Dr. Giacaglia received his Master's degree in physics from the Faculty of Sciences in 1962 and his Ph. D. in astronomy from Yale University in 1965. Since 1967, he has been Professor in the Chair of General Mechanics of the Polytechnical School of the University of São Paulo.

Dr. Giacaglia came to SAO in 1968 on a leave of absence from the University. He is currently working in Research and Analysis as a geophysicist, where he is specializing in research in celestial mechanics.

NOTICE

This series of Special Reports was instituted under the supervision of Dr. F. L. Whipple, Director of the Astrophysical Observatory of the Smithsonian Institution, shortly after the launching of the first artificial earth satellite on October 4, 1957. Contributions come from the Staff of the Observatory.

First issued to ensure the immediate dissemination of data for satellite tracking, the reports have continued to provide a rapid distribution of catalogs of satellite observations, orbital information, and preliminary results of data analyses prior to formal publication in the appropriate journals. The Reports are also used extensively for the rapid publication of preliminary or special results in other fields of astrophysics.

The Reports are regularly distributed to all institutions participating in the U. S. space research program and to individual scientists who request them from the Publications Division, Distribution Section, Smithsonian Astrophysical Observatory, Cambridge, Massachusetts 02138.